INFORMATION TO USERS

This manuscript has been reproduced from the microfilm master. UMI films the text directly from the original or copy submitted. Thus, some thesis and dissertation copies are in typewriter face, while others may be from any type of computer printer.

The quality of this reproduction is dependent upon the quality of the copy submitted. Broken or indistinct print, colored or poor quality illustrations and photographs, print bleedthrough, substandard margins, and improper alignment can adversely affect reproduction.

In the unlikely event that the author did not send UMI a complete manuscript and there are missing pages, these will be noted. Also, if unauthorized copyright material had to be removed, a note will indicate the deletion.

Oversize materials (e.g., maps, drawings, charts) are reproduced by sectioning the original, beginning at the upper left-hand corner and continuing from left to right in equal sections with small overlaps. Each original is also photographed in one exposure and is included in reduced form at the back of the book.

Photographs included in the original manuscript have been reproduced xerographically in this copy. Higher quality 6" x 9" black and white photographic prints are available for any photographs or illustrations appearing in this copy for an additional charge. Contact UMI directly to order.

UMI

A Bell & Howell Information Company
300 North Zeeb Road, Ann Arbor MI 48106-1346 USA
313/761-4700 800/521-0600

Abnormal lipoprotein metabolism in animal models of intrahepatic cholestasis induced by α-naphthylisothiocyanate

by

Jeffrey W. Chisholm

Submitted in partial fulfillment of the requirements for the

Doctor of Philosophy Degree

at

Dalhousie University

Halifax, Nova Scotia

December, 1996

DALHOUSIE UNIVERSITY

FACULTY OF GRADUATE STUDIES

The undersigned hereby certify that they have read and recommend to the Faculty of Graduate Studies for acceptance a thesis entitled "Abnormal lipoprotein metabolism in animal models of intrahepatic cholestasis induced by α-naphthylisothiocyanate"

by Jeffrey W. Chisholm

in partial fulfillment of the requirements for the degree of Doctor of Philosophy.

Dated: December 9, 1996

External Examiner

Research Supervisor

Examining Committee

DALHOUSIE UNIVERSITY

DATE: December 18, 1996

AUTHOR: Jeffrey W. Chisholm

TITLE: "Abnormal lipoprotein metabolism in animal models of intrahepatic cholestasis induced by α-naphthylisothiocyanate"

DEPARTMENT OR SCHOOL: Biochemistry

DEGREE: Ph.D. CONVOCATION: May YEAR: 1997

Permission is herewith granted to Dalhousie University to circulate and to have copied for non-commercial purposes, at its discretion, the above title upon the request of individuals or institutions.

Signature of Author

Table of Contents

List of Figures

List of Tables

Abstract

The α-naphthylisothiocyanate (ANIT) treated rat and mouse were evaluated as models of abnormal lipoprotein metabolism in familial lecithin: cholesterol acyltransferase (LCAT) deficiency and cholestatic liver disease.

In the rat, alterations in plasma lipoprotein composition were studied from 0 to 120 h. By 48 h, plasma free cholesterol (FC), cholesteryl ester (CE) and phospholipid (PL) were increased 9.4, 2.9 and 6.1 fold with a concomitant reduction in the CE/FC ratio. LCAT and lipoprotein lipase (LPL) activities were near normal while hepatic triacylglycerol lipase (HTGL) was decreased. Elevated FC and PL were primarily associated with an increase in lipoproteins within the low density lipoprotein (LDL) density range that contained apolipoprotein (apo) A-I and E. The composition of these lipoproteins was consistent with the presence of abnormal lipoprotein-X-like vesicles. By 120 h, vesicles within the LDL density range were cleared through apparent movement of PL and FC into high density lipoproteins (HDL). In ANIT-treated human apo A-I transgenic rats, a positive correlation between plasma apo A-I levels, CE and a reduction in the accumulation PL and FC-rich lipoproteins within the LDL density range was demonstrated.

These results indicate that the ANIT-treated rat is a reversible model of abnormal lipoprotein metabolism in transient intrahepatic cholestasis where LCAT is functional and that the clearance of PL and FC-rich LDL lipoproteins is limited by the apo A-I mediated generation of LCAT substrate HDL and not LCAT activity.

In the ANIT-treated mouse, plasma PL and FC concentrations at 48, 72 and 168 h were increased 10, 11, 13 and 17, 20, 45 fold respectively. Elevations in these lipids were followed by very low CE levels, CE/FC ratio and LCAT activity (48 h). As in the rat, the ratio of FC and PL within the LDL density region was consistent with the presence of vesicles. These results suggest that the ANIT-treated mouse may be a useful model for studying the abnormal lipoproteins of LCAT deficiency and intrahepatic cholestasis.

Abbreviations and Symbols

ALT-alanine aminotransferase

ANIT-α-naphthylisothiocyanate

Apo-apolipoprotein

APOBEC- apolipoprotein B mRNA editing complex 1

AST-aspartate aminotransferase

BCA-bicinchoninic acid

BSA-bovine serum albumin

CE-cholesteryl ester

CETP-cholesteryl ester transfer protein

cyp7-7α-hydroxylase gene

DOPC-1,2-di[cis-9-octodecanoyl] *sn* glycero-3-phosphocholine

Na_2EDTA-disodium ethylenediamine tetra-acetic acid

ER-endoplasmic reticulum

FC-free cholesterol

HDL-high density lipoprotein

HMG CoA reductase-hydroxy methylglutaryl Co-enzyme A reductase

HTGL-hepatic triacylglycerol lipase

IDL-intermediate density lipoprotein

LCAT-lecithin: cholesterol acyltransferase

LDL-low density lipoprotein

LDLR-low density lipoprotein receptor

LPL-lipoprotein lipase

Lp-X-lipoprotein X

Lp-Y-lipoprotein Y

LRP-low density lipoprotein receptor related protein

PAGE-polyacrylamide gel electrophoresis

PL-phospholipid

PLTP-phospholipid transport protein

RER-rough endoplasmic reticulum

rHDL-recombinant high density lipoprotein

SER-smooth endoplasmic reticulum

TAG-triacylglycerol

TBS-tris buffered saline

TC-total cholesterol

TgR[HuAI]-transgenic rat expressing the human apolipoprotein A-I gene

TLC-thin layer chromatography

VLDL-very low density lipoprotein

Acknowledgments

I thank **Dr. Peter J. Dolphin** for his supervision and generous support throughout my tenure in his lab. I must also thank **Mr. Bruce Stewart** for his excellent technical assistance, routine analysis of rat plasma lipids by gas chromatography and help with the TgR[HuAI] rat colony. **Mrs. Jacquie Froom** and **Ms. Danita Volder** in **Dr. Meng Tan's Lab** deserve special recognition and sincere thanks for their assistance in the routine analysis of human apolipoprotein A-I in the TgR[HuAI] rats.

I would also like to thank my supervisory committee which consisted of **Dr. Carl Breckenridge, Dr. Ted Palmer** and **Dr. Neale Ridgeway** for their knowledgeable advice and support during the course of this thesis research.

Over the past 4 plus years, a number of faces have passed through the Dolphin Lab making my residency both interesting and immensely enjoyable. In particular, I would like to thank in no particular order **Ms. Cynthia Coffill** who is doing doctoral studies with **Dr. Dan Sparks** at the Ottawa Heart Institute, **Mr. Denis Blinn** a former honors student in our lab currently studying kinesiology and **Ms. Jocelyn Johnston** a summer student who left the lab in search of bigger and better things in medicine. I also must acknowledge and thank **Ms. Evelyn Teh** a current Ph.D. student and **Mr. Jason Dube** a current honors student in the lab for putting up with me, making me laugh and making life bearable over the last few stressful months.

Dr. Lou Agellon and the members of his lab at the University of Alberta deserve special thanks for giving me the opportunity to collaborate on the ANIT-treated mouse project and in the process learn more about the world of bile acid metabolism.

Dr. Jim Paterniti, formerly of Sandoz and now employed with Ligand Pharmaceuticals, CA., deserves recognition for both collaborating and entrusting the welfare of the TgR[HuAI] rat colony to me.

Last but certainly not least, I owe my deepest gratitude and thanks to **my parents** and **family** for always believing in me and offering support whenever it was needed.

Thesis research and my stipend were supported by a research grant to **P.J. Dolphin** from **The Heart and Stroke Foundation** of **New Brunswick** and latterly **Nova Scotia**.

Chapter 1- Introduction

1.1 Dietary lipid absorption

All mammals require cholesterol for the maintainence and synthesis of cellular membranes, production of sterols and synthesis of metabolically active steroids. Mammals may obtain cholesterol from both endogenous (synthesis primarily in the liver) and exogenous sources. The relative importance of the exogenous source to cholesterol homeostasis is probably metabolically regulated at the level of intestinal cholesterol absorption (1). Exogenous cholesterol is absorbed by the intestinal endothelium as free cholesterol with dietary cholesteryl esters having been hydrolysed in the gut by cholesterol esterase (E.C. 3.1.1.13). Dietary phospholipid is absorbed as *sn-1* lysophospholipid after phospholipase A_2 (E.C. 3.1.1.4) mediated hydrolysis of the *sn-2* fatty acyl moiety and triacylglycerol is absorbed as *sn-2* monacylglycerol and free fatty acids after hydrolysis by pancreatic lipase (E.C. 3.1.1.3). Both lysophospholipid and monoacylglycerol may then be resynthesized into phospholipid and triacylglycerol by the action of acyltransferases in intestinal endothelium cells. Much of the free cholesterol may be esterified via acyl CoA:cholesterol acyltransferase (ACAT) (E.C. 2.3.1.26) before being packaged with triacylglycerol and phospholipid into chylomicrons (dietary lipoproteins) (2).

1.2 Lipoprotein structure

Normal circulating lipoproteins are spherical macromolecular complexes composed of a core of hydrophobic, neutral lipid and a surface monolayer of amphipathic

lipid. Cholesteryl ester and triacylglycerol are the primary neutral lipids, whereas phospholipid and free cholesterol are the major surface lipids. Lipoproteins also have a protein constituent and these are referred to as apolipoproteins. Apolipoproteins tend to function in programming the metabolism of the lipoprotein. Some of the major lipoprotein species are shown in **Table 1.1** and are generally differentiated by their lipid and apolipoprotein composition, size, floatation density (**Figure 1.1**), electrophoretic mobility and function, if known. In general, lipoproteins can be divided into two physiological types, anabolic and catabolic by their primary functions.

Figure 1.1- Schlieren patterns of human serum lipoproteins
Svedberg coefficients of floatation (S_f) as determined in an analytical ultricentrifuge are shown (lower scale). Svedberg coefficients of floatation for chylomicrons through to Lp_{a1} were determined at a density of 1.063 g/ml and and for $Lp_{a(A1+A2)}$ through to HDL_3 at a density of 1.20 g/ml. The uppermost scale correlates S_f units with floatation density. Figure adapted from Lindgren (3).

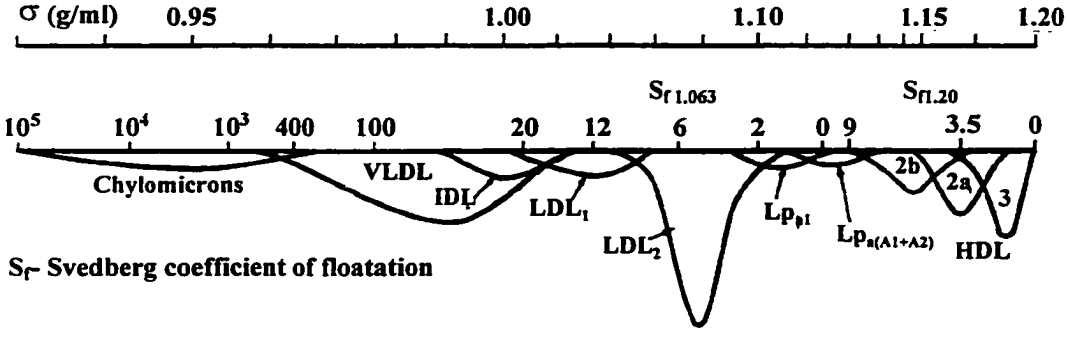

1.3 Anabolic lipoprotein species

Chylomicrons, (see **Table 1.1**) form part of a complex system that facilitates the movement of cholesterol and triacylglycerol between tissues and organs. Chylomicrons primarily are responsible for moving dietary cholesterol, triacylglycerol and other lipophilic molecules such as vitamin E from the intestine into the circulation. These large

particles are primarily associated with apolipoprotein B_{48}. Triacylglycerol-rich very low density lipoprotein (VLDL) are synthesized in the liver and are functional precursors to intermediate density lipoprotein (IDL) and the major anabolic cholesterol delivery lipoprotein, low density lipoprotein (LDL). VLDL function primarily as carriers of liver derived triacylglycerol. IDL are normally found in very low concentrations in plasma and are lipolysis products of apolipoprotein B_{100} containing VLDL that are further catabolized by the action of hepatic lipase [E.C. 3.1.1.3] to LDL. In some species such as the rat and the mouse, the liver also secretes apolipoprotein B_{48} containing VLDL that are thought to be metabolized in an identical manner to chylomicrons (4).

1.4 Catabolic lipoprotein species

A number of different species of high density lipoprotein (HDL) make up what is thought to be a catabolic lipoprotein pathway which facilitates the removal of excess cholesterol from extrahepatic cells back to the liver for catabolism through bile acid synthesis and/or recycling. Recycling may occur either through the secretion of new VLDL or by transfer of cholesteryl ester from HDL by the cholesteryl ester transfer protein (CETP) to VLDL and LDL. This combined process is often referred to as "reverse cholesterol transport" (5-7). There have been numerous different HDL species reported in the literature ranging from so-called lipid-free apolipoprotein A-I, preβ-HDL, γ-HDL through to a variety of α-HDL species. Background aspects of HDL metabolism as necessary for this dissertation will be discussed later, and for a detailed account, the reader is directed to a number of excellent recent reviews (6-9).

Table 1.1- Physical properties of some of the major lipoprotein species found in plasma. Lipid compositional data is from normolipidemic humans.

Lipoprotein Species *(Abr.)*	Lipoprotein Species *(Full Name)*	Density Range *(g/ml)*	Particle Diameter (nm)	Electrophoretic Mobility in Agarose	Associated Apolipoproteins *(circulating)*	Protein *(%)*	FC *(%)*	PL *(%)*	CE *(%)*	TAG *(%)*
Chylo	Chylomicron	d<1.006	75-1200§	pre-β	B_{48}, C's, E†	2†	<1†	5†	<1†	93†
VLDL	Very Low Density Lipoprotein	d<1.006†	30-80§	pre-β†	B_{100}, B_{48}(rat), C's, E†	10†	6†	15†	14†	53†
IDL	Intermediate Density Lipoprotein	1.006<d<1.019†	25-35§	pre-β	B_{100}, E†	18†	7†	22†	23†	31†
LDL	Low Density Lipoprotein	1.019<d<1.063†	18-25§	β†	B_{100}†	25†	9†	21†	42†	4†
HDL	High Density Lipoprotein	1.063<d<1.21†	5-12§	α†	A-I, A-II, A-IV, E, C's , D	-	-	-	-	-
HDL1	High Density Lipoprotein 1	1.050<d<1.063		α	A-I, A-II E, A-IV, C's	32	8	36	23	2
HDL2	High Density Lipoprotein 2	1.063<d<1.12†		α	A-I, A-II, A-IV, C's	43†	5†	30†	20†	2†
HDL3	High Density Lipoprotein 3	1.12<d<1.21†		α	A-I, A-II, A-IV, C's	55†	3†	25†	16†	1†
VHDL	Very High Density Lipoprotein	1.21<d<1.25†	5-6	pre-β1‡	A-I‡	47.5‡	7.6‡	44‡	0‡	0‡
VHDL	Very High Density Lipoprotein	1.21<d<1.25†		pre-β2‡	A-I‡	21.5‡	5.7‡	73.8‡	0‡	0‡
VHDL	Very High Density Lipoprotein	1.21<d<1.25†		pre-β3‡	A-I, LCAT, CETP and D*	-	-	-	-	-
VHDL	Very High Density Lipoprotein	1.21<d<1.25†		γ	E	-	-	-	-	-

† Data from Fielding and Fielding (10)

‡ Data from Castro and Fielding (11)

* Data from Francone *et al.* (12)

§ Data from Davis and Vance (13)

1.5 Chylomicron metabolism

Newly secreted chylomicrons are large triacylglycerol-rich lipoproteins that in addition to lipid, contain metabolically important apolipoproteins. These include apolipoprotein B_{48}, A-I and sometimes A-IV. Apolipoprotein A-I, C-III, and A-IV form a gene cluster (14) that contains a common intestinal-specific transcriptional promoter (15) and as a possible result, apolipoprotein C-III may also be secreted with the nascent particle and then be transferred to HDL. In the circulation, apolipoprotein A-I and A-IV are transferred to HDL in exchange for apolipoprotein E, C-I and C-II (16,17).

Apolipoprotein B_{48} is the amino terminal 48% of apolipoprotein B_{100} and is synthesized by a mRNA editing event (18) (for a recent review see (19)) caused by the deamination of cytidine 6666 to uridine resulting in an in-frame codon change from CAA to the stop codon UAA (20). Recent work has demonstrated that a unique mRNA editing protein named APOBEC-1 (apoB- mRNA editing enzyme catyalytic peptide 1) (21) is involved. In most species, apolipoprotein B only undergoes editing in the intestine and full length apolipoprotein B_{100} is expressed in the liver. However, in rats, mice, dogs and horses, VLDL are secreted by the liver containing either apolipoprotein B_{48} or B_{100} (22). Metabolically, once secreted, apolipoprotein B_{48} VLDL remnants are indistinguishable from chylomicron remnants and are thought to be processed in the same manner (4).

1.6 Lipoprotein remnant catabolism

Shortly after entering the blood stream, chylomicrons and VLDL are thought to acquire apolipoprotein E and the C apolipoproteins from HDL (16,17). The presence of

apolipoprotein C-II is necessary for the activation of the endothelium bound triacylglycerol lipase, lipoprotein lipase (LPL, E.C. 3.1.1.34) which catalyzes the lipolysis of triacylglycerol (23). Relatively insoluble fatty acids are produced and are reversibly bound to albumin prior to uptake by tissues where they may be used for energy production and/or storage. As the core of the triacylglycerol-rich particle becomes "deflated" (depleted) of triacylglycerol, a remnant lipoprotein is formed, and the excess surface phospholipid and free cholesterol are transferred to HDL and/or free apolipoprotein A-I (24). The precise mechanism by which excess surface phospholipid and free cholesterol is moved into HDL has yet to be elucidated.

The remnant lipoprotein may then be catabolized by receptor mediated endocytosis either by the LDL receptor (LDLR), LDL receptor related protein (LRP) or other structurally related candidate receptors (25). Apolipoprotein B_{100} is the primary ligand for uptake of LDL by the LDL receptor, whereas apolipoprotein E facilitates the binding of remnants to either the LDL receptor or LRP. In an excellent review, Havel (25), reviews recent experimental evidence and concludes that physiologically, remnants are normally taken up by the LDL receptor with the LRP only becoming important when the LDL receptor is down regulated, inhibited or genetically absent. Recent evidence (4,25) suggests that lipolysis and uptake of the chylomicron may occur in a coordinated fashion involving binding of the chylomicron to hepatic endothelium-bound heparin sulfate proteoglycans, lipoprotein lipase and/or hepatic lipase. Once bound, the chylomicron undergoes lipolysis, becomes enriched with apolipoprotein E present in the microvilli (26) and is finally taken up by the appropriate proximal receptor. This process has been referred to as "secretion recapture" by Brown *et al.* (27). New evidence from

hypertriglyceridemic apolipoprotein C-III transgenic mice has provided evidence that apolipoprotein C-III is also important in the catabolism of remnant lipoproteins (28). The hypertriglyceridemia associated with elevated apolipoprotein C-III levels appears to be due to displacement of apolipoprotein E and decreased remnant catabolism via reduced apolipoprotein E mediated interaction with cell surface heparin sulfate proteoglycans and thus reduced interaction with LPL. Apolipoprotein C-III rich VLDL from both normal and human apolipoprotein C-III transgenic mice interacted normally with purified LPL *in vivo* (28), casting doubt on the possiblity that apolipoprotein C-III metabolically inactivates lipoprotein lipase. Apolipoprotein C-I has also been shown to decrease remnant clearance *in vitro* (10); however, this finding is contadicted by *in vivo* studies in the apolipoprotein C-I knockout mouse in which mice lacking apolipoprotein C-I had defective remnant clearance (29). Clearly the role of apolipoprotein C-I in remnant lipoprotein metabolism is not well understood.

1.7 VLDL synthesis

Endogenously synthesized cholesterol and cholesterol from dietary lipoproteins are packaged by the liver along with endogenously synthesized triacylglycerol into apolipoprotein B_{100} VLDL which is the macromolecular precursor to LDL. Production of VLDL appears to be primarily post-translationly regulated by triacylglycerol (30) and possibly cholesterol (31) availability as the change in mRNA levels for apolipoprotein B_{100} in response to dietary and hormonal stimulation are modest in comparison to apolipoprotein B_{100} secretion rates (30,32). It appears that apolipoprotein B_{100} is translated, translocated and packaged into VLDL by a process differing from typical

secretory proteins. Normally, proteins translated on the rough endoplasmic reticulum (RER) membrane are translocated into the lumen of the RER co-translationally; however, apolipoprotein B_{100} which possesses a normal, albeit long, signal peptide appears to become associated with the endoplasmic reticulum either co-translationally or immediately post-translationally (30). It has been suggested that this abnormal association with the endoplasmic reticulum membrane may be due to information within the signal peptide (33). The result is that apolipoprotein B_{100} appears to have transmembrane topology with the endoplasmic reticulum and this may predispose the protein to degradation by cellular proteases and provide the basis for post-translational regulation of VLDL synthesis (30). When triacylglycerol and/or possibly cholesteryl ester is available, degradation of apolipoprotein B_{100} is reduced, and conversely elevated when lipid availability is reduced (30). This suggests that under conditions where VLDL synthesis is favorable, apolipoprotein B_{100} is protected from degradation and this is thought to occur through translocation into the lumen of the endoplasmic reticulum and co-ordinated lipid addition through a direct interaction with a microsomal transfer protein (MTP)/protein disulfide isomerase (PDI) heterodimeric complex (34) which appears to be obligatory for secretion (35,36). Further maturation of nascent VLDL may occur through fusion with a triacylglycerol-rich lipid droplet in what has been termed a "two step model" (37). Nascent VLDL, appears to be then secreted through the normal secretory protein pathway involving vesicular transport from the endoplasmic reticulum to the Golgi stacks where N-glycosylation, phophorylation and fatty acylation of apolipoprotein B in the nascent particle are thought to occur. The final steps are the formation of secretory vesicles from the *trans*-Golgi, fusion with the plasma membrane and release of

nascent VLDL into the circulation (13). Whether or not nascent VLDL is secreted with apolipoproteins in addition to apolipoprotein B or if they are provided by other lipoproteins like HDL, remains unclear. However, Dolphin *et al.* (16) have demonstrated that nascent rat hepatic VLDL acquires additional apolipoprotein E and all of the CII and CIII after secretion.

1.8 LDL metabolism

LDL, as previously discussed, is the metabolic product of the lipolysis of apolipoprotein B_{100} containing triacylglycerol-rich VLDL by lipoprotein lipase. In the process of lipolysis, the C apolipoproteins are lost and the lipoprotein becomes relatively enriched in apolipoprotein E (38). This apolipoprotein B_{100} VLDL remnant is referred to as IDL due to its floatation properties in the ultracentrifuge ($1.019<d<1.063$ density range). IDL is thought to be further metabolized by the action of hepatic lipase to LDL, with a resulting loss of apolipoprotein E to HDL, as mature LDL has an almost exclusive association with apolipoprotein B_{100} (see **Table 1.1**). LDL is the primary carrier of cholesterol in the form of cholesteryl ester to extrahepatic peripheral tissues and in humans, LDL levels correlate with atherosclerotic risk. Additionally in some species including humans, VLDL and LDL are further enriched in cholesteryl ester by the exchange of triacylglycerol for HDL cholesteryl ester by CETP (for a review see (39,40)). Whether or not CETP plays a role in atherosclerosis is still speculative as its function in humans seems contradictory, by both raising and maintaining LDL cholesteryl ester levels and being a participant "in reverse cholesterol transport". Interestingly, species lacking CETP, like rats, mice and also genetically CETP deficient humans (39,40), have

what are thought be anti-atherosclerotic lipoprotein profiles. However, species like the rat and mouse secrete a large proportion of apolipoprotein B_{48} containing VLDL and alterations in the distribution of lipoprotein species in their plasma may be due to the enhanced catabolism of apolipoprotein B_{48} VLDL remnants and concomitant reduction in LDL formation (4). It should be noted that *in vivo,* both VLDL and IDL may be taken up by receptor mediated endocytosis without conversion to LDL. Unlike chylomicrons, remnants, and apolipoprotein E rich VLDL and IDL, the LDL receptor is the primary pathway for apolipoprotein B mediated uptake of LDL into cells (4).

LDL is delivered to extra-hepatic tissues and the liver via the LDL receptor (41) and this process plays an important role in the maintenance of whole-body cholesterol homeostasis (42). After endocytosis of LDL, the particle is transferred to the lysosome where apolipoprotein B is degraded by lysosomal proteases, the cholesterol component is transferred into the hepatocellular cholesterol pool and the LDL receptor is recycled to the cell surface (41). Changes in cellular cholesterol levels are regulatory and influence anabolic and catabolic cholesterol modulating systems within the liver (42). In response to elevated cellular cholesterol, hydroxy methyl glutaryl CoA reductase (HMG CoA reductase) [E.C. 1.1.1.34] the rate limiting enzyme for cholesterol synthesis, hydroxy methyl glutaryl CoA synthetase (HMG CoA synthetase) [E.C. 4.1.3.5] and the LDL receptor are down regulated while ACAT is upregulated. Both the LDL receptor and HMG CoA reductase may be transcriptionally regulated in parallel due to the presence of nearly identical sterol regulatory elements (SRE). In addition HMG CoA reductase is regulated post-translationally by phosphorylation and by product level inhibition (41,43). Excess cholesterol may be esterified via ACAT (41) and/or excreted by conversion to bile

acids which is a catabolic pathway regulated by 7α hydroxylase (44).

1.9 "Reverse cholesterol transport" and HDL metabolism

As defined by Barter and Rye (7), "reverse cholesterol transport" can be broken down into four coordinated processes.

1. Efflux of cholesterol from a donor membrane to an acceptor particle in the extra-cellular fluid.
2. Esterification of cellular derived HDL cholesterol into cholesteryl ester by lecithin: cholesterol acyltransferase (LCAT) [E.C. 2.3.1.43]
3. In species having CETP, transfer of cholesteryl ester to VLDL and LDL
4. Delivery of cholesteryl esters back to the liver for catabolism or resecretion.

HDL levels have been found to be inversely correlated with risk of atherosclerosis (45,46). If the protective affect of HDL is due to its ability to return excess cholesterol from peripheral tissues to the liver for catabolism, the question arises, are all HDL particles equally able to facilitate "reverse cholesterol transport"? While there is not yet a conclusive answer, work by Fielding and Fielding (47) have implicated a small subfraction of HDL containing only apolipoprotein A-I (Lp-AI). Further resolution of this subfraction has identified at least 3 pre-β migrating Lp-AI HDL lipoproteins that appear to be the initial acceptors of cell derived free cholesterol and possibly percursors to the major α-migrating HDL fraction (11). Pre-β1 Lp-AI (one molecule A-I) HDL have been estimated to have a diameter of 50-60 Å and comprise 2-5% of total plasma HDL (6) with higher concentrations being found in peripheral lymph (48,49). Analysis of the 10-40% lipid associated with these particles further implicates them in early

association with the plasma membrane as their sphingomyelin:lecithin ratio more closely resembles outer-leaflet plasma membrane than α-HDL (6). Pre-β2 are disc shaped Lp-AI HDL particles that are thought to be the product of pre-β1 particles and by comparison to pre-β1 particles contain an increased lecithin content and more copies of apolipoprotien A-I (6,11). Like pre-β1, the concentration of these particles is increased within the lymph (48,49). A high molecular weight pre-β3 Lp-AI HDL particle has also been isolated in association with LCAT (12) and Fielding and Fielding (6) suggest this may be a pre-β2 HDL bound to LCAT. This may turn out to be the final intermediate particle prior to the conversion of lipid-poor pre-β HDL to spherical α-HDL by the action of LCAT.

There are three working models describing possible mechanisms for cholesterol efflux mediated by HDL, as outlined by Rothblat *et al.* (8). The best described has been termed "aqueous diffusion" (50) and envisions the diffusion of free cholesterol in the donor membrane to acceptor particles. The efficiency of the transfer depends upon the physical properties of the acceptor such as size, surface area and apolipoprotein content (50). Secondly, the HDL receptor mediated mobilization and desorbtion of cholesterol model as proposed by Oram (51,52), suggests that HDL binding to a putative HDL receptor (53) initiates a protein kinase C mediated cell signaling event resulting in the intracellular mobilization of cholesterol to the cell surface followed by efflux of free cholesterol to HDL (54,55). Thirdly and perhaps the least well documented proposal is that HDL in some cell types undergoes receptor mediated retroendocytosis that results in HDL internalization by the cells, followed by resecretion of intact cholesteryl ester enriched HDL (56). The physiological implications of this phenomenon to *in vivo*

cholesterol efflux remain to be determined.

Rothblat *et al.* (8) have combined the results of numerous cholesterol efflux studies and computer modeling to propose a working model to describe cholesterol efflux kinetics. The model was developed from these kinetics, accumulated evidence for cholesterol domains within membranes (57,58) and lipoprotein membrane interactions as described by Tabas and Tall (59) and Leblond and Marcel (60). Briefly, the model (8) predicts that cholesterol within the outer plasma membrane of cells contains cholesterol-poor and cholesterol-rich domains with cholesterol-rich domains being associated with increased sphingomyelin content. Contrary to what might be expected, the cholesterol-poor domains (fast pool) more readily provide cholesterol to acceptor particles due to enhanced interactions with the postulated lipid-binding hinge domain of apolipoprotein A-I, as described by Segrest *et al.* (61), whereas the cholesterol in the cholesterol-rich domain (slow pool) is much more organized and tightly packed. The resulting interaction of HDL with the cholesterol-poor domain would promote an apolipoprotein mediated and accelerated desorbtion of free cholesterol as compared to much slower diffusional efflux from the cholesterol-rich domain (8). This model is extremely attractive in light of Fielding and Fielding's (6) findings implicating the pre-β1 HDL subpopulation as the prime facilitators of efflux. Interestingly, Rothblat *et al.* (8) have suggested that the apparent intracellular mobilization of cholesterol observed by Oram (51,52) as a result of a possible cell signaling event is not incompatible with their model and could be triggered by interaction of the apolipoprotein hinge domain with the cell membrane. More recently, Fielding and Fielding (6) have suggested that pre-β HDL are involved in

cholesterol efflux from the cholesterol-poor domain in an LCAT dependent reaction that strongly implicates a specific cell signaling event, whereas efflux from the cholesterol-rich domain is diffusional to acceptor particles not thought to be major LCAT substrates, such as albumin, LDL and Lp AI/AII HDL. HDL cholesterol or HDL apolipoprotein A-I concentration may not be the best indicator of the capacity of HDL to mediate cholesterol efflux, as Fournier *et al.* (62) have demonstrated *in vitro* that cholesterol efflux mediated by TgR(hAI) rat HDL is best correlated with HDL phospholipid and not cholesterol or apolipoprotein A-I.

According to Fielding and Fielding's model (6) of "reverse cholesterol transport", sometime during the conversion of pre-β2 to pre-β3 and movement of the particle out of the extra-cellular space into the circulation, LCAT mediated esterification with the 3β-OH of cholesterol to the *sn-2* fatty acyl groups of phospholipid begins to occur. This results in the conversion of the HDL disc to a spherical α-HDL.

In rats and mice that lack CETP, the spherical HDL may increase in size, from a small spherical HDL_3 to HDL_2 through to HDL_1. Isolated HDL_1 is usually enriched in apolipoprotein E which is probably acquired through exchange with other lipoproteins. HDL_1 may eventually be taken up by the liver, either by the LDL receptor and/or the LDL receptor related protein and/or by some other poorly understood mechanism. Additionally, there is evidence in rats and steroidogenic cell lines that metabolize cholesterol, that HDL derived cholesteryl ester can be internalized without apolipoprotein A-I (63). Pittman, has termed this "selective uptake" (63). In humans and other species having CETP, newly formed cholesteryl ester may be transferred to VLDL and LDL

acceptor particles in exchange for triacylglycerol. Liang *et al.* (64) have also demonstrated that this process, as well as the action of hepatic lipase on HDL (65-67), may result in the creation of lipid-poor apolipoprotein A-I which presumably may be recycled into pre-β HDL by movement into the peripheral lymph or possibly cleared from the plasma by the kidney (68). Forte *et al.* (69) have shown that lipid-free apolipoprotein A-I when incubated with chinese hamster ovary (CHO) cells results in the formation of LCAT reactive discs. Czarnecka and Yokayama (70) have confirmed this and identified the discs as pre-β HDL. More recently, Von Eckardstein *et al.* (28) have shown that the phospholipid transfer protein (PLTP) may also generate pre-β1 HDL in the process of converting HDL_3 to HDL_2. While the lack of CETP certainly may contribute to the larger HDL observed in rat and mouse plasma, recent work in human apolipoprotein A-I transgenic mice (71,72) also indicates that mouse apolipoprotein A-I has a structural preference for forming larger HDL particles.

Uptake of HDL derived cholesteryl ester by the liver is not well understood, but as Barrans *et al.* (9) suggest, recent work (28,64-67) demonstrating the generation of pre-β1 HDL during the course of HDL remodelling may in part explain the phenomenom of "selective uptake of HDL cholesteryl esters". The possiblity that HDL apolipoprotein A-I is recycled may explain the disproportional mass of cholesteryl ester to apolipoprotein A-I observed to be cleared by the liver in these studies (63,73,74). Exciting new studies in transgenic mice (75) and rabbits (76) over-expressing human hepatic lipase further implicate this enzyme as having a role in the catabolism of HDL cholesterol. Furthermore, studies by Marques-Vidal *et al.* (77) have shown that uptake of

reconstituted HDL by the perfused liver may be dependent on the phospholipase A_1 activity of hepatic lipase. Perhaps in the future, hepatic lipase will be identified as a key component in facilitating HDL cholesterol uptake either through a hepatic HDL receptor or by some other novel endocytotic mechanism.

1.10 Abnormal lipoproteins in LCAT deficiency and liver disease

As outlined above, the liver plays a central role in the metabolism and provision of cholesterol to peripheral tissues; therefore, it is not surprising that alterations in liver function as a result of disease, drugs or surgical intervention will have a profound effect on lipoprotein metabolism. Interestingly, many similar alterations in lipoprotein metabolism are also observed in familial LCAT deficiency (78-81).

In the mid 19th century, Flint first reported the elevation of plasma "cholesterine" (cholesterol) in jaundiced patients (82). This was later confirmed by Widal *et al.* (83) and the increased cholesterol was identified as being primarily unesterified. As well, the increase in free cholesterol was found to be followed by an equi-molar increase in lecithin (84,85) which, as Miller (86) points out, are the primary substrates for the LCAT reaction (5,87).

The characteristic lipoproteins of liver disease have been comprehensively reviewed by Miller (86). Seidel *et al.* (88) have reported the presence of β migrating VLDL, which are characteristically rich in free cholesterol and phospholipid and depleted in triacylglycerol and cholesteryl ester (89). In some types of liver disease, triacylglycerol levels have been reported to be elevated (85,89,90) and studies in the bile-duct ligated rat suggest this may be due to reduced remnant catabolism (91). In the LDL

density range, up to 3 different particles (89,90,92) have been purified from human plasma in which LCAT activity was reduced (89), and these were a large triacylglycerol rich lipoprotein referred to as Lipoprotein Y (Lp-Y) (92), Lipoprotein X (Lp-X) and a 20 nm diameter LDL deficient in core cholesteryl esters. Lp-Y has been reported (89,90) to have a diameter of 100-300 nm and composition of 35% triacylglycerol, 20% cholesterol and 20% phospholipid with apolipoprotein B and the C apolipoproteins making up the 25% protein constituent. Muller *et al.* (90) have suggested that Lp-Y is formed as a result of hepatic lipase deficiency, while Agorastos *et al.* (89) found Lp-Y only when LCAT activity was low. Additionally, Felker *et al.* (93) have identified Lp-X-like vesicles and possibly Lp-Y in their studies of cholestatic (extrahepatic) perfused rat livers.

Lp-X is a vesicular lipoprotein that, unlike normal lipoproteins, contains an aqueous core and appears under the electron microscope as stacked discs of 30-70 nm length. Lp-X has been identified as having a composition of 3% triacylglycerol, 23% free cholesterol, 2% cholesteryl ester, 66% phospholipid and 6% protein (mainly C apolipoproteins and albumin) (94). Associated albumin may only be identified after lysis of the vesicle and this is evidence for albumin being trapped within the core of the vesicle. Additionally, Lp-X may form a heterogeneous population of particles as Patsch *et al.* (95) have purified 3 different Lp-X particles of increasing density, namely Lp-X_1, Lp-X_2 and Lp-X_3 from the ultacentrifuge with Lp-X_2 and Lp-X_3 being associated with apolipoproteins A-I and E.

A landmark study by Manzato *et al.* (96) demonstrated that bile micelles could be converted to Lp-X by the addition of albumin and this process could be reversed by the addition of bile salts to Lp-X. The presence of Lp-X in liver disease is usually correlated

with a deficiency of LCAT activity; however, there appear to be exceptions to this relationship in cases where the influx of biliary derived phospholipid and free cholesterol exceed the esterifying capacity of functioning LCAT (86). This appears to be the case in the α-naphthylisothiocyanate (ANIT) treated rat (97) as described in this thesis, bile-duct ligated dogs (98), some cases of human liver disease (99), following Intralipid™ administration where large amounts of lipolysis products are generated (100-103) and possibly in the bile-duct ligated rat (104,105). A similar effect has also been observed in familial LCAT deficient patients fed a high fat diet (106).

Whether or not Lp-X is a substrate for LCAT is not clear, Wengler and Seidel (107) could not demonstrate cholesterol esterification when Lp-X was incubated with semi-purified LCAT and this was confirmed by Utterman *et al.* (108). Patsch *et al.* (109) showed evidence of a small amount of Lp-X esterification after a 45 hour incubation of purified Lp-X and LCAT. However, a small amount of α-migrating material was identified following the incubation and this raises the probability that some apolipoprotein A-I may have been present in the Lp-X preparation. Indeed O and Frohlich (110) in a recent study have demonstrated that although LCAT will bind to Lp-X, significant esterification and size reduction of Lp-X will only occur in the presence of LCAT, apolipoprotein A-I and albumin. Unfortunately, this study did not fully investigate the role of apolipoprotein A-I in the reaction and the possibilty that HDL-like particles were generated. This result combined with the possibility that the LCAT and/or Lp-X preparations used by Patsch *et al.* (109) may have contained some apolipoprotein A-I are suggestive that apolipoprotein A-I may bind to Lp-X, activate LCAT and result in

apparent cholesteryl ester enrichment of Lp-X through the generation of an HDL-Lp-X complex. New HDL could disassociate and generate new α-HDL with an accompanying reduction in Lp-X size. Following LCAT mediated cholesteryl esterification, the characteristic cathodal migration of Lp-X was abolished in both of these studies (109,110). Anodal migration of Lp-X has been reported previously and a negative result on agar electrophoresis is not conclusive evidence against the presence of Lp-X (111,112). Additionally, Ritland *et al.* (38), have demonstrated that hepatic lipase may also play a role in the catabolism of Lp-X, as Lp-X in LCAT deficient patient's plasma was found to virtually disappear 10 minutes after the injection of heparin.

Whether or not Lp-X is cleared from the blood as a result of the indirect action of LCAT or by some other mechanism remains to be determined and is probably dependent upon whether LCAT and/or hepatic lipase is functional. This might be best accomplished *in vivo* in a reversible model of LCAT deficiency or cholestasis.

When Lp-X containing radiolabelled albumin was injected into normal rats, the majority of label was recovered in the liver with the spleen accumulating the most on a mass basis (113). Although Lp-X is thought to interact with the LDL receptor related protein (113) and inhibit the uptake of apolipoprotein B_{48} remnants (113,114), there is little evidence for its uptake by either this receptor or the LDL receptor (113,115). Possibly, this apparent receptor interaction may be due to binding of Lp-X to hepatic lipase.

Apolipoprotein A-I, the major HDL apolipoprotein, is often reduced in liver disease (88,116) and Seidel *et al.* (88) have postulated that this is due to decreased

binding of apolipoprotein A-I to cholesteryl ester depleted HDL and a resultant increase in apolipoprotein A-I catabolism. An analogous situation has been reported in familial LCAT deficiency (79) where decreased levels of apolipoprotein A-I have been shown to be associated with HDL discs having a diameter of 13-24 nm (117). As well, apolipoprotein E is usually observed to be increased in liver disease (116,118,119) and familial LCAT deficiency (79,120,121). This may be attributed to the lack of LCAT activity as the increased plasma apolipoprotein E content has been shown to be associated with large phospholipid and free cholesterol-rich HDL discs having a diameter of 14-40 nm (117).

1.11 Animal models of LCAT deficiency and liver disease

The study of abnormal lipoprotein metabolism in familial LCAT deficiency has provided insight into the importance of the LCAT reaction (5,87) in lipoprotein metabolism. Upon initiating this project, the initial question raised was why do most patients afflicted with genetic familial LCAT deficiency develop renal failure by their 4^{th}-5^{th} decade? Interestingly, the renal failure appears to be due to the development of atherosclerotic lesions characterized by deposition of osmophilic material in the glomeruli (subendothelial), basement membrane and mesangial regions (122). LCAT deficiency is also associated with corneal arcus, xanthoma, anemia and almost always proteinurea when renal insufficiency is present (79). The development of atherosclerosis in LCAT deficiency perhaps should not be surprising given the postulated role of LCAT in "reverse cholesterol transport"; however, even in the most serious cases of atherosclerosis due to hypercholesterolemia, renal atherosclerosis is usually not the

primary problem or cause of death. If the low levels of apolipoprotein A-I observed in LCAT deficiency are due to increased catabolism by the kidney, could this lead to renal lipid deposition? Current knowledge suggests that in order for this to happen, the apolipoprotein A-I being taken up by the kidney would need to have associated lipid, particularly cholesterol and phospholipid, and secondarily the plasma must have a very low capacity for returning lipid accumulated by the kidneys back to the plasma. In LCAT deficiency these criteria may possibly be met. The situation is further complicated by the proposal of Guérin *et al.* (79) that there may be a positive relationship between increased levels of Lp-X and the progression of renal dysfunction, a casual relationship that was first observed by Gjone *et al.* (123). Further evidence for the possible role of Lp-X in renal dysfunction comes from the observation of renal lipid deposition in dogs subjected to choledochocaval anastomosis (124).

In any case, this relationship has been difficult to study fully, due to the lack of a model of human familial LCAT deficiency that allows for the in depth study of the *in vivo* metabolism of the abnormal lipoproteins. The obvious model of choice would be an inexpensive animal that has genetic LCAT deficiency, either through a naturally occurring mutation, artificially induced by homologous recombination in stem cells (LCAT knockout) or possibly by gene therapy. The other ideal characteristic would be that the animal have a human-like lipoprotein metabolism (as discussed earlier). Unfortunately, this model does not exist, although an LCAT knockout mouse has very recently been produced. The phenotypic details however, have not been published to date. The LCAT knockout mouse by itself or in combination with some of the many mouse transgenics currently available offer many exciting research possibilities in the

future (transgenic mouse models of human lipoprotein metabolism have been reviewed in (125,126)). The next choice for an *in vivo* model would be one with a transient and artificially induced LCAT deficiency either by injection of a specific LCAT inhibitor or inhibitory antibody. However, to date, a specific *in vivo* inhibitor of LCAT has not been identified and the feasibility of using antibodies to inhibit LCAT has not been examined. Perhaps the next best option would be a model of secondary LCAT deficiency as the result of liver disease.

1.12 Experimental rationale

Initial studies as described in this thesis, were performed in the D-(+) galactosamine rat which is a transient and reversible model of hepatitis associated with a secondary LCAT deficiency and decreased plasma cholesteryl ester (127). *In vivo*, D-(+) galactosamine exerts its hepatotoxic effect by sequestering cellular UDP (uridyl diphosphate) and as such would be expected to have deleterious affects on cellular processes dependent on glycosylation. For these reasons and from interpretation of preliminary results that will be shown in this thesis, studies in the D-(+) galactosamine rat were discontinued.

This decision made, the apparent relationship between LCAT deficiency and

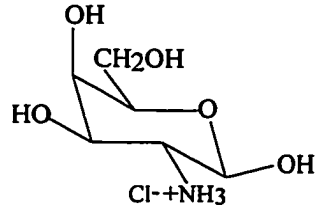

Figure 1.2- The molecular structure of D-(+) galactosamine HCl

some types of cholestasis was recognized and the ANIT (α-naphthylisothiocyanate) treated rat was identified as a possible candidate animal model. As described below, the pathological effects of ANIT treatment have been intensively studied, but little has been done to examine the alterations in lipoprotein metabolism as a result of ANIT-induced cholestasis. Therefore, the focus of this thesis research was firstly to investigate the changes in lipoprotein metabolism in the rat following ANIT treatment and evaluate the potential application of the model to the study of LCAT deficiency. Secondly, in collaboration with Dr. Lou Agellon at the University of Alberta, to extend these studies into the mouse with an added emphasize on the regulation of bile acid metabolism. The final focus of the thesis work was to extend the ANIT treated rat model into transgenic rats which over express human apolipoprotein A-I and investigate the role of apolipoprotein A-I in the metabolism of cholestatic lipoproteins.

1.13 ANIT-induced intrahepatic cholestasis

A single dose of ANIT (α–naphthylisothiocyanate) (**Figure 1.3**) when given by gavage to rats (128,129), mice (129), and guinea pigs, (129) produces a transient intrahepatic cholestasis (128,130), necrosis of the bile-duct endothelium and areas of focal injury to the hepatocytes in periportal areas of the liver (131-133). ANIT does not appear to produce cholestasis in hamsters and rabbits (129).

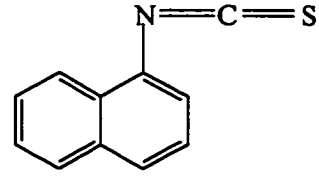

Figure 1.3- The molecular structure of ANIT (α-naphthylisothiocyanate)

The pharmacological action of ANIT remains unclear, but appears to be related to effects of the drug directly upon the hepatocytes and not bile canalicular cells (130). ANIT is thought to be bioactivated by cytochrome P-450 dependent mixed function oxidases (134-136) and/or "fusion" to hepatic glutathione (137). This theory is largely based on observations showing that induction of NADPH dependent cytochrome P-450 mixed function oxidases by phenobarbital increased ANIT hepatotoxicity, while inhibition of mixed function oxidase activity by SKF 525-A (diethylaminoethyl-2,2-diphenylvalerate) reduced the effect of ANIT (134). More recently, Traiger *et al.* (135,136) have shown using rat liver microsomes that ANIT bioactivation may involve *S*-oxidation mediated by cytochrome P-450 dependent mixed function oxidases leading to desulphation of ANIT. Bioactivation of ANIT is further supported by radioactive tracer studies showing that intact ANIT is not secreted into the urine of animals (129) and by a correlation between *in vivo* hepatotoxicity and ^{35}S sulfate excretion, both of which were dependent on cytochrome P-450 dependent mixed function oxidase activity (136). Species-specific effects of ANIT may be the result of differences in the biotransformation of ANIT and the action of metabolites on hepatocytes (129). In ANIT treated animals, microsomal mixed function and cytochrome P-450 oxidase activities have been shown to be decreased (138,139) together with their drug-metabolizing activities (138-140). Kosser *et al.* (133) have suggested that the onset of ANIT-induced cholestasis is biphasic. Initially changes in hepatocanicular function and increased tight junction permeability are observed and these are followed by bile-duct obstruction and hepatocellular dysfunction. The second phase appears to begin with near complete cessation of bile flow between 16 and 24 hours (128,133) which is followed by increased levels of bile components within

the plasma compartment possibly due to leakage through tight cell junctions (141). Maximal plasma concentrations of bile acids (128,133) are observed by 24 hours (128,138,139), while conjugated bilirubin (142,143) and liver enzymes are maximally elevated by 48 hours (138,139). These abnormal plasma levels return to near normal by 96 hours (138).

In rats, Schaffner *et al.* (139), examined hepatic bile acid composition (**Table 1.2**) and found an approximately 2.5 fold increase in liver bile acid concentration. Overall the precentage composition of cholic acid (3α, 7α, 12α hydroxy bile acid) remained unchanged while β-murocholic acid (3α, 6β, 7β hydroxy bile acid) increased from approximately 10% to 46% becoming the major secondary hepatic bile acid. On the basis of these results, they suggested that there was a defect in rat bile acid metabolism favoring the production of trihydroxy bile acids instead of more lithogenic bile acid species which would have significant detergent properties and be conceivably more

Table 1.2- Liver bile acid composition data in normal and ANIT-treated (48 h) rats
Data reprinted from Schaffner *et al.* (139).

Bile Acid	OH Groups	Normal[a]	ANIT (48 h)[b]	Normal[c]	ANIT (48 h)[c]
		nmol/g liver	*nmol/g liver*		
Lithocholic	3α	Trace	Trace	Trace	Trace
Deoxycholic	3α 12α	22±10	Trace	13%	Trace
Chenodeoxycholic	3α 7α	21±8	Trace	12%	Trace
Hyodeoxycholic	3α 6α	12±12	Trace	7%	Trace
Ursodeoxycholic	3α 7β	Trace	Trace	Trace	Trace
Cholic	3α 7α 12α	97±19	195-249	57%	54%
β–muricholic	3α 6β 7β	17±8	154-219	10%	46%

[a] n=7
[b] n=3
[c] Percentage composition calculated from original data

damaging in cholestasis.

Changes in plasma lipoproteins resulting from ANIT-induced cholestasis have not been extensively studied. Katterman and Wolfrum (144) have shown that ANIT treatment results in increased plasma free cholesterol and a decreased CE/FC ratio in the presence of increased LCAT activity. In the liver, both free and esterified cholesterol were elevated, but in contrast to plasma the CE/FC ratio was increased. This suggests that ANIT-induced intrahepatic cholestasis, like extrahepatic cholestasis in the rat, occurs under conditions were liver cholesterogenesis is upregulated (113,145). More recently, Mitamura (146) was able to demonstrate that ANIT induced cholestasis resulted in large elevations of plasma phospholipid and free cholesterol, smaller increases in cholesteryl ester, little change in triacylglycerols and the presence of phospholipid-rich HDL.

1.14 Human transgenic apolipoprotein A-I rats (TgR[HuAI] rats)

Transgenic rats expressing the human apolipoprotein A-I gene were developed by Swanson *et al.* (147) using the 13 kbp construct shown in **Figure 1.4.** The authors included an extra 10 kbp of the 5' flanking region of the human apoplipoprotein gene in an attempt to get intestinal promotion of the transgene. This was not achieved as the intestinal promoter was not present in the construct. The promoter has recently been localized to 3' region of the apolipoprotein A-I gene and within the 5' promoter region of the apolipoprotein C-III gene (15,148). Transgenic rats generated from this construct were found to have high levels of human apolipoprotein A-I gene expression in the liver and immunologicaly measurable human apolipoprotein A-I in their serum (147).

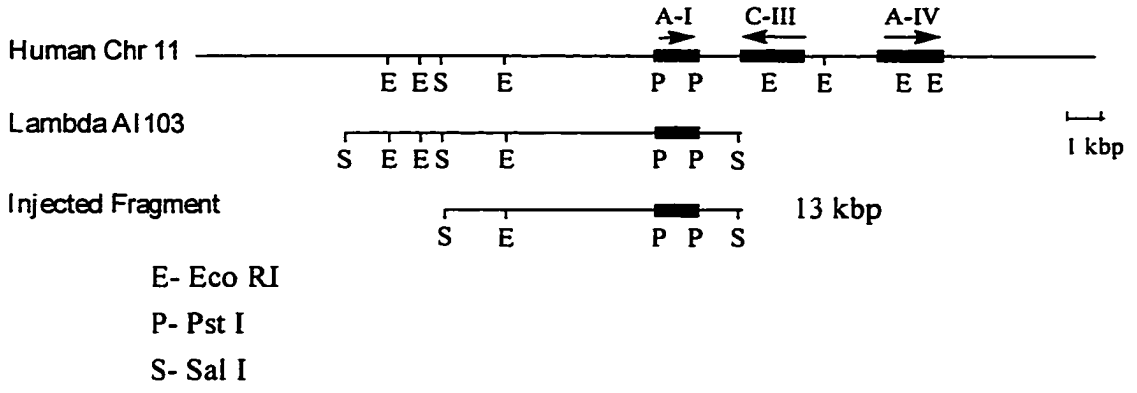

Figure 1.4- Human apolipoprotein A-I DNA construct used for production of TgR[HuAI] rats
Adapted from Swanson *et al.* (147).

Initial analysis of the high line rats (TgR[HuAI]) demonstrated plasma human apolipoprotein A-I levels ranging from 500-1000 mg/dl and endogenous rat apolipoprotein A-I levels ranging from 42 mg/dl to 0 mg/dl. The lower levels of endogenous rat apolipoprotein A-I were found in those rats expressing the most human apolipoprotein A-I. This inverse relationship has also been reported in human apolipoprotein A-I transgenic mice (71).

Swanson *et al.* (147) also observed by Superose 6B gel filtration that increased plasma concentrations of apolipoprotein A-I were associated with increased levels of HDL but not qualitative changes in HDL size. Further analysis of TgR[HuAI] rat HDL by non-denaturing electrophoresis clearly showed that there were major alterations in HDL composition due to expression of the transgene, as polydispersity in the HDL region was clearly evident (149). This finding has been previously reported in human

apolipoprotein A-I transgenic mice (72). In these mice, HDL particles of 11.4, 10.2 and 8.7 nm corresponding to HDL_1, HDL_2 and HDL_3 were observed in comparison to a monodisperse HDL characterized by a 10 nm particle in non-transgenic mice. Further, analysis of the distribution of rat and human apolipoprotein A-I in HDL and the d>1.21 g/ml fraction of rat plasma has indicated that human apolipoprotein A-I preferentially binds HDL over rat apolipoprotein A-I (149). Similar observations have been observed in apolipoprotein A-I transgenic mice (71,72) and it has been suggested this may account for the inverse relation between human and rodent apolipoprotein A-I (62,150) and be a result of structural differences between the two apolipoproteins (72,151). Additionally, a very recent study of experimental nephrosis in the TgR[HuAI] rats found that transgenic rats in comparison to control rats did not accumulate HDL lipids as a result of nephrosis and the authors attributed this to enhanced filtration of an 8.2 nm member of the polydisperse transgenic HDL over the 11 nm particles identified in non-transgenics (150).

In human apolipoprotein A-I transgenic mice, enhanced expression of human apolipoprotein A-I has been observed to prevent or diminish atherosclerosis in a number of atherosclerotic mouse models (38,152-155). Since overexpression of human apolipoprotein A-I appears to have anti-atherosclerotic properties in mice it was hypothesized that overexpression of human apolipoprotein A-I in the rat might prevent some of the lipid accumulation observed in the ANIT-treated rat and give insight into the role of apolipoprotein A-I in the metabolism of cholestastic lipoproteins. As a result, the effect of ANIT on TgR[HuAI] rats was investigated.

1.15 7α-hydroxylase regulation and bile acid metabolism

A crucial step in the maintenance of cholesterol homeostasis is excretion of cholesterol and the liver through bile acid synthesis is the major facilitator of this process. The conversion of cholesterol to bile acids requires at least 14 enzymes and is regulated at the first committed step (44). The enzyme responsible is cholesterol 7α-hydroxylase [E.C. 1.14.13.17] which is a member of the cytochrome P-450 enzyme family and a product of the cyp7 gene. Transcription and translation of the gene give rise to a 503 and 504 amino acid protein in rat and human respectively. The enzymatic conversion of cholesterol to 7α-hydroxy cholesterol occurs in the endoplasmic reticulum and requires molecular oxygen, NADPH and cytochrome P-450 reductase (44). The further conversion of 7α-hydroxy cholesterol to primary bile acids has been reviewed (44,156) and consists of at least 14 separate steps in varying cellular locations including side chain oxidation in the peroxisome (157) by a process similar to β-oxidation of fatty acids (158). The final step in primary bile acid synthesis is conjugation of the bile acid to either glycine or taurine which most likely takes place in the peroxisome (159). In the human, hamster and rat the major primary bile acids are cholic and chenodeoxycholic acids (160). The water soluble aminoacyl bile acids are secreted by the liver into the common bile duct (161) and stored in the gallbladder (humans) until released by hormonal stimulation into the duodenum (162).

The co-secretion of cholesterol and phospholipid is not well understood and a number of hypothesis exist (163) including co-transport of cholesterol, phospholipid and bile, as well as bile micelle mediated efflux of membrane cholesterol and phospholipid.

It is apparent however, that the detergent abilities (hydrophobicity) and bile acid concentration influence biliary lipid secretion (164,165). In the case of phospholipid, it is becoming increasingly clear that a p-glycoprotein phosphatidylcholine transporter/flippase encoded by the mdr2 gene is essential for phosphatidylcholine secretion and may function by translocating phosphatidylcholine from the inner to outer cannicular membrane leaflet (165). Secretion into the duodenum aids in the solubilization and absorption of dietary fats, cholesterol and hydrophobic nutrients by the enterocytes. Additionally, the actions of bacterial enzymes in the intestine give rise to the many secondary and tertiary bile acids identified in mammals (44). Bile acids in addition to biliary cholesterol and phospholipid become mixed with dietary cholesterol and the majority are absorbed by the intestine. This appears to serve as a very efficient mechanism for the conservation of both cholesterol and bile acids. Absorption or rather reabsorption of bile acids in the ileum may occur via nonionic diffusion or active transport (44) with the latter being via the ileal sodium-dependent bile acid transporter (166). These bile acids may then travel via the circulatory system back to the liver where they are reabsorbed possibly by a sodium dependent transporter or other candidate transporters (167) and resecreted into bile (168).

Much of the information on the regulation of bile acid synthesis and 7α-hydroxylase comes from studies performed in the rat. Due to the absence of a gallbladder and the unusually long small intestine that results in high levels of bile acid biosynthesis (169), the rat as a model of human bile acid metabolism has been criticized. Furthermore, unlike humans, cyp7 in the rat is only responsive to negative feedback control by

hydrophobic and not hydrophilic bile acids (170-172). 7α-hydroxylase is thought to be almost exclusively regulated at the level of cyp7 gene transcription, as message, protein mass and activity always correlate (44). The cyp7 gene is repressed by bile acids, diurnal rhythm (light), starvation, and glucocorticoids and derepressed by intestinal bile acid binding resins, cholesterol, diurnal rhythm (dark) and thyroid hormone (44). The putative transcriptional inhibition by bile and activation by cholesterol has led to the suggestion that cyp7 may be coordinately regulated by both a bile acid responsive element (BARE) and a modified sterol responsive element (SRE) (44,173). The modified SRE would activate transcription unlike the inhibitory SRE involved in the regulation of cholesterol synthesis and LDL receptor regulation (41).

The possible alterations in bile acid metabolism resulting from ANIT-induced intrahepatic cholestasis in the rat or mouse, have never been investigated. Since the rat may not be the best model for study of bile acid metabolism for reasons already mentioned, an investigation in the ANIT-treated mouse was undertaken. This project has two components, firstly to characterize the abnormal lipoproteins in the ANIT-treated mouse and secondly in collaboration with Dr. Lou Agellon at the University of Alberta to study cyp7 regulation and cholesterol homeostasis in the ANIT-treated mouse liver.

Chapter 2- Materials and Methods

2.1 Animals

2.1.1 NORMAL RATS

Female Spraque Dawley rats (Charles River Laboratories) (225-275 g) were used for all normal rat experiments. Rats were pair fed regular rat chow, given water *ad libetum*, housed under 12 hour light/dark conditions and fasted for 12 hours prior to treatment. Rats were lightly anesthetized by intraperitoneal administration of Ketamine/Xylazine (3%/0.37% w/v) at a dosage of 0.8-1.0 ml/kg and given either 100 mg/kg ANIT (Sigma) in 25 mg/ml corn oil (Mazola) or 150 mg/kg ANIT (Sigma) in 30 mg/ml corn oil (Mazola) by gavage. Control rats received a similar amount of corn oil by weight. At the indicated experimental time points, fasted rats were deeply anesthetized by an intraperitoneal injection of Ketamine/Xylazine 2.0-2.5 ml/kg and blood was collected from the descending aorta into tubes containing Na_2EDTA to a final concentration of 1 mg/ml. For post-heparin plasma collection, blood was collected from fasted anesthetized rats 8 minutes after an intrajugular injection of 100 U/kg sterile heparin (Sigma) saline solution (150 U/ml, pH 7.4). Plasma was isolated by centrifugation at 3000 x g for 30 minutes at 4 °C. A preservative cocktail containing thimerosal (Sigma, St. Louis, MO), aprotinin (Sigma), Na_2EDTA, and sodium azide was added to yield respective final concentrations of 0.005%, 0.001%, 0.01% and 0.02%.

2.1.2 TRANSGENIC RATS (TGR[HUAI])

TgR[HuAI] rats were received from Sandoz Pharmaceuticals as a gift through Dr. Jim Paterniti (currently employed with Ligand Pharmaceuticals, California) in the wake of the closing of the Cardiovascular Research Division at Sandoz. All TgR[HuAI] rats used in this study were bred in-house and identified phenotypically by measurement of human apolipoprotein A-I levels by immunoelectrophoresis or immunoturbidometrically by nephelometry. Preliminary identification was performed on a 0.5-1.0 ml blood sample obtained from the jugular vein under Ketamine/Xylazine (3%/0.37% w/v) anesthesia at a dosage of 1.5-2 ml/kg. To minimize the effects of dehydration, rats sampled in this way were routinely administered 5-10 ml of sterile saline subcutaneously. In some cases it was possible to identify rats genotypically after breeding.

Experimentally, transgenic rats used in these studies were treated using the same protocol as for normal Spraque Dawley rats, with the exception that rats were chosen for experiments based primarily on their human apolipoprotein A-I levels and secondly their sex and weight. This was necessary to keep animal costs to a minimum.

2.1.3 C57BL/6 MICE

Female C57BL/6 mice (Charles River Laboratories) (16-20 g) were used for all mouse studies. Mice were group fed (4-6) regular rat chow, given water *ad libetum,* housed under 12 hour light/dark conditions and fasted for 8-10 hours prior to ANIT treatment. Mice were lightly anesthetized by intraperitoneal administration of Ketamine/Xylazine (2%/0.4% w/v) at a dosage of 1-1.5 ml/kg and given 100 mg/kg

ANIT (Sigma) in a 10 mg/ml corn oil (Mazola) bolus by gavage. Control mice received a similar amount of corn oil by weight. At the indicated experimental time points, fasted mice were deeply anesthetized by an intraperitoneal injection of Ketamine/Xylazine (2%/0.4% w/v) at a dosage of 2-3 ml/kg and blood was collected from the descending aorta into tubes containing Na_2EDTA to a final concentration of 1 mg/ml.

For some experiments, the gallbladder and mouse livers were immediately excised, washed in saline, and the liver was dissected into 4-5 sections. Each section was weighed and immediately frozen in liquid N_2 and stored at -80 °C or room temperature in phosphate buffered formalin. Frozen sections were used either for liver lipid analysis (174) after lipid extraction (175) or sent on dry ice to Dr. Lou Agellon at the University of Alberta for analysis of 7α-hydroxylase (cyp7 gene product) [E.C. 1.14.13.17] and/or HMG CoA reductase [E.C. 1.1.1.88] activity and mRNA levels. Formalin preserved liver samples were sent to Dr. Lou Agellon at room temperature for histological and pathological examination. For intestinal bile acid transporter analysis, an intestinal section was excised leading from the cecum until almost halfway to the stomach (approx. 10 cm). The section was cannulated, washed with saline, weighed and frozen immediately in liquid N_2, and shipped to the University of Alberta for analysis. Excised gallbladders were washed in saline, placed in 1.5 ml microfuge tubes, and spun to the bottom of the tube by pulse centrifugation in a microfuge (Beckman). The contents of the gallbladders were removed using 25 µl capilliary micropipettes and placed in 400 µl microfuge tubes which were quick frozen in liquid N_2 and stored at -80 °C. Plasma was isolated by centrifugation at 3000 x g for 30 minutes at 4 °C. A preservative cocktail

containing thimerosal (Sigma), aprotinin (Sigma), Na_2EDTA, and sodium azide was added to yield respective final concentrations of 0.005%, 0.001%, 0.01% and 0.02%.

2.2 Enzymatic and lipid analysis

Aspartate aminotransferase (E.C. 2.6.1.1), alanine aminotransferase (E.C. 2.6.1.2), alkaline phosphatase (E.C. 3.1.3.1), bilirubin and bile acids were measured manually using commercial kits (Boehringer Mannheim and Sigma). Initial analysis of rat aminotransferase activities were performed by kinetic methods (Boehringer Mannheim) and latterly in mice using a colorimetric endpoint method (Sigma) optimized to give results comparable to the kinetic methodology. Total cholesterol, free cholesterol, triacylglycerols and phospholipids were measured either directly by enzyme kits (Boehringer Mannheim) or by gas chromatographic total lipid profiling (174). When enzyme kits were employed, cholesteryl ester mass was calculated from total cholesterol and free cholesterol by mole subtraction using an average rat cholesteryl ester molecular weight of 660 g/mol. All plasma samples were measured by gas chromatographic total lipid profiling, as an unidentified component of plasma from ANIT-treated rats completely inhibited the choline oxidase method of phospholipid determination used in the enzymatic kits. The enzymatic inhibition was not present in the lipoprotein positive fractions of plasma from treated rats after ultracentrifugation, suggesting that the unknown inhibitor was associated with the lipoprotein free (d_{15}> 1.21 g/ml) plasma component.

2.3 LCAT activity assays

LCAT activity was measured in early work using the exogenous synthetic proteoliposome substrate method of Chen and Albers (176) as previously described by Jauiainen and Dolphin (87) and latterly using the exogenous recombinant HDL (rHDL) method of Sparks *et al.* (177).

The rHDL, 80:10:0:1 phosphadityl choline:free cholesterol:cholesteryl ester:protein substrate of Sparks *et al.* (177) was prepared by reducing to dryness 56 µl of 20 mg/ml 1,2-di[cis-9-octodecanoyl] *sn* glycero-3-phosphocholine (DOPC), 34 µl of 2 mg/ml cholesterol (Sigma 99.9+%) in hexane and 12 µCi (12 µl) fresh [1,2-^{3}H]-cholesterol (Dupont- NEN) in a screw top culture tube under N_2 without heating. The resulting lipid film was dispersed by vortexing at room temperature in TBS (10 mM Tris-HCl, 140 mM NaCl, 1mM Na_2EDTA, 0.01% NaN_3, pH 8.0). To the resulting emulsion, 28 µl of 30 mg/ml sodium cholate (Sigma) in TBS pH 8.0 was added and vortexed for 3 minutes prior to incubation at 37 °C on an orbital shaker for 3 hours. To insure adequate mixing and optimal micelle formation, the solution was vortexed every 15-30 minutes on high for 30 seconds and then centrifuged in a clinical tabletop centrifuge to collect the sample. To this micellar solution, 0.5 mg of previously purified human apolipoprotein A-I (87) was added in a total volume of 600 µl TBS pH 8.0 and incubated by gentle inversion on a mechanical inverter for 1 hour at 37 °C. The bile acids were removed by aspirating the apolipoprotein A-I micellar solution into a 3 ml luerlok™ syringe (BDH) containing 0.6 g of prepared Biobeads (see **Appendix A**). The syringe was capped with a 0.45 µm syringe filter (Gelman Supor Acrodisc 13, Cat #54604) and the syringe plunger

pulled back to the 3.0 ml stop. The syringe was capped with parafilm and inverted on a mechanical inverter for at least 3 hours at 4 °C to facilitate cholate removal. The resulting rHDL solution was then expelled through the syringe filter and residual rHDL solution was washed out of the syringe and filter with 100 ul of cold TBS pH 8.0. The resulting rHDL solution was then assayed for protein concentration by the modified BCA method (as described under protein mass analysis) and the volume adjusted with TBS 8.0 to give a final concentration of 20 μg apolipoprotein A-I per 100μl and a lipid/ A-I ratio of 90:1.

Exogenous LCAT activity was measured by combining 200 μl of Tris pH 8.0, 100 μl of rHDL substrate solution and 125 μl of 2% fatty acid free BSA (Sigma) in a teflon stoppered culture tube and incubating for 15 minutes in a shaking water bath. To each tube, 25 μl of 10 mM β-mercaptoethanol was added in addition to 25-50 μl of plasma in a total volume of 50 μl. The tubes were then mixed by gentle vortexing and incubated at 37 °C in a shaking water bath for exactly 15 minutes. The reaction was stopped by the addition of 2 ml of absolute ethanol and vortexing. To extract the lipids, 4.0 ml of hexane containing 100 μg/ml cholesterol (Sigma) and 50 μg/ml cholesterol oleate (Sigma) was added. The tube was then vortexed and centrifuged for 10 minutes in a clinical centrifuge to separate the organic and aqueous phases. The upper organic phase was removed by aspiration, placed in a screw top culture tube and reduced to dryness under N_2 at 37 °C. The lipid residue was redissolved in 200 μl of chloroform (BDH) and 50 μl was spotted on a preactivated TLC (thin layer chromatography) plate (see **Appendix A)** and allowed to dry, prior to being developed for approximately 15 minutes

in 90:10:1 hexane:diethyl ether: glacial acetic acid. Inclusion of H_2O in this TLC system should be avoided as small amounts have deleterious affect upon the lipid class separation. Once the solvent front reached the top of the plate, the plate was removed, the solvent allowed to evaporate and the cholesteryl ester and free cholesterol bands identified by reversible iodination in I_2 vapor. The bands were marked with pencil and to avoid I_2 quenching during [^{3}H] counting the I_2 was allowed to sublime. The marked bands were then cut out of the plate and dissolved in 20 ml of scintillation cocktail (Ready Safe, Beckman) and the β-emissions of ^{3}H counted for 10 minutes in a scintillation counter (Beckman). LCAT activity was then calculated by the following equation:

Activity (nmol CE formed $ml^{-1}h^{-1}$) =

$$\frac{(\textbf{CPM}\text{ CE spot} - \textbf{CPM}\text{ CE spot Blank}) \times \mathbf{40}\ [40 \times 25\mu l\ plasma = 1ml] \times \mathbf{4}\ [15\ min \times 4 = 1\ h]}{(\textbf{CPM}\text{ of FC spot} + \text{CE spot})\ /(\mathbf{8.9}\text{ nmol FC in } 100\ \mu l\text{ substrate})}$$

2.4 Triacylglycerol lipase activity assays

Plasma triacylglycerol lipase activities were measured by the method of Jackson and MacLean (178). The assay was performed on the day of plasma collection and all samples were determined in triplicate. To ensure endogenous apolipoprotein C-II was not limiting in samples, pooled rat plasma was heat-inactivated at 62 °C for 10 minutes to denature lipases (179) and 20% v/v was added to control and total lipase sample tubes as a source of apolipoprotein C-II. Hepatic triacylglycerol lipase was measured in the presence of 1 M NaCl to inhibit lipoprotein lipase. Lipoprotein lipase activity was calculated as the difference between total lipase and hepatic triacylglycerol lipase activities.

2.5 Immunoassay of plasma apolipoproteins

Rat plasma samples were assayed for rat apolipoproteins B, E and A-I by a slight modification of the electroimmunoassay described by Krul and Dolphin (180). In the modified assay, the barbital buffer system was replaced with a Tris-Tricine buffer pH 8.3 (80 mM Tris HCl, 24 mM Tricine). Apolipoprotein A-I in TgR[HuAI] rats was assayed by a similarly modified electroimmunoassay (181) or immunoturbidometrically by nephelometry (Behring clinical autoanalyzer).

2.6 Density gradient ultracentrifugation

Rat plasma samples to be analyzed by density gradient ultracentrifugation were

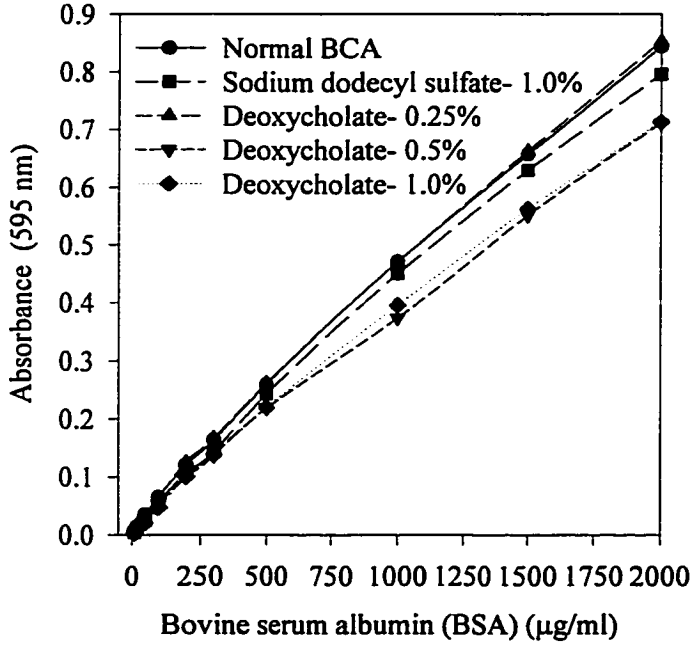

Figure 2.1- The effect of added detergents on the absorbance of a BSA standard curve BCA reagent was prepared at a ratio of 50:1 reagent B:reagent A and 1 part H_2O or detergent was added to yield a final detergent concentration as shown.

processed on the afternoon of plasma collection by the method of Chapman *et al.* (182). Sample tubes were centrifuged in an SW-41 rotor (Beckman) at 15 °C for 44 hours at 40,000 rpm. Completed gradients were fractionated manually into 400 µl fractions using a Gilson micropipette and stored for further analysis.

2.7 Protein mass analysis

Protein mass in gradient fractions was measured by a sodium dodecyl sulfate-modified Lowry procedure (183) and using the BCA protein assay (Pierce) modified by the addition of 0.25% deoxycholate. Bovine serum albumin (BSA) (Sigma or Pierce) was used as a standard. The Lowry assay was replaced by the BCA assay due to

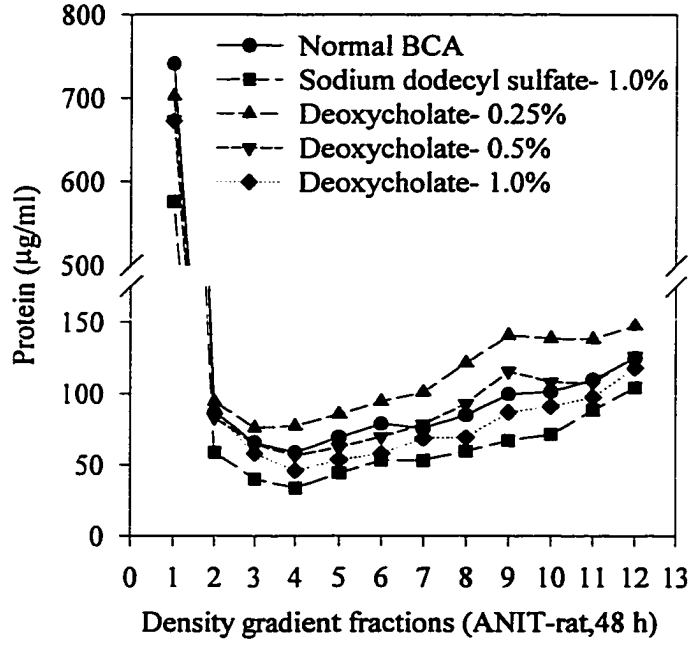

Figure 2.2- Effect of detergents in the BCA assay on protein recovery
Density gradient ultracentrifugation fractions 1-12 from an ANIT treated rat (100 mg/kg) were analysed in the presence of detergents and the protein concentrations interpolated against Bovine serum albumin standards run under indentical detergent conditions.

interfering substances in some samples that led to the formation of precipitin complexes and a resulting turbidity. The BCA assay also has the advantage of being relatively linear over a wide concentration range (0-2000 μg/ml) and can be performed on microtitre plates. The BCA reagent was prepared by mixing 50:1 reagent A: reagent B plus 1.25 parts of 10.5% deoxycholate to yield a final reagent containing approximately 0.25% deoxycholate. The assay consisted of incubating 200 μl of BCA reagent with 10-50 μl (10 μl for standards) of sample for 1-1.5 hours. The microplate was then read on a microplate reader (Biorad) at 595 or preferably 562 nm and sample protein concentrations calculated by interpolation form the standard curve. Differences in absorbances due to sample volumes were normalized to 10 μl using Beer's Law.

During initial evaluation of the assay, 0.25% deoxycholate was found not to alter the absorbance of a BSA standard curve ranging from 0-2000 μg/ml (**Figure 2.1**) and enhance the recovery of protein in lipid-rich lipoprotein fractions (**Figure 2.2**) when compared to the normal BCA reagent and several other detergent conditions.

2.8 Electrophoresis under denaturing conditions

Sodium dodecyl sulfate polyacrylamide 5-19% gradient gel electrophoresis of density gradient ultracentrifugation fractions 1-24 or chromatographically purified lipoproteins was performed by a modification of the method of Irwin *et al.* (184). The samples (50 μl) were loaded onto the 5-19% gradient gels together with broad range molecular weight standards (Bio-Rad) and run at 3-3.5 mA/gel (10 °C) until the bromophenol blue just began to exit the gel (approx. 3.5 h). Gels were then stained overnight with 0.1% Coomassie Blue R-250 (Fisher Scientific) in 50% methanol and

10% acetic acid. Gels were destained with the stain solution less Coomassie Blue R-250 (Fisher) and then photographed and/or scanned.

2.9 Non-denaturing electrophoresis

Non-denaturing 2.5-16% and 4-30% polyacrylamide gradient gels used for early anlaysis were prepared using the formulation of Asztalos *et al.* (185) that was adapted for use in an 18 cm long Bio-Rad Protein II apparatus. Due to problems with consistency between gel preparations, chromatographically purified lipoproteins (chapter 5) were run on commercial 2-16 and 4-30 PAA gels (Isolab) as described by Nichols *et al.* (186). The loaded gels were run at 125 volts for 24 hours before Coomassie Blue R-250 (Fisher) staining and in some cases were subsequently lipid stained with 0.2% Sudan Black (Fisher) in 60% ethanol. To aid in the quantification of particle sizes, high molecular weight standards (Pharmacia) of known particle diameter were run concurrently and particle diameters were estimated using a second order linear regression equation of R_f vs. Log (particle diameter). The gels were photographed and/or scanned.

2.11 Purification of lipoprotein particles

Fresh rat plasma (2.5-4.0 ml) was adjusted to d_{15}=1.21 g/ml by the addition of dry solid KBr and mixed by inversion at 4 °C. The plasma was then overlayered by a d_{15}=1.21 g/ml KBr solution containing 0.01% Na_2EDTA, 0.01% NaN_3 and 0.05% Gentamicin and spun in a Ti 50.3 rotor (Beckman) for 25 hours at 50,000 rpm (179,760 x g). The top d_{15}<1.21 g/ml lipoprotein fraction (1-2 ml) was collected by tube slicing and the free cholesterol and cholesteryl ester composition was determined enzymatically.

Two or more ANIT-treated or control rats having a similiar free cholesterol and cholesteryl ester composition were pooled for Heparin-Sepharose affinity chromatography.

2.11.1 HEPARIN-SEPHAROSE CL-6B AFFINITY CHROMATOGRAPHY

The methodology used was slightly modified from that described by Weisgraber and Mahley (187). The crude d_{15}<1.21 g/ml lipoprotein samples were dialyzed against pre-chromatography dialysis buffer (5 mM Tris-HCl, pH 7.4, 25 mM NaCl and 0.02% NaN_3) overnight (10- 12 h) with 2 buffer changes prior to Heparin-Sepharose CL-6B chromatography. The samples were then adjusted to 25 mM $MnCl_2$ by the addition of 1 M $MnCl_2$ (pH 7.4, 25 mM NaCl) and loaded onto a Heparin-Sepharose column (1.6 cm x 10 cm, 20 ml Heparin-Sepharose CL-6B gel, Pharmacia) using a peristaltic pump (P-1, Pharmacia) at a flow rate of 0.1 ml/min and then allowed to bind to the column overnight (10- 12 h)prior to elution. The sample was eluted at a flow rate of 0.4 ml/minute using

Table 2.1- Elution scheme for Heparin-Sepharose chromatography of lipoproteins
The above table shows the salt elution profile used to elute lipoprotein fractions (d_{15}<1.21 g/ml plasma fraction) from a Heparin-Sepharose affinity column. The above parameters were used to program a step gradient on a Waters Protein Purification system 650 at 0.4 ml/min.

Time *(minutes)*	**Fraction #**	**25 mM NaCl 25 mM $MnCl_2$** *(%)*	**95 mM NaCl** *(%)*	**1000 mM NaCl** *(%)*	**NaCl** *(mM)*
0	1-13	100	0	0	**25**
140	14-21	0	95	0	**95**
220	22-29	0	94	6	**150**
300	30-37	0	77	23	**300**
380	38-45	0	39	61	**650**
460	46-53	0	0	100	**1000**
540	54-60	100	0	0	**25**
600	-	0	0	0	**0**

the elution profile shown in **Table 2.1,** and resulted in the dialyzed d_{15}<1.21g fraction being fractionated into 5 peaks. Fractions were collected at 10 minute intervals using a fraction collector (Frac-100, Pharmacia) and the fractions making up each individual peak were pooled and concentrated by dialysis against icing sugar. The concentrated samples were then dialyzed against 25 mM Tris, 154 mM NaCl, 0.01% Na_2EDTA and 0.02% NaN_3 at 4 °C overnight (10-12 h) before gel filtration.

2.11.2 SUPEROSE 6B GEL FILTRATION OF LIPOPROTEINS

Superose 6B (Pharmacia) gel filtration was performed on either 2-3 ml of rat plasma, d_{15}<1.21 g/ml lipoprotein fraction or 1-3 ml of concentrated sample partially purified by Heparin-Sepharose chromatography. A 100 cm column (Pharmacia SR) was siliconized by a light coating of Sigmacote™ (Sigma) and packed to yield a column of 1.6 x 90 cm. Depending on the efficiency of packing, the column had a void volume of 48-60 mls and an operating pressure of 36-40 P.S.I. at a flow rate of 0.4 ml/min. Samples were loaded manually with a syringe through a bypass valve and fractions were eluted at 10 minute intervals using a Waters Protein Purification System 650, ultra-violet detector and fraction collector (Frac-100, Pharmacia). Depending on the experiment, fractions were either analysed individually or pooled. Pooled fractions were concentrated by dialysis against icing sugar and the salt and sugar were removed by dialysis against 20 mM ammonium bicarbonate and 0.01% Na_2EDTA buffer (pH 7.4). Concentrated fractions were then characterized by lipid analysis, electron microscopy, denaturing and/or non-denaturing polyacrylamide electrophoresis.

2.11.3 ELECTRON MICROSCOPY OF NEGATIVELY STAINED LIPOPROTEINS

Fresh lipoproteins isolated by ultracentrifugation (d_{15}<1.21 g/ml) and/or gel filtration chromatography were dialyzed against 20 mM ammonium biocarbonate and 0.01% Na_2EDTA buffer (pH 7.4) in preparation for electron microscopy. Negative staining of lipoproteins was performed by the method of Forte and Nordhausen (188). Briefly, a drop of lipoprotein containing solution was placed on Formvar coated copper grids and allowed to settle for 1 minute before excess liquid was wicked away with filter paper. The sample was then stained by the addition of one drop of 2% sodium phosphotungstate acid (pH 7.4) and stained for 0.5-1 minute prior to the removal of excess stain. The samples were then visualized and photographed in the electron microscope (Phillips).

2.12 Statistical analysis

All rat and mouse plasma data are presented as the means of like measurements ± the standard error of the mean for the sample size. Changes in rat and mouse plasma data following ANIT treatment were assessed for statistical significance using a one way repeated measures analysis of variance (ANOVA RM) or a Friedman repeated analysis of variance on ranks. Individual time points were further identified as significant using Dunnetts or Dunns multiple comparison method ($p > 0.05$). Density gradient data were based upon single determinations of plasma from individual animals. Statistical correlation of TgR[HuAI] rat data was performed by linear regression analysis.

Results

Chapter 3- D-(+) galactosamine-HCl induced hepatitis

Initial thesis research was performed in the galactosamine rat (D-(+) galactosamine-HCl, 750 mg/kg I.P.) which has been reported to be a reversible animal model of hepatitis resulting in secondary LCAT deficiency and a dramatic reduction in

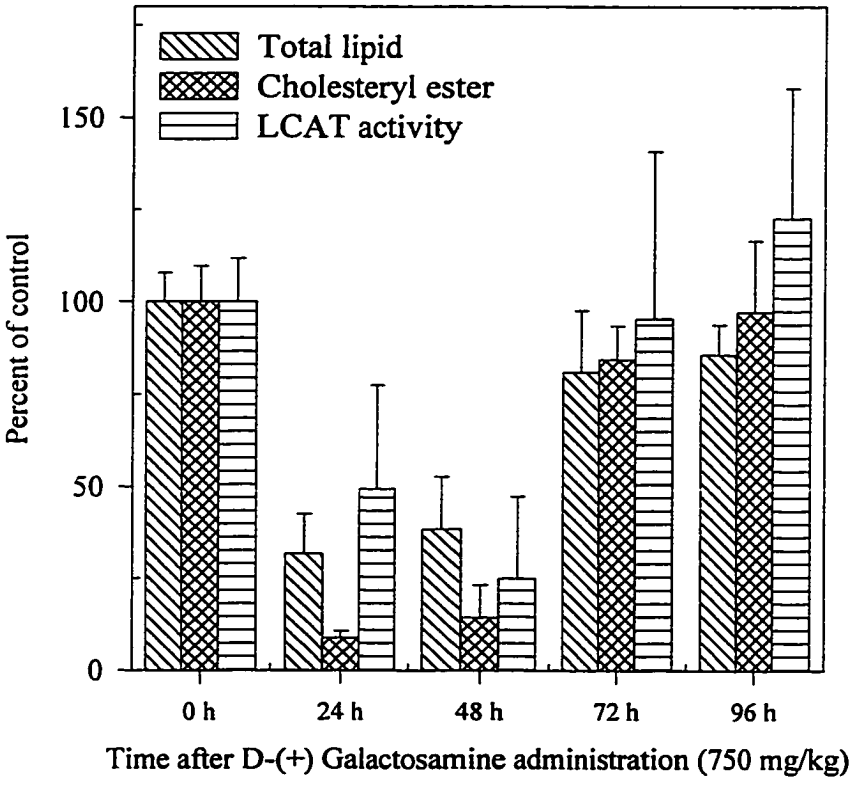

Figure 3.1- Preliminary time course of D-(+) galactosamine induced hepatitis in the rat Plasma LCAT activity was assayed by an exogenous proteoliposome method (87), and plasma lipids were measured enzymatically (as described in methods). Values are presented as percentage of control ± S.E.M. (0, 24 and 48 h, n=8; 72 and 96 h, n=3 and 4).

plasma cholesteryl esters (127). The LCAT deficiency, cholesteryl ester reduction and reversibility were confirmed over a time course of 96 hours (**Figure 3.1**) and these findings were paralleled by impressive reductions in plasma total lipids.

Further preliminary characterization and assessment of the galactosamine rat as a suitable model for studying the abnormal lipoproteins in familial LCAT deficiency were carried out by measuring hepatic triacylglycerol lipase and lipoprotein lipase activities. These results are shown in **Table 3.1** and clearly demonstrate that galactosamine induced hepatitis results in a marked deficiency of not only LCAT but also both lipase activities. These reductions in plasma lipolytic enzyme activities most likely reflect under-glycosylation of the enzymes due to UDP sequestration by galactosamine resulting in impaired secretion and/ or activity of the enzymes. A deficiency of all 3 major plasma lipolytic enzymes would have major consequences for lipoprotein metabolism in the galactosamine rat, not to mention that many other metabolically important processes

Table 3.1- Effect of galactosamine-induced hepatitis on plasma lipids and lipolytic enzyme activities 48 h following D-(+) galactosamine administration

LCAT activity was assayed by an exogenous proteoliposome method (87) and lipoprotein and hepatic triacylglycerol lipase activities were assayed using a trioleoylglycerol and Triton N-101 emulsion (178) as described in methods. Plasma lipids were measured enzymatically. Values are expressed as ± S.E.M. (n=8). For LPL and HTGL assays, control (n=1); 48 h, (n=4). LCAT, lecithin: cholesterol acyltransferase; LPL, lipoprotein lipase; HTGL, hepatic triacylglycerol lipase; FC, free cholesterol; CE, cholesteryl ester; PL, phospholipid; TAG, triacylglycerol.

	LCAT*	LPL**	HTGL**	FC	CE	PL	TAG
	(nmol/ml/h)	*(nmol/ml/h)*	*(nmol/ml/h)*	*(mg/dl)*	*(mg/dl)*	*(mg/dl)*	*(mg/dl)*
Control	18±2	4278	2408	22±1	85±8	156±3	44±11
Galactosamine (48 h)	5±4	620±390	222±90	28±7	12±8	61±10	16±19
% of control	25±22	14±9	9±4	131±31	14±9	44±7	35±44

*nmol cholesteryl ester formed ml^{-1} h^{-1}

**nmol oleic acid released ml^{-1} h^{-1}

would likely be perturbed to a similar extent. These factors in addition to the difficulties in characterization and metabolic experimentation introduced by the very low levels of plasma lipids, resulted in a decision not to proceed with studies in this animal model.

It is worth noting that density gradient ultracentrifugation of a galactosamine rat 48 hours after treatment was highly suggestive of low levels of Lp-X like particles in the LDL density fractions (8-11) (see **Figure 3.2)** as these fractions were near devoid of neutral lipid and were approximately 30% free cholesterol and 60% phospholipid, which is characteristic of Lp-X.

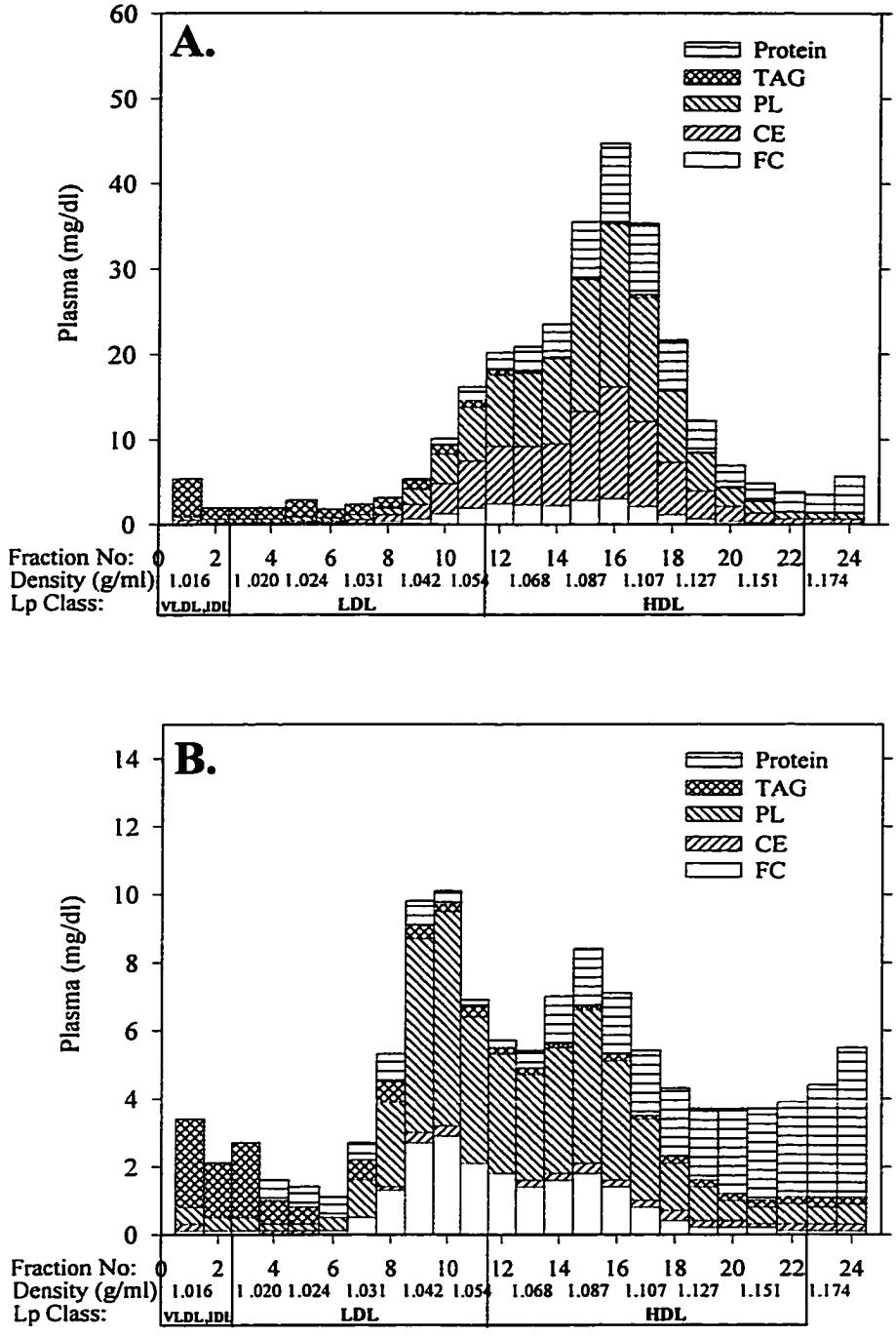

Figure 3.2A and B- Lipoprotein distribution profile of a control and D-(+) galactosamine treated rat (750 mg/kg, 48 h) after density gradient ultracentrifugation

Density gradient profiles of a control (A.) and a D-(+) galactosamine treated rat (B.) are shown. Lipids were measured enzymatically using kits, and protein was measured by a modified Lowry method (183). Only fractions 1-24 are shown, as fractions 25-30 were devoid of lipid. FC, free cholesterol; CE, cholesteryl ester; PL, phospholipid; TAG, triacylglycerol; Lp, lipoprotein.

Chapter 4- The ANIT rat

ANIT-induced (100mg/kg) reversible intrahepatic cholestasis in the rat resulted in very significant alterations in the composition of rat plasma. The major changes occurred after 18 hours, peaked at 48 hours and returned to near normal by 120 hours. **Figure 4.1** shows that after 18 hours the plasma total bile acid concentration increased rapidly to a peak maximum at 24 hours. Bilirubin was similarly increased reaching maximum plasma

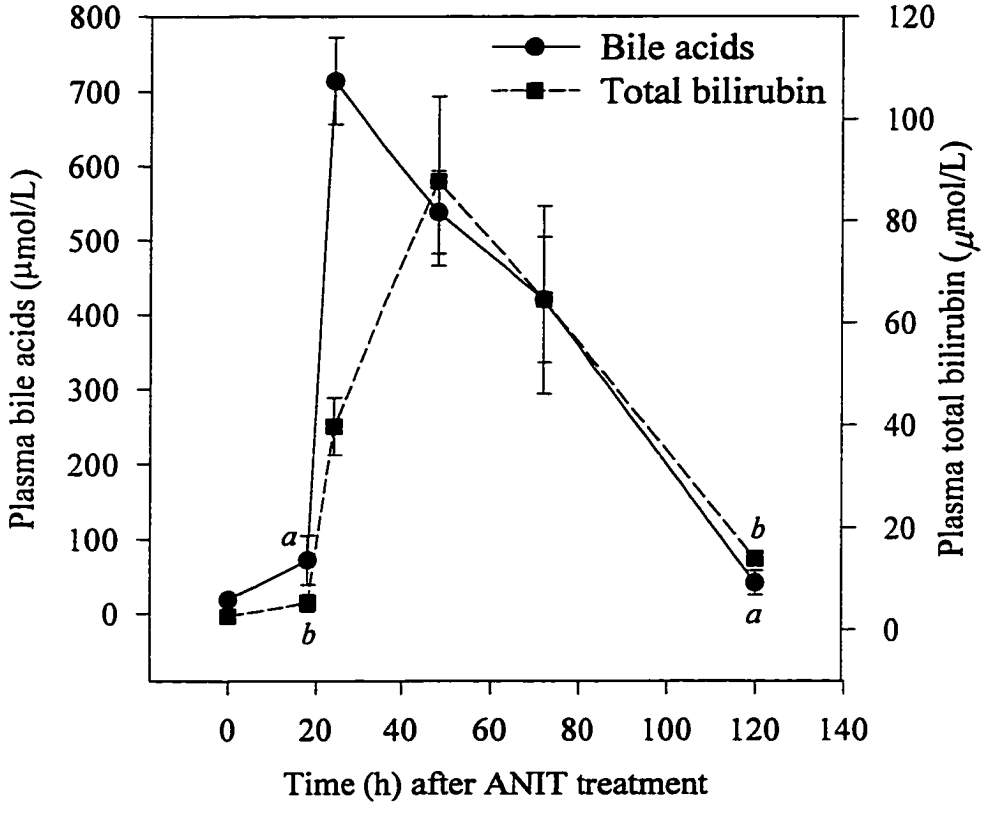

Figure 4.1- Plasma total bile acids and bilirubin after ANIT administration
Points shown are for fasted rats and are the mean ± S.E.M. (n=6). The ANIT dosage was 100 mg/kg. ^{a}Bile acids and ^{b}Bilirubin measurements were not significantly different ($p < 0.05$) versus controls (0 h).

Table 4.1- Plasma markers of liver damage
Values are given as mean ± S.E.M (n=6 except where noted). Units are I.U. (37 °C). Alk Phos, alkaline phosphatase; AST, aspartate aminotransferase; ALT, alanine aminotransferase. ^{a}n=5; ^{b}n=2; ^{c}n=10; *significant ($p < 0.05$) versus controls (0 h).

	0 h	18 h	24h	48 h	72 h	120 h
Alk Phos	53 ± 0^{b}	-	-	$214 \pm 19^{c*}$	-	-
AST	103 ± 7	160 ± 39^{a}	396 ± 37^{a}	$2513 \pm 345^{*}$	$1069 \pm 120^{*}$	117 ± 10
ALT	43 ± 6	65 ± 10^{a}	210 ± 19^{a}	$1916 \pm 312^{*}$	$1130 \pm 197^{*}$	76 ± 9

values at 48 hours. In addition, ANIT-induced hepatic liver damage was characterized by significant elevations in the plasma concentration of liver enzymes. **Table 4.1** shows that at 48 hours, there was a 4 fold increase in alkaline phosphatase, 24 fold increase in aspartate aminotransferase and 45 fold increase in alanine aminotransferase activities.

Elevations in plasma bilirubin, bile acids and liver enzymes were followed by increases in plasma lipids (**Figure 4.2**). Elevated concentrations of plasma phospholipid and free cholesterol were observed after 18 hours and were followed by maximal increases of 611% and 935% respectively at 48 hours. The phospholipid and free cholesterol values then began to decrease to near normal values by 120 hours. The elevation in plasma free cholesterol was paralleled by increases in cholesteryl ester. However, the CE/FC ratio decreased after 18 hours to a near 1:1 mass ratio by 48 hours, after which the ratio began to return towards normal.

These changes occurred in the presence of normal to moderately increased LCAT activity (**Figure 4.3**) such that the decrease in CE/FC ratio did not result from a deficiency in LCAT esterifying activity. Plasma triacylglycerol levels were not significantly increased as a result of cholestasis. Lipoprotein lipase activity was increased to 130% of control levels at 48 hours and hepatic triacylglycerol lipase activity

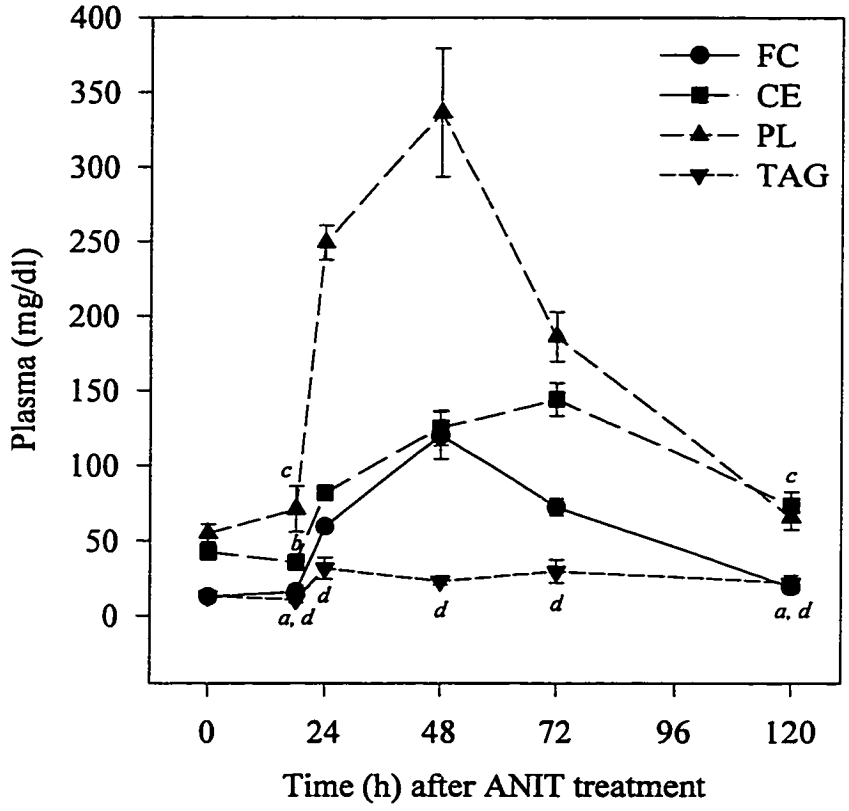

Figure 4.2- Plasma lipids after ANIT administration (100 mg/kg)
Points shown are for fasted rats and are the mean ± S.E.M. (n=6). [a]Free cholesterol (FC), [b]Cholesteryl ester (CE), [c]Phospholipid (PL) and [d]Triacylglycerol (TAG) measurements were not significantly different ($p < 0.05$) versus controls (0 h).

was decreased to 43% of control values at 48 hours (**Figure 4.3**). The phospholipase activity of hepatic lipase was not measured, but was likely affected to a similar extent.

ANIT-induced cholestasis also resulted in altered concentrations of the main rat plasma apolipoproteins B, E, and A-I. Apolipoprotein E was increased by 3.0 fold, apolipoprotein A-I by 1.9 fold and apolipoprotein B by 1.6 fold at 48 hours (**Figure 4.4**) suggesting the increased lipid mass observed in this cholestatic model was predominantly associated with apolipoprotein E and A-I and not with apolipoprotein B.

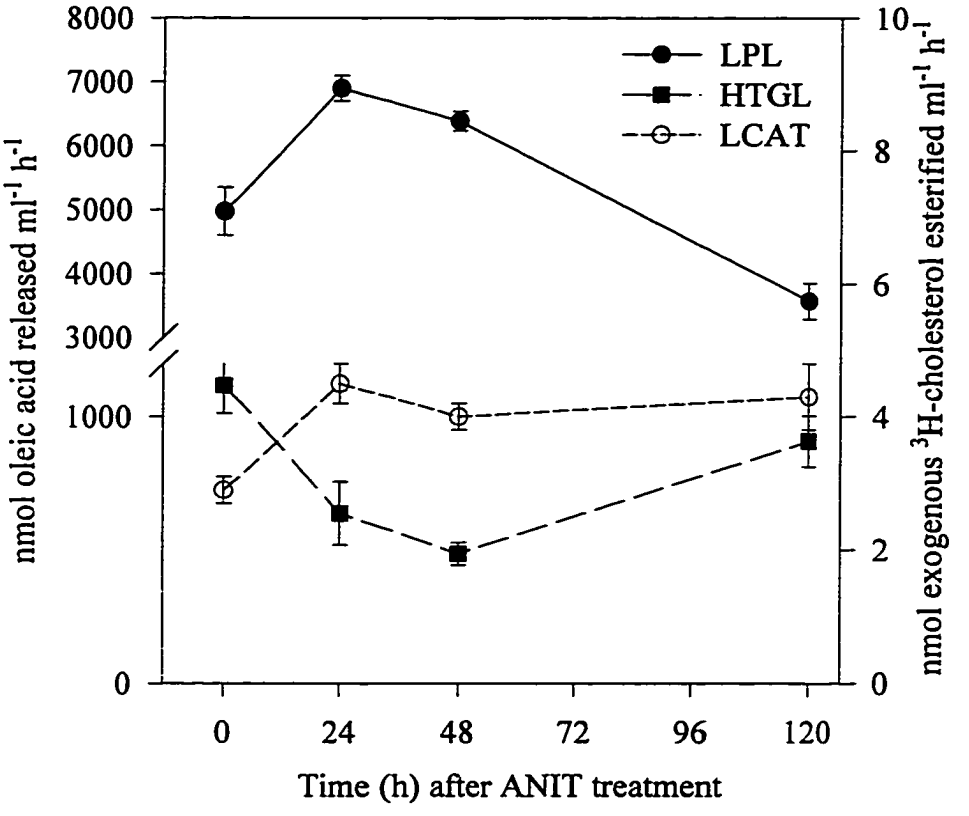

Figure 4.3- Plasma lipolytic enzyme activities after ANIT administration
Points shown are for fasted rats and are the mean ± S.E.M. (n=6). Lecithin: cholesterol acyltransferase (LCAT) activity was measured using an exogenous proteoliposome substrate (87) and lipoprotein lipase (LPL) and hepatic triacylglycerol lipase (HTGL) activities were measured using a trioleoylglycerol emulsion as substrate (178). [a]Lipoprotein lipase (LPL), [b]Hepatic triacylglycerol lipase (HTGL) and [c]Lecithin cholesterol acyltransferase (LCAT) measurements were not significantly different ($p < 0.05$) versus controls (0 h).

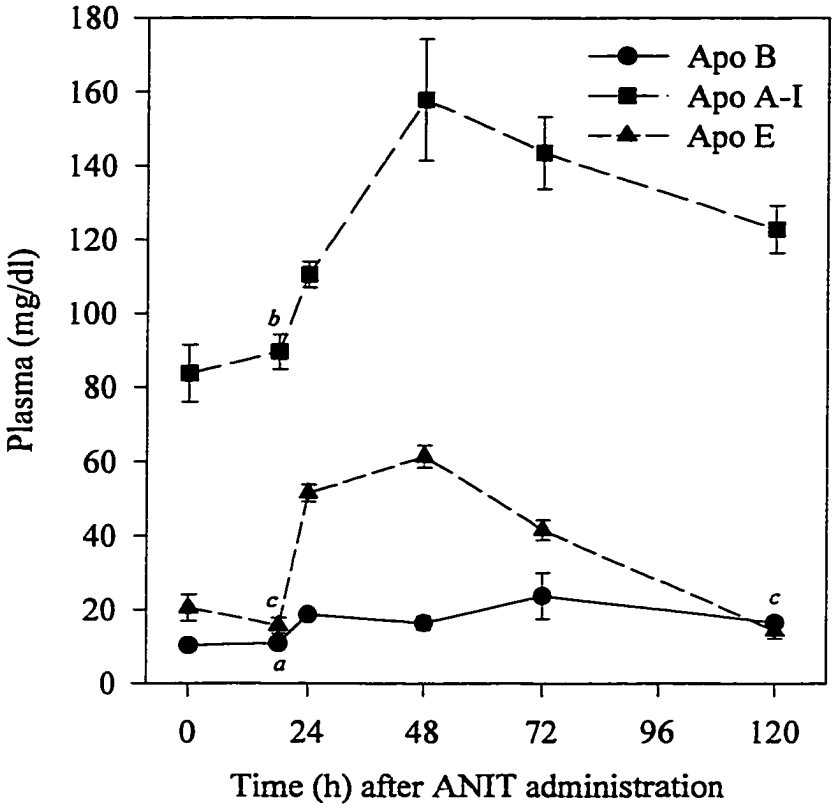

Figure 4.4- Plasma apolipoprotein B, E, and A-I concentrations with time after ANIT administration (100 mg/kg)

Points for fasted rats are the mean ± S.E.M. (n=5) and were measured by electroimmunoassay (180). ^{a}Apo B, ^{b}Apo A-I and ^{c}Apo E measurements were not significantly different ($p < 0.05$) versus controls (0 h). Apo, apolipoprotein.

Table 4.2- Plasma phospholipid:apo A-I and cholesteryl ester:apo A-I ratios with time after ANIT administration (100 mg/kg)
Values are given as mean ± S.E.M. (n=5). Apo A-I, apolipoprotein A-I; PL, phospholipid; CE, cholesteryl ester.

Time (h)	Apo A-I (μM)	PL (mM)	CE (mM)	PL/A-I (molar ratio)	CE/A-I (molar ratio)
0	30±3	0.7±0.1	0.7±0.1	24±5	22±5
18	32±2	0.9±.02	0.6±0.1	29±8	17±3
24	39±1	3.2±0.1	1.3±0.1	82±6	32±2
48	56±5	4.3±0.6	1.9±0.2	77±17	34±6
72	51±3	2.4±0.2	2.2±0.2	47±7	44±6
120	44±2	0.9±0.1	1.1±0.1	19±3	26±4

The molar ratio of phospholipid to apolipoprotein A-I in plasma increased from 24 to a peak of 82 molecules phospholipid/A-I molecule by 24 hours (**Table 4.2**). The cholesteryl ester/apolipoprotein A-I molar ratio, by contrast, rose steadily from an initial value of 22 to a peak of 44 molecules cholesteryl ester per molecule apolipoprotein A-I by 72 hours (**Table 4.2**). Although not quantitated by immunoassay, sodium dodecyl sulfate polyacrylamide gel electrophoresis of density gradient fractions (**Figure 4.10**) indicated that apolipoprotein A-IV levels were also increased by 48 hours.

Molecular species analysis by gas chromatography of the phospholipid and cholesteryl esters present during the course of ANIT-induced intrahepatic cholestasis clearly showed that the increased levels of phospholipid were due predominantly to increases in medium chain species (**Figure 4.5**) containing a sum of 34, 36 or 38 carbons in both fatty acyl side chains. These species likely correspond, respectively, to phospholipids containing C-16/18, C-18/18 and C-18/20 fatty acyl chains.

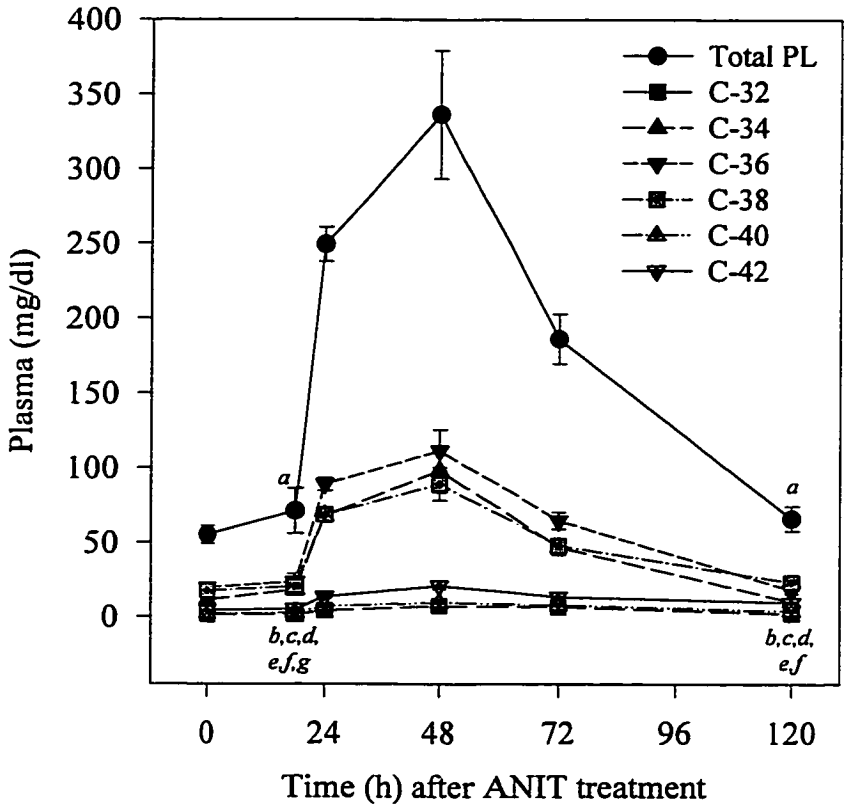

Figure 4.5- Plasma phospholipid molecular species with time after ANIT administration (100 mg/kg)

Points shown are for fasted rats and are the mean ± S.E.M. (n=6). Carbon numbers in the legend refer to the total carbons from the two fatty acyl moieties and do not include the 3 carbons in the glycerol backbone. C-16/18, C-18/18 and C-18/20 are likely the major fatty acid combinations represented by C-34, C-36 and C-38 molecular species as identified by gas chromatographic total lipid profiling (174). ^{a}Total plasma phospholipid (PL), ^{b}C-32, ^{c}C-34, ^{d}C-36, ^{e}C-38, ^{f}C-40 and ^{g}C-42 phospholipid measurements were not significantly different ($p < 0.05$) versus controls (0 h).

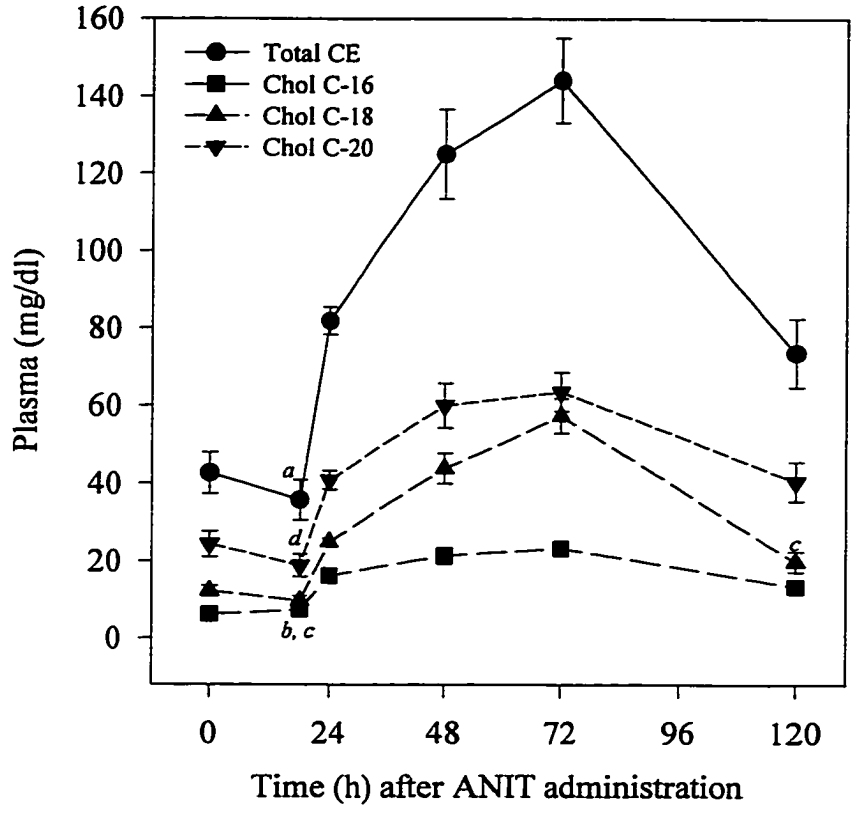

Figure 4.6- Plasma cholesteryl ester molecular species with time after ANIT administration (100 mg/kg)

Points shown are for fasted rats and are the mean ± S.E.M. (n=6). Carbon numbers in the legend refer to total fatty acyl chain carbons as determined by gas chromatographic total lipid profiling (174) and do not include carbons derived from cholesterol. ^{a}Total cholesteryl ester (CE), ^{b}C16, ^{c}C-18 and ^{d}C-20 cholesteryl ester measurements were not significantly different ($p < 0.05$) versus controls (0 h).

Similar analysis of cholesteryl esters, (**Figure 4.6**) showed that the major cholesteryl ester species found within plasma from the ANIT-treated rats were those containing 18 and 20 carbon fatty acyl moieties. Although both C-20 and C-18 cholesteryl esters increased substantially by 48 hours, the overall percentage of C-16 and C-18 fatty acids esterified was increased at the expense of C-20. The percentage by mass of cholesteryl esters containing C-16, C-18 and C-20 fatty acids was 14%, 29% and 57%

respectively in untreated rats. In the ANIT-treated rat the respective values were 17%, 35% and 48% at 48 hours and 16%, 40% and 44% at 72 hours. The ratios returned to normal by 120 hours. These results may indicate in rats that the species-specific substrate requirements sometimes ascribed to LCAT may be more dependent upon the nature of the phospholipid substrate available than a particular structural preference.

As a result of the increased plasma lipids following ANIT treatment, significant alterations in the plasma lipoprotein distribution were observed. **Figure 4.7** demonstrates the shift in lipoprotein mass from the HDL to the LDL density range at 48 hours, the time

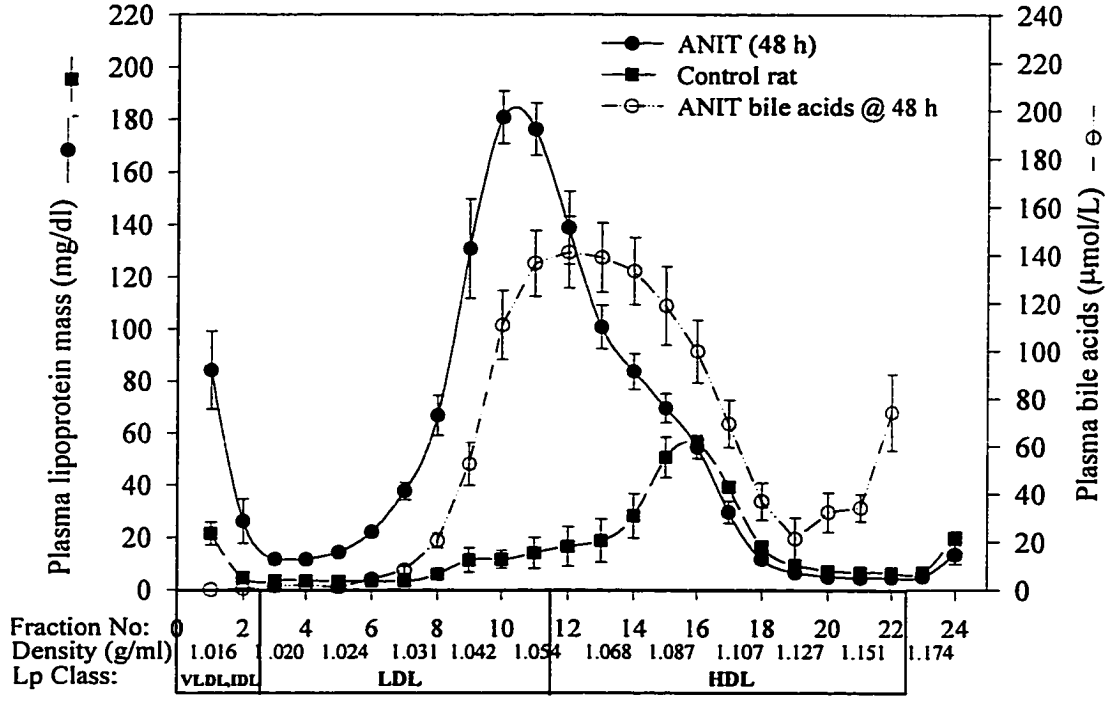

Figure 4.7- Control and ANIT-treated rat (48 h) lipoprotein and bile acid distributions Lipoprotein mass was calculated from lipid plus protein. For controls, ANIT-treated rats (100 mg/kg) and bile acid analysis, n=3, 4 and 4 respectively. No bile acids were detected in control rat gradient fractions.

of maximum effect. Additionally, bile acids associated with treated rat fractions were measured and are shown. Detected bile acids were most highly concentrated in the HDL density fractions and were present in fractions 8-18 and fractions above 24. It should be noted that the total recovery of lipoprotein-associated bile acids after density gradient ultracentrifugation was approximately 10% of total plasma bile acids. No bile acids were detected in control rat fractions. To further analyze the changes in lipoprotein composition, individual lipoprotein components of density gradient fractions in control and ANIT-treated rats are shown in **Figure 4.8 and 4.9**. Profiles of ANIT-treated rats at 24 hours (**Figure 4.9A**), 48 hours (**Figure 4.9B**), 72 hours (**Figure 4.9C**) and 120 hours (**Figure 4.9D**) revealed profound changes in the distribution of lipoproteins over the cholestatic time course when compared to a control rat profile (**Figure 4.8**). At 24 hours (**Figure 4.9A**) there was a noticeable increase in lipid mass within the LDL density range (fractions 3-11) mainly as a result of phospholipid and free cholesterol enrichment. HDL was moderately enriched in phospholipid. At 48 hours (**Figure 4.9B**), the time point of peak plasma lipid levels, there was a marked elevation in the lipid (primarily free cholesterol and phospholipid) distributed throughout density gradient fractions 1-24. In the LDL density range (fractions 9-11), particles were particularly deficient in core neutral lipid suggesting the presence of vesicles. For example, fraction 9 is composed of FC/18%, CE/6%, PL/59%, TAG/3% and Prot/14%. HDL (fractions 12-18) was cholesteryl ester deficient and phospholipid enriched when compared to control rat plasma. By 72 hours (**Figure 4.9C**) the plasma cholesteryl ester content (**Figure 4.2**) began to return towards normal and the lipid mass associated with the LDL density region at 48 hours (**Figure 4.9B**) decreased such that there was a clearly discernible

separation (fraction 13-14) between the LDL and HDL density regions. The lipid composition of fractions in the LDL region (fractions 3-11) remained enriched in phospholipid. The cholesteryl ester composition of HDL was increased and there was reduced phospholipid enrichment. By 120 hours (**Figure 4.9D**) the lipid distribution returned to near normal and the excess phospholipid and free cholesterol were cleared from the plasma.

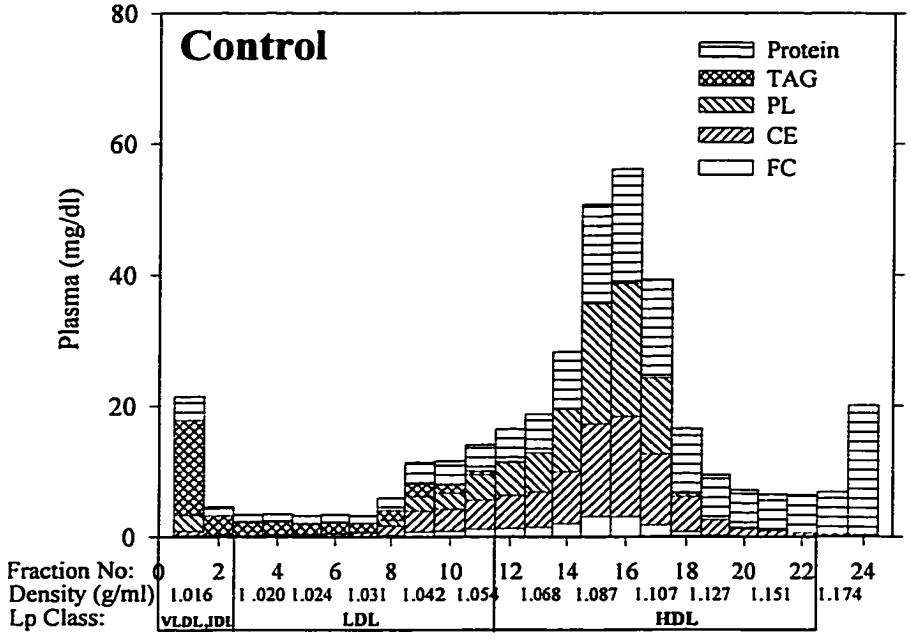

Figure 4.8- Lipoprotein mass distribution of a control rat after density gradient ultracentrifugation

Only fractions 1-24 are shown, as fractions 25-30 were devoid of lipid. FC, free cholesterol; CE, cholesteryl ester; PL, phospholipid; TAG, triacylglycerol; Lp, lipoprotein.

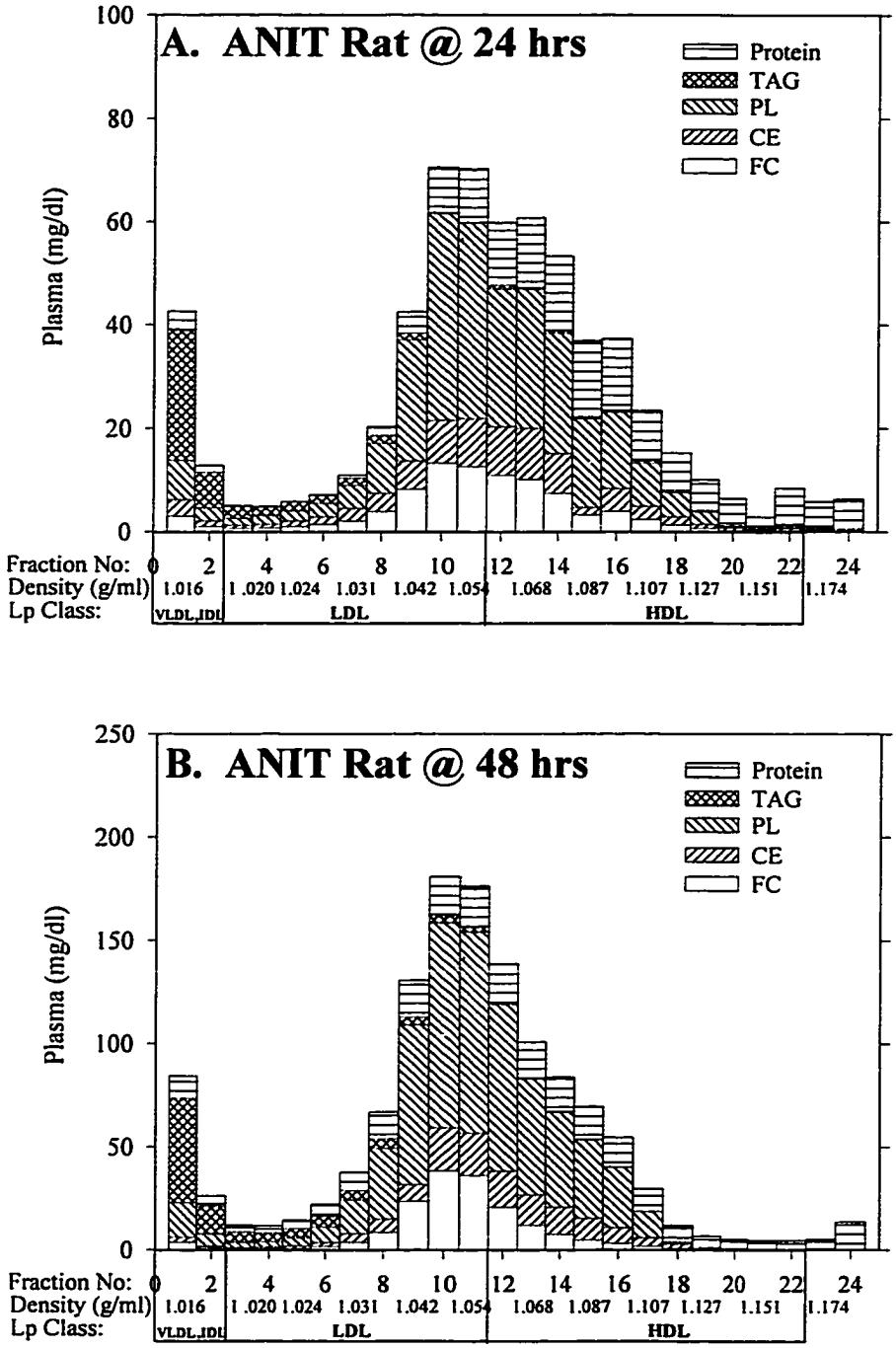

Figure 4.9A and B

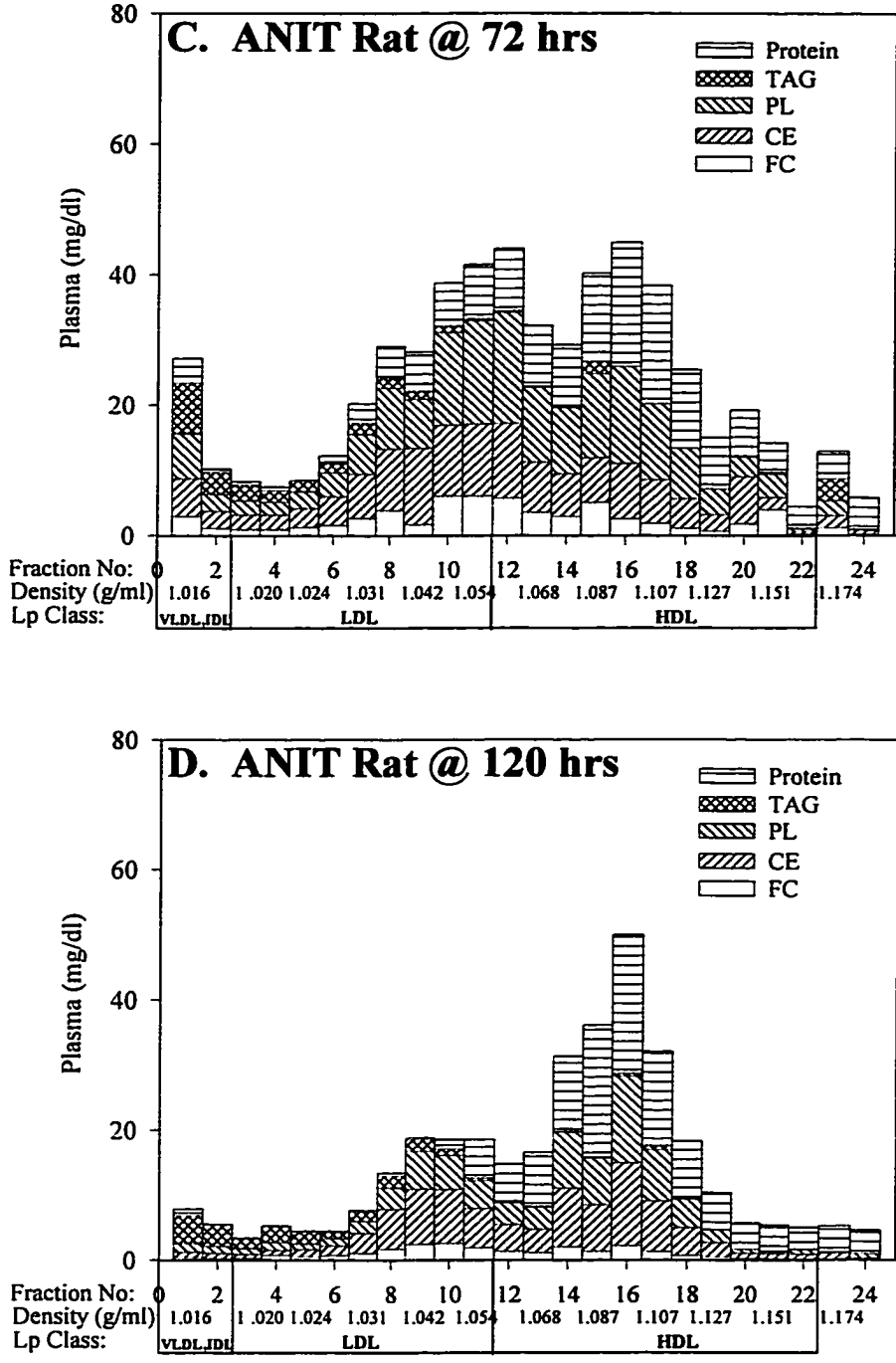

Figure 4.9A-D- Profiles (24, 48, 72 and 120 h) of ANIT-treated rat lipoprotein mass distribution after density gradient ultracentrifugation

(A.) 24, (B.) 48, (C.) 72 and (D.) 120 h after ANIT treatment. Only fractions 1-24 are shown as fractions 25-30 were devoid of lipid. FC, free cholesterol; CE, cholesteryl ester; PL, phospholipid; TAG, triacylglycerol; Lp, lipoprotein.

To further analyze the alterations in lipoprotein metabolism occurring at 48 hours, density gradient fractions 1-24 were analyzed for apolipoprotein content by sodium dodecyl sulfate polyacrylamide gel electrophoresis on 5-19% gradient gels. **Figure 4.10A**, shows the distribution throughout the gradient fractions of apolipoproteins in an untreated rat. LDL fractions 6-10 (d_{15}= 1.028- 1.048 g/ml) which corresponded to rat LDL, as expected contained apolipoprotein B and some apolipoprotein E. High density fractions contained increasing quantities of apolipoprotein E, A-I and A-IV, with the major apolipoprotein E containing fractions being fractions 11-18. Apolipoprotein A-I rich HDL was centered around fractions 14-20 and co-fractionated with apolipoprotein A-IV. Sodium dodecyl sulfate polyacrylamide gel electrophoresis of gradient fractions 8-12 at 48 hours after ANIT treatment (**Figure 4.10B**) revealed movement of apolipoproteins A-I and A-IV into the lower density ranges. The presence of apolipoprotein B_{48} in HDL fractions 13-15 suggests these rats have impaired remnant removal. The major apolipoprotein E containing fractions were fractions 8-16, approximately 2-3 fractions less dense than that observed in an untreated rat. Apolipoprotein A-I and A-IV distribution appeared to be more wide-spread as significant amounts were found outside of the normal HDL density range (fractions 14-20). Additionally, Fractions 8-12 were shown by lipid analysis (**Figure 4.9B**) to be deficient in core neutral lipid and also to contain a band corresponding to albumin. These results suggest Lp-X like vesicles may be present.

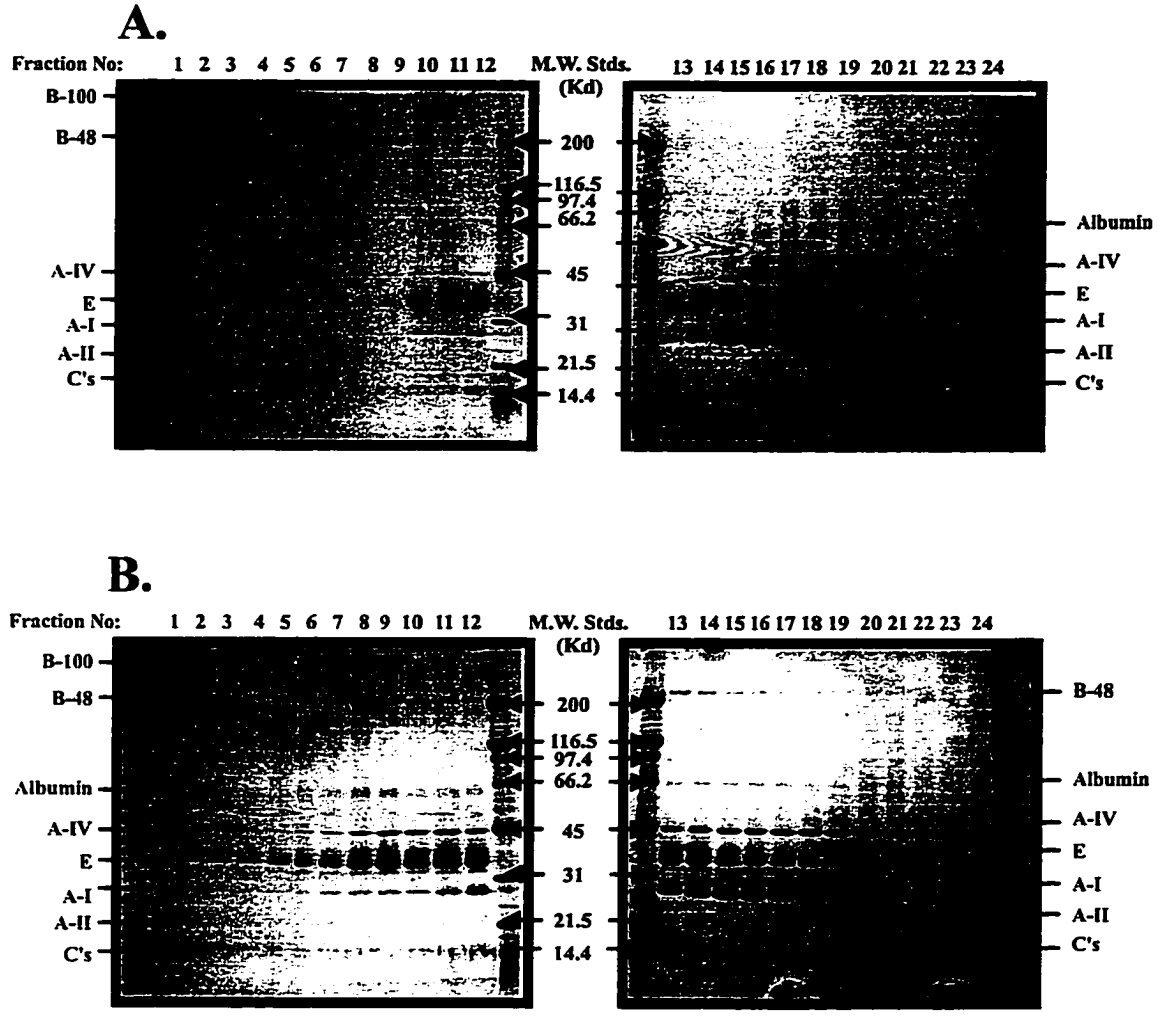

Figure 4.10A and B- Sodium dodecyl sulfate polyacrylamide gel electrophoresis (5-19%) of density gradient fractions 1-24 after ultracentrifugation
A control rat (A.) is shown compared to an ANIT rat 48 h post-treatment (B.). Twenty μg of protein was loaded in each lane (Fig. 4.10A., fractions 1-9 <20 μg; Fig. 4.10B., fractions 1-6 <20 μg). Molecular weight standards were broad range (Bio-Rad) of the indicated molecular weights.

Density gradient fractions from an untreated and an ANIT-treated rat were subjected to non-denaturing polyacrylamide gel electrophoresis. The results are shown in **Figure 4.11**. Particle diameters above 170 Å are estimates. **Figure 4.11A** indicates the size distribution of lipoproteins in fractions 1-12 of a control rat. Fractions 1-8, were each homogeneous for a single particle population, whereas fractions 9-11 were

heterogeneous and contained two populations of particles, likely LDL and a large HDL. This was not surprising given the presence of apolipoprotein B, E, A-I and A-IV within these fractions (**Figure 4.10A**). Fractions 1-7 of treated rats (**Figure 4.11B**) also contained single particle populations slightly smaller than those observed in untreated rats. This was probably due to decreased core cholesteryl esters. Fractions 9-12 of ANIT-treated rats (**Figure 4.11B**) appeared to contain at least four particle populations and these may correspond to vesicles (370-340 Å), small LDL (260 Å), VLDL and chylomicron remnants (220 Å) and a large HDL (180-140 Å). The putative LDL and HDL populations in this range appear to be smaller than their normal counterparts (**Figure 4.11A**) probably as a result of decreased cholesteryl ester content and phospholipid enrichment. **Figure 4.11C** and **4.11D** document the particle diameters for fractions 13-24 of a control and ANIT-treated rat. In general, the major differences were that the HDL from treated rats appeared to be slightly smaller in fractions 13-15 and markedly smaller in fractions 16-20. The smaller sized HDL in fractions 13-15 were possibly the result of reduced cholesteryl ester content and relative phospholipid enrichment. The very small HDL in fractions 16-20 may represent discoidal particles. Additionally, as shown in **Figure 4.10B**, apolipoprotein B_{48} was present in fractions 13-16 possibly denoting impaired remnant removal. The remnants may be too large to enter a 4% gel such that bands corresponding to these particles (**Figure 4.11D**) may be present at the top of lanes 13-15.

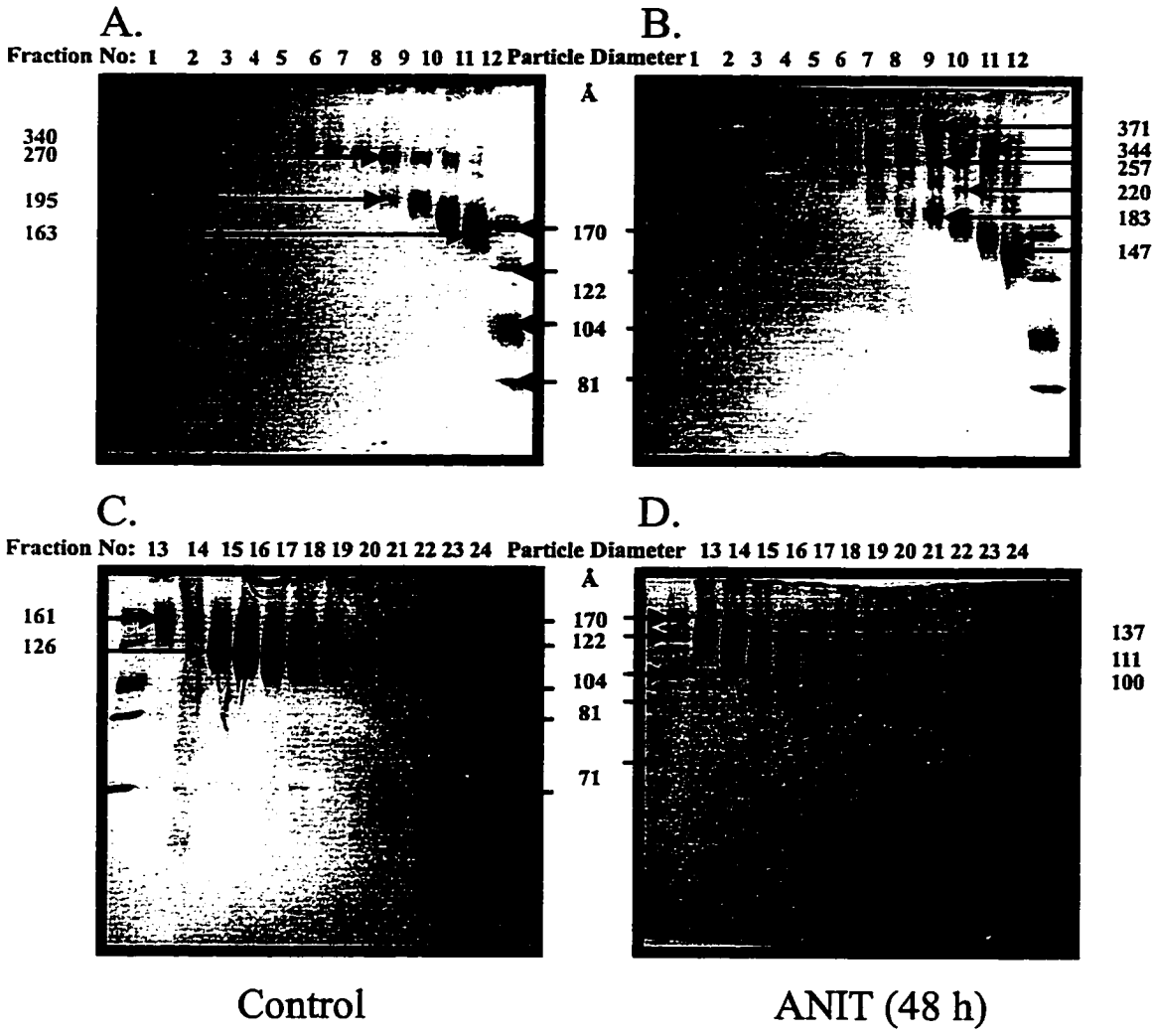

Figure 4.11A-D- Non-denaturing polyacrylamide gel electrophoresis of ANIT (48 h) and control density gradient fractions (1-24)

Nondenaturing 2-16% polyacrylamide gradient gels of density gradient ulracentrifugation fractions 1-12 (LDL range) (Fig. 4.11A and B) and 4-30% polyacrylamide gradient gels of fractions 13-24 (HDL range) (Fig. 4-11C and D). A control rat (Fig. 4.11A and C) is shown as compared to an ANIT-treated rat 48 h post-treatment (Fig. 11B and D). Twenty μg of protein was loaded in each lane (Fig. 4.11A, fractions 1-9 < 20 μg; Fig. 4.11B, fractions 1-6<20 μg). Gels were stained with Coomassie Blue R-250, destained and documented. Particle diameters above 170 Å were estimated by extrapolation using the equation of the second order regression curve of R_f versus log particle diameter (high molecular weight standards, Pharmacia).

Chapter 5- Characterization of the abnormal lipoproteins in the ANIT rat

The results from the ANIT-treated rat time course study (chapter 4), clearly demonstrated lipoprotein heterogeneity in the LDL density range at the 48 hour time point. The near lack of neutral core lipid in this region combined with the phospholipid to free cholesterol ratio strongly supported the presence of Lp-X-like vesicles. However, further purification of the lipoproteins in this density range was required for conclusive proof, as Lp-X could not be demonstrated by agar electrophoresis (results not shown). To this end a purification procedure modified slightly from that of Weisgraber and Mahley (187) was developed to separate apolipoprotein B and E associated particles by their affinities to heparin sulfate immobilized on Sepharose (Heparin-Sepharose CL-6B, Pharmacia). Fractions separated by this chromatographic step were then further subfractionated by size on a Superose 6B gel filtration column. The results presented here are preliminary as the procedure is lengthy, technically difficult and was complicated by numerous problems with equipment. However, the separation, although not entirely optimized, yielded a reasonably good separation and with some modifications may be promising.

At the time this separation was performed, problems developed with the ANIT stock and a dosage of 150 mg/kg was necessary to achieve similar lipid values (48 h) to those observed in the ANIT-treated rat time course study. This procedural modification does limit the value of the results and requires cautious interpretation of the lipoprotein characterization when compared to the results documented in the ANIT-treated rat time course study.

The d_{15}<1.21 g/ml fraction of two ANIT-rat plasmas (48 h) isolated by a single ultracentrifugation (described in methods) were pooled. The pooled lipoprotein fraction was dialyzed to the initial chromatography conditions of 25 mM NaCl and 25 mM $MnCl_2$ was added to enhance the interaction and binding of the lipoproteins to the column,. The sample was then loaded and incubated for 12 hours to facilitate complete lipoprotein binding prior to being eluted using a step NaCl gradient (as described in methods). The results of this separation as monitored at 280 nm for both an ANIT pool (2 rats, 7.4 ml plasma) and a control pool (4 rats, 13.2 ml plasma) are shown in **Figure 5.1.** The separation using a multi-step NaCl gradient of 25 mM to 1000 mM resulted in a very defined separation of 4 fractions from the control pool (**Figure 5.1A**) and 5 fractions from the ANIT pool (**Figure 5.1B**). The Heparin-Sepharose chromatographic method employed elutes fractions (peaks) according to increasing apolipoprotein E composition (peaks II-IV) and latterly apolipoprotein B content (peak V).

The Heparin-Sepharose chromatographic fractions (II to V control and I to V ANIT) were concentrated against icing sugar and dialyzed against gel filtration buffer prior to size separation on a Superose 6B gel filtration column (1.6 x 90 cm). The elution profiles of the control pool (**Figure 5.2**) and ANIT pool (**Figure 5.3**) Heparin-Sepharose fractions as monitored at 280 nm are shown.

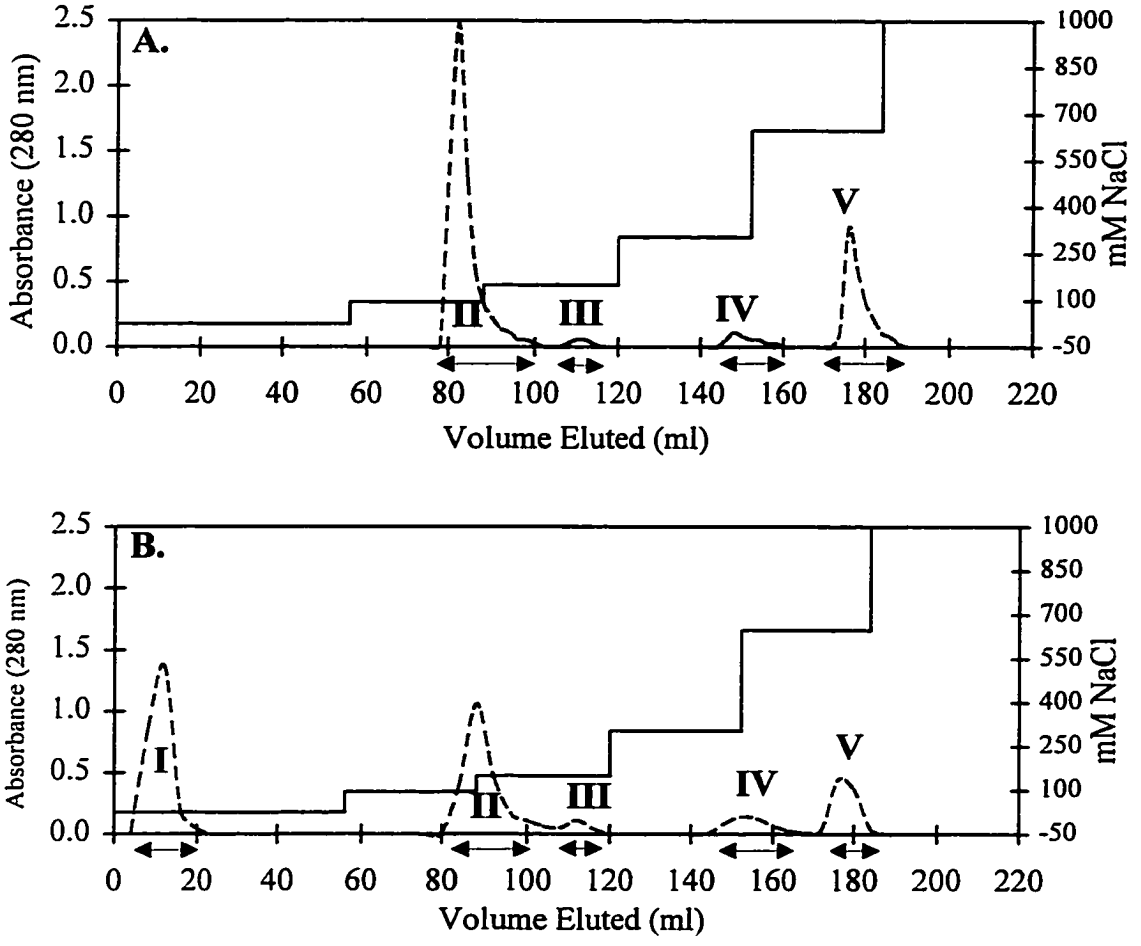

Figure 5.1A and B- Heparin-Sepharose chromatography of the pooled d_{15}<1.21 g/ml fraction of ANIT-treated (48 h, 150 mg/kg) and control rat plasma

The Heparin-Sepharose chromatographic separation (column 1.6 x 10 cm) of the d_{15}<1.21 g/ml fraction of pooled control rat (A.) and ANIT-treated rat (B.) plasma is shown. The elution profile (0.4 ml/min, 10 min/fraction) as measured at 280 nm is shown and the NaCl concentrations of the step gradient are indicated. Individual fractions, under peaks marked I to V were pooled as indicated by the arrows (◄—►) in preparation for further subfractionation by Superose 6B gel filtration.

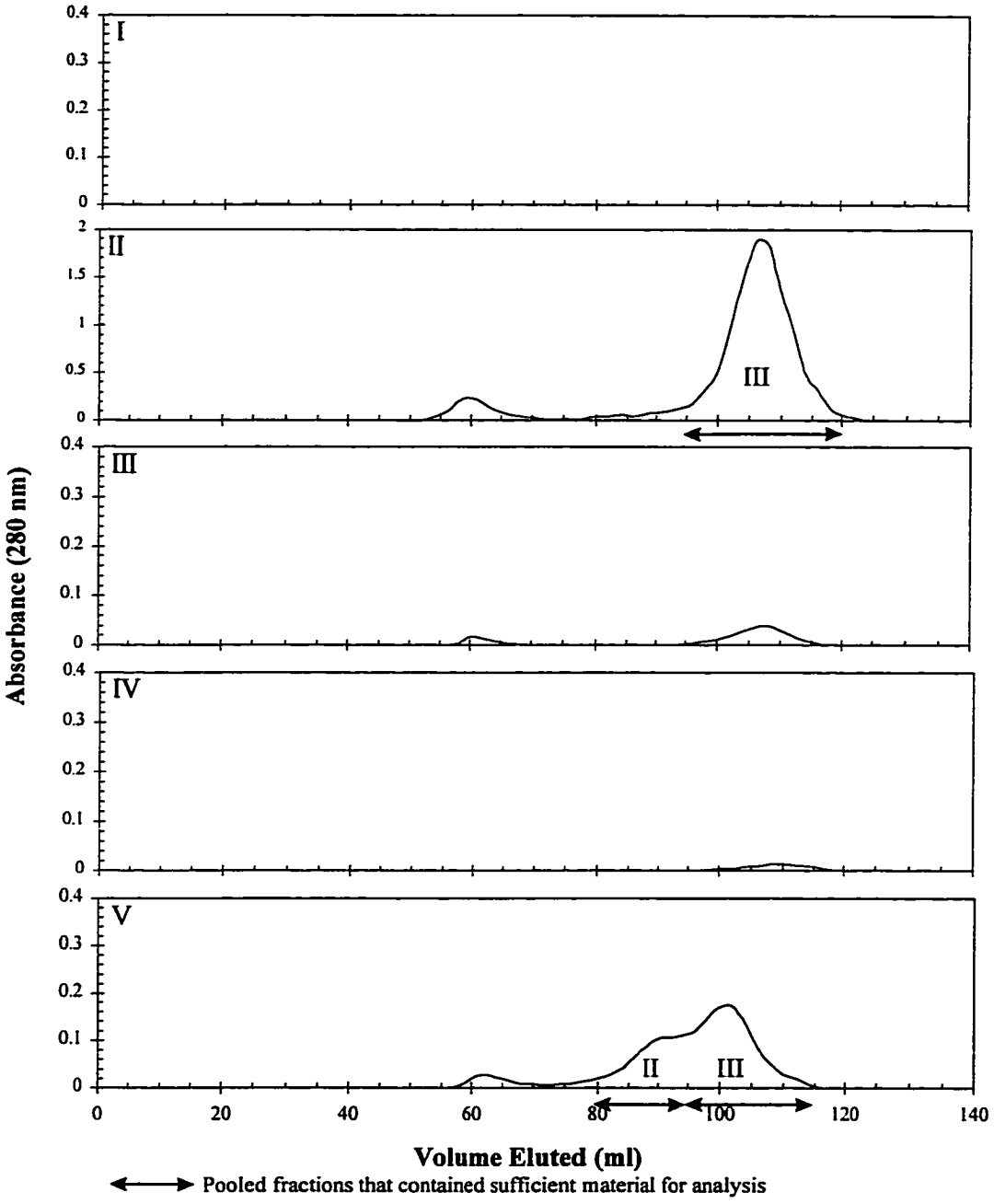

Figure 5.2- Superose 6B gel filtration elution profiles of Heparin-Sepharose chromatography fractions from the pooled d_{15}<1.21 g/ml fractions of control rats

Concentrated and dialyzed samples previously isolated by Heparin-Sepharose chromatography (**Figure 5.1A**) were separated by particle size on a Superose 6B gel filtration column (1.6 x 90 cm) and the elution (0.4 ml/min, 10 min/fraction) was monitored at 280 nm. Fractions under major peaks, as indicated by the arrows, were pooled, concentrated by dialysis and prepared for further characterization.

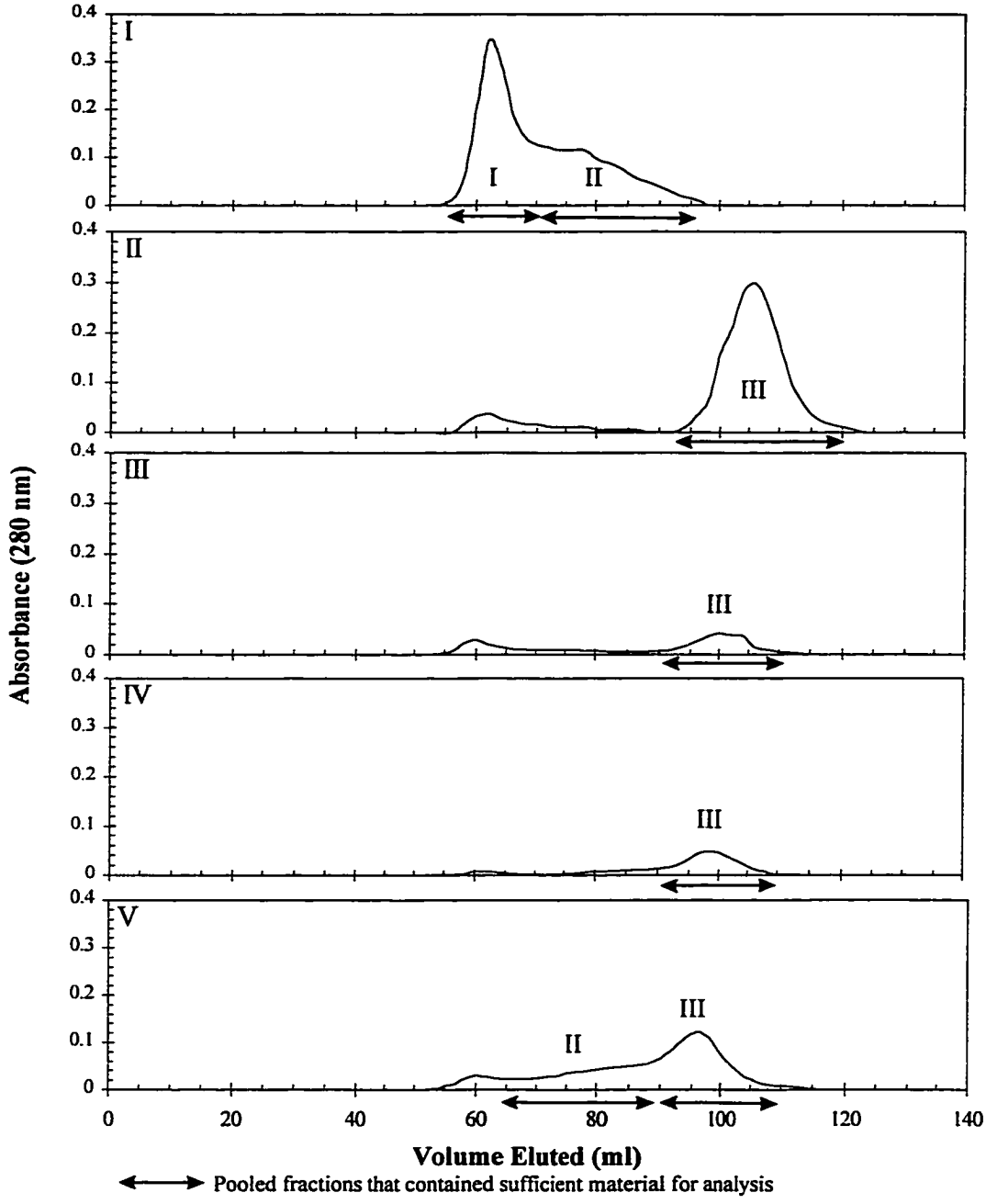

Figure 5.3- Superose 6B gel filtration elution profiles of Heparin-Sepharose chromatography fractions from the pooled d_{15}<1.21 g/ml fraction of ANIT-treated rats

Concentrated and dialyzed samples previously isolated by Heparin-Sepharose chromatography (**Figure 5.1B**) were separated by size on a Superose 6B gel filtration column (1.6 x 90 cm) and the elution (0.4 ml/min, 10 min/fraction) was monitored at 280 nm. Fractions under major peaks, as indicated by the arrows, were pooled, concentrated by dialysis and prepared for further characterization.

As expected from the ANIT-treated rat time course study (chapter 4), the separation procedure demonstrated significant particle heterogeneity in the pooled d_{15}<1.21 g/ml fraction of ANIT-treated rat plasma as compared to that of a control. Of particular note was the appearance of unbound material (**Figure 5.1B**, profile I) that was not present after Heparin-Sepharose chromatography of the control pool (**Figure 5.2A**). While there appeared to be relative changes in the distribution of lipoprotein classes as indicated by comparison of the control and ANIT profiles in **Figure 5.2** and **5.3**, overall conclusions cannot be made as recoveries of the total lipid present in the plasma of rats used for the purification were 26% for the control pool and only 11% for the ANIT pool after Superose 6B gel filtration.

The major losses did not occur as a result of the ultracentrifugation step, as control and ANIT pool recoveries were 101 and 96% respectively. However, as the characterization results will suggest, this does not rule out the possibility that the single spin ultracentrifugation method used may have resulted in aggregation of the lipoproteins to the top of the ultracentrifuge tube. This may have especially been a problem in the ANIT pool, as material at the top of the tube was very dense and packed. Even though the material did resolubilize during sample collection, the strong possibility exists that large aggregates were formed which would not pass through the column filter onto the Heparin-Sepharose column causing a concomitant loss of lipoprotein particles. While this may in part explain some of the losses in the ANIT particle purification, it is unlikely that significant aggegration occurred in the control purification as most of the expected particles would be HDL, which do not aggregate as easily as larger particles. Furthermore, no material needed to be resolubilized after the ultracentrifugation step.

This suggests that the majority of sample lost in the control purification came during the many handling steps, including possible aggregation and adherance to the dialysis membrane during the multiple dialysis steps. It should be noted, that in **Figures 5.2** and **5.3** there appear to be small peaks in chromatograms II, III, IV and V of large diameter material. An attempt was made to analyse these for lipid and protein content; however, there was little recoverable material associated and as such their absorbance (280 nm) relative to characterizable peaks may be more reflective of turbidity in the fraction and less on protein content.

Qualitative apolipoprotein distribution analysis in the purified fractions was performed by sodium dodecyl sulfate polyacrylamide gradient gel electrophoresis and non-denaturing gradient gel electrophoresis was used to estimate purified particle size. Lipid and protein compositional data was obtained by total lipid profiling and a modified BCA protein assay (described in methods). Finally phosphotungstic acid negative staining electron microscopy was employed to verify particle size and look for abnormalities in lipoprotein structure. The following data is only for lipoprotein fractions isolated from the ANIT pool as only HDL and a small LDL were recovered from the control pool. There was not enough normal LDL (**Figure 5.3, fraction V-II**) to fully characterize, nor was the electron microscopy successful in providing images of any particles from the control pool. However, a reasonable comparison can be made between the lipoproteins purified from the ANIT pool and the characterization performed at the 0 and 48 hour time points of the ANIT-treated rat time course study.

Sodium dodecyl sulfate polyacrylamide gradient gel electrophoresis of the lipoproteins purified from the ANIT pool (**Figure 5.4**) showed that gel filtration fractions I-I and I-II (**Figure 5.3**) from the unbound Heparin-Sepharose fraction I (**Figure 5.1**) contained apolipoprotein E, B_{100}, B_{48} and A-IV but no albumin. This result was unexpected for two reasons, firstly Lp-X was expected to be found in these fractions with associated albumin and not apolipoprotein B. Secondly, apolipoprotein B was expected to bind with high affinity to the column. While it might be argued that the presence of apolipoprotein B in the unbound fraction indicated column overloading, this was not likely the case as apolipoprotein B was present in fraction I-I (**Figure 5.4**) which did not have a corresponding bound apolipoprotein B containing fraction (**Figure 5.3**, profile V).

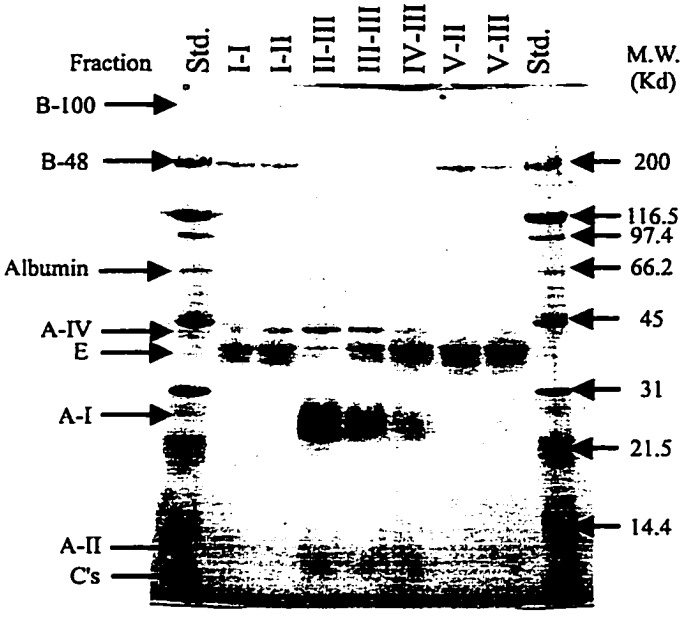

Figure 5.4- Sodium dodecyl sulfate polyacrylamide gel electrophoresis (5-19%) of purified ANIT rat (48 h, 150 mg/kg) lipoproteins

Fractions from the purification procedure containing sufficient protein for complete characterization were analyzed for apolipoprotein composition by sodium dodecyl sulfate polyacrylamide gradient gel electrophoresis (5-19%). Twenty μg of protein was loaded in each lane. Molecular weight standards were broad range (Bio-Rad) of the indicated molecular weights.

Therefore, this result indicated either the presence of very unusual apoliprotein B containing particles that do not bind to Heparin-Sepharose and/or aggregation of apolipoprotein B containing particles to themselves and/or Lp-X like lipoproteins.

The weak binding of lipoproteins containing primarily apolipoprotein A-I and A-IV (**Figure 5.4**, fraction II-III) and not apolipoprotein E was not expected, however this does not appear to be specific for ANIT-treated rat lipoproteins, as a similar result was obtained with the corresponding fraction from a control pool (data not shown). Fractions III-III and IV-III appear to contain lipoproteins associated with apolipoprotein A-I and E and as expected there appears to be a quantitative relationship between apolipoprotein E composition and NaCl elution concentration. Based on this data alone, fraction II-III appears to correspond to HDL_3, fraction III-III to HDL_2 and fraction IV-III to HDL_1. Fraction V-II was found to contain apolipoprotein E, B_{48} and B_{100} with fraction V-III being similar to V-II but containing more apolipoprotein B_{48} and less B_{100}. As such these fractions may be expected to correspond to either LDL, IDL, VLDL, remnants and/or unusual cholestatic apolipoprotein B containing lipoproteins.

Estimation of particle diameter by non-denaturing polyacrylamide gel electrophoresis was performed on the purified fractions from the ANIT pool and these results (**Figure 5.5**) were compared to those from a control rat in the ANIT-treated rat time course study (chapter 4, **Figure 4.11**). The particles in fraction I-I did not enter the gel matrix of the 2-16% gel which has an exclusion limit of about 400 Å (diameter) and as such can only be characterized as being >400 Å. The particles in fraction I-II entered the gel and a monodisperse population of particles ranging from an estimated 400 to 230 Å diameter were observed. Particle diameter estimation of fractions II-III, III-III and IV-

III further supported their tentative identifications as HDL_3, HDL_2 and HDL_1 respectively. Fraction II-III was polydisperse containing 3 identifiable populations having diameters of 170-100, 81-78 and 71-66 Å which were comparable to control rat HDL_3 diameters estimated from **Figure 4.11** at 140-110, 80 and 70 Å. The larger subfraction of ANIT HDL_3 does however, appear to have a larger diameter than the corresponding subfraction of control HDL_3. ANIT HDL_2 (III-III) was estimated to be monodisperse and range in diameter from 180-100 Å and was comparable to control HDL_2 having an estimated diameter (**Figure 4.11**) of 160-100 Å. ANIT HDL_1 (IV-III) was mondisperse and estimated to have a diameter ranging from 200-100 Å, a slightly broader distribution than control HDL_1 which had an estimated diameter of 200-140 Å. Fraction V-II contained a monodisperse lipoprotein distribution ranging from 350-220 Å which is comparable to control LDL (**Figure 4.11**) having a diameter of 340-260 Å. These particles which contain apolipoprotein B_{100} may correspond to LDL. The lipoproteins in fraction V-III also yielded a single broad band ranging from 270-140 Å, a size which is intermediary between control LDL and HDL_1. This fraction may consist of a heterogenous population of apolipoprotein B_{48} remnants and apolipoprotein E rich HDL_1.

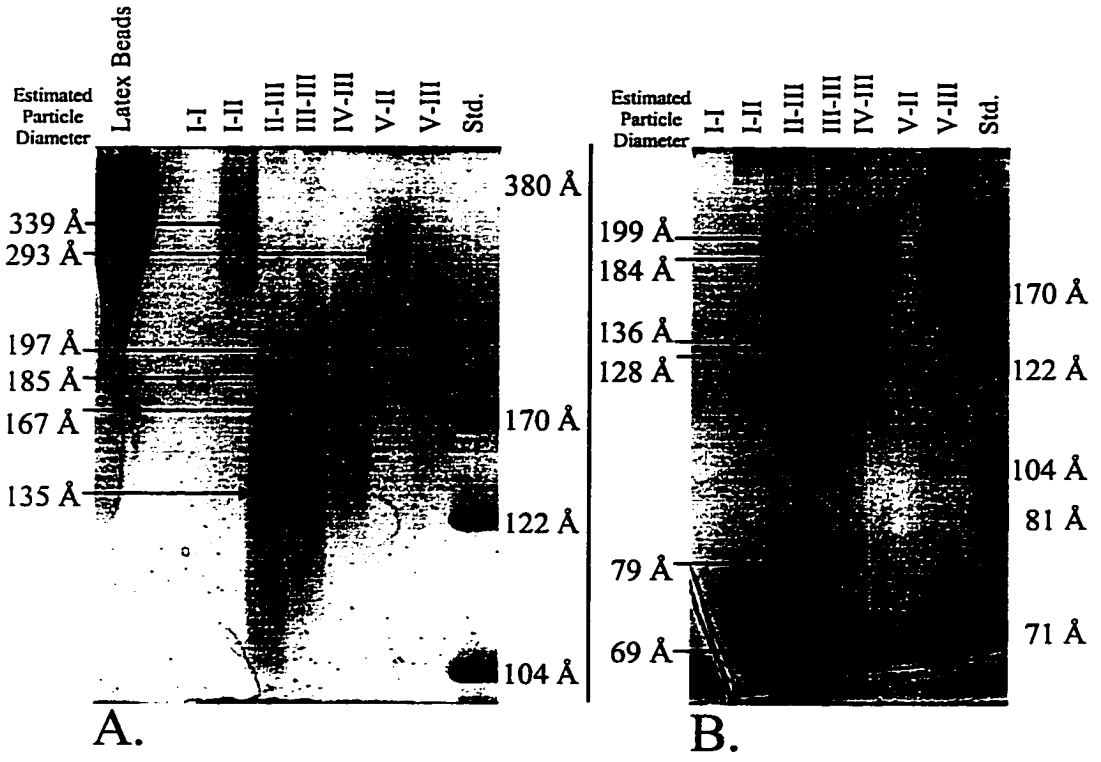

Figure 5.5- Non-Denaturing gels showing the estimated particle diameter of Heparin Sepharose and gel filtration purified lipoproteins from the ANIT pool

PAA gels (Isolab) 2-16% (A.) and 4-30% (B.) were loaded with 20 μg protein/lane, electrophoresed under non-denaturing conditions and stained with 0.2 % Coomassie Blue R-250 (186). Non-denatured high molecular weight standards of known stokes diameter (Pharmacia) and 0.038 μm latex beads (Duke Scientific) (2-16% gels) were run concurrently and the particle diameters were estimated by interpolation using the second order regression equation of R_f versus log (particle diameter).

Table 5.1- Comparison of isolated lipoprotein fractions between an ANIT-treated rat (150 mg/kg, 48 h) and a control rat. Lipoproteins (d_{15}>1.21 g/ml) characterized after isolation by a combination of Heparin-Sepharose affinity and gel filtration chromatography of pooled ANIT-treated rat plasma (48 h) were compared to control rat fractions isolated by density gradient ultracentrifugation. For ANIT-treated fractions, the approximate corresponding density range is given and for control rat fractions, the estimated chromatography fractions are shown. Chromatography fractions for control rats were correlated to the approximately equivalent density gradient fraction (based on preliminary chromatography results), as results from a complete separation were unavailable. Protein estimations for lipid-rich control fractions may be low as they were measured by a modified Lowry method (183) which yields lower protein concentrations than the modified BCA assay (described in methods) used for ANIT fractions.

ANIT Rat (48 h)

Lipoprotein Density	Chromatography Fraction	FC	CE	PL	TG	Prot	Surface: Core Ratio	Apo Distribution (approx.)	Est. Particle Diameter
?	I-I	17%	5%	57%	6%	16%	6.8	E>>B48≈B100≈AIV	>40 nm
?	I-II	10%	11%	58%	5%	18%	4.4	E>>B48≈B100≈AIV	40-23 nm
LDL	V-II	15%	9%	43%	0%	33%	6.3	E>>B48≈B100	35-22 nm
HDL_1/LDL	V-III	8%	14%	36%	0%	41%	3.0	E>>B48>B100	27-14 nm
HDL_1	IV-III	5%	12%	28%	0%	55%	2.7	E>AI≈AIV	20-11 nm
HDL_2	III-III	5%	13%	34%	0%	48%	3.1	AI>>E≈AIV>ALB	18-10 nm
HDL_3	II-III	4%	12%	38%	0%	46%	3.5	AI>>>AIV>E≈ALB	17-10, 8.1-7.8, 7.1-6.6 nm
Control Rat									
VLDL	V-I	3%	5%	19%	68%	6%	0.3	E>B100≈B48>C's>AI>A-IV	>40 nm
LDL	V-II	10%	32%	34%	18%	7%	0.9	E≈B100>B48	34-26 nm
HDL_1	IV-III	9%	27%	32%	3%	30%	1.4	E>>AI>AIV	20-14 nm
HDL_2	III-III	5%	22%	31%	1%	43%	1.6	AI>E≈AIV≈C's>AII>ALB	16-10 nm
HDL_3	II-III	4%	15%	21%	0%	61%	1.7	AI>>AIV>>E>AII>C's	14-11, 8, 7 nm

The results of the preliminary purification and characterization of the abnormal lipoproteins in the ANIT-treated cholestatic rat after 48 hours are presented with lipid and protein compositional data in **Table 5.1**. ANIT rat data, in the table, was organized according to purification fraction identification number (I.D.) with the approximate corresponding density class being indicated. Control rat data were obtained from density gradient ultracentrifugation results as shown in **Figure 4.11** and this data combined with preliminary control pool purification data were used to correlate density class with an approximate corresponding chromatography fraction.

All identified ANIT lipoprotein fractions had a very large surface to core ratio (6.8 to 2.7) compared to controls (1.7 to 0.3), due to the depletion of neutral lipid (mostly cholesteryl ester) and phospholipid enrichment. ANIT HDL fractions, although somewhat depleted in cholesteryl ester and rich in phospholipid would not be expected to be discoidal. The percentage compositional data support functioning LCAT activity in the ANIT rat (48 h) as significant cholesteryl ester was present in all HDL fractions. ANIT LDL, in comparison to normal rat LDL was extremely core depleted and enriched in phospholipid and free cholesterol. ANIT pool fractions I-I and I-II, although core depleted, contained significantly more cholesteryl ester and triacylglycerol than would be expected for vesicle-like particles (Lp-X). This data, combined with particle diameter and apolipoprotein compositional data strongly supports the conclusion that these particles are either extremely abnormal, phospholipid enriched apolipoprotein B containing remnant lipoproteins or aggregates of aplipoprotein B containing remnants

and vesicular lipoproteins like Lp-X.

Analysis of ANIT pooled fractions by electron microscopy (**Figure 5.6**) supported the particle diameter estimation data obtained by non-denaturing polyacrylamide gradient gel electrophoresis. The electron micrographs were not of high enough quality to support particle diameter measurements and population subspecies analysis. None of the electron micrographs support the presence of discoidal lipoproteins or stacked discs, as would be expected if discoidal HDL and Lp-X were present, however all of the particles appeared to have an irregular non-spherical shape and this may be the result of cholesteryl ester depletion and phospholipid enrichment and/or degradation of the lipoproteins as a result of the extensive and lengthy purification.

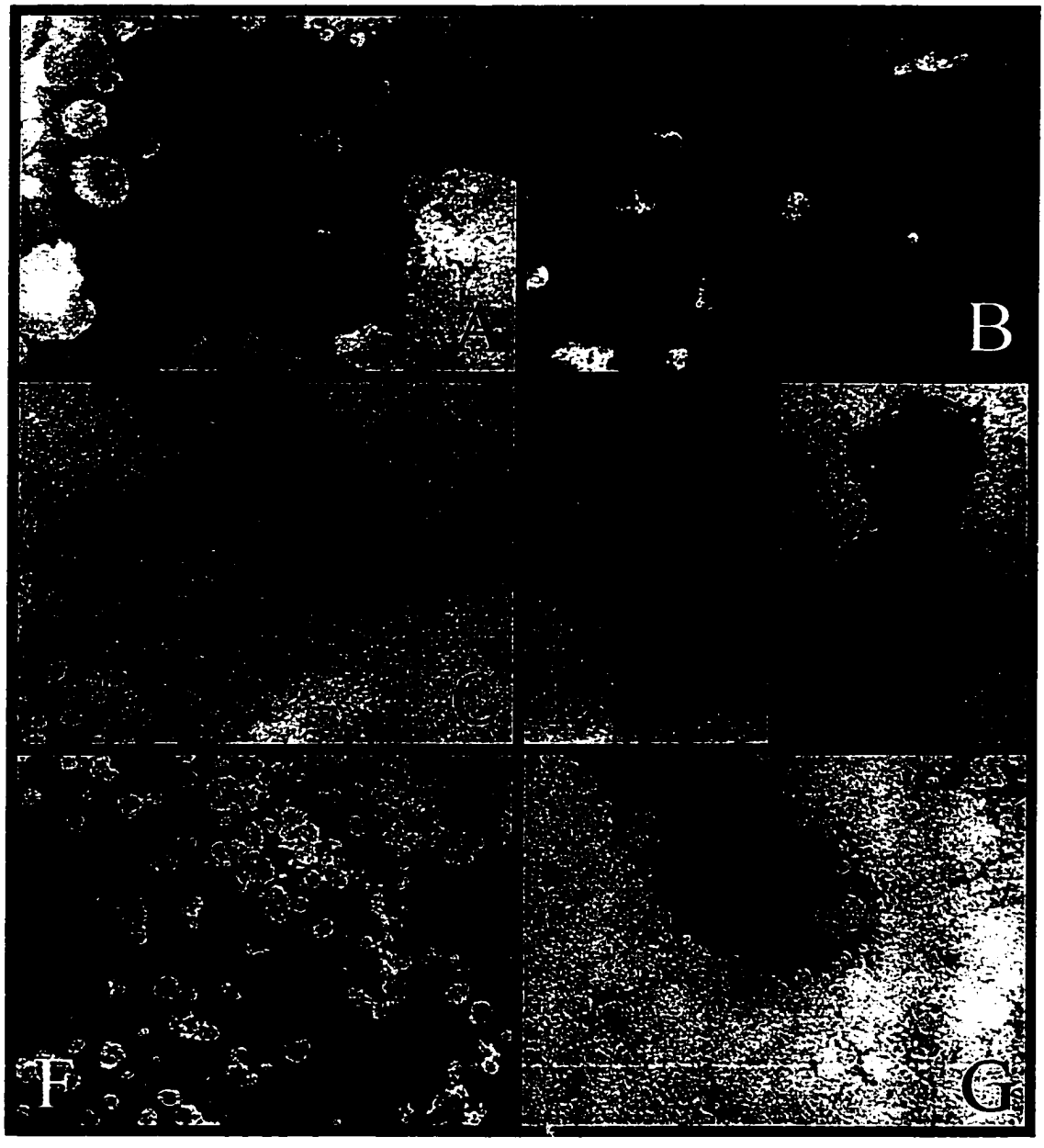

Figure 5.6- Electron micrographs of lipoprotein fractions purified from ANIT-treated rat (150 mg/kg, 48 h) plasma

Purified lipoprotein fractions were dialyzed against 20 mM ammonium bicarbonate, 0.01% Na_2EDTA buffer (pH 7.4) and and negatively stained on formvar coated copper grids with 2% sodium phosphotungstic acid (pH 7.4) (188) and photographed after viewing in an electron microscope (Phillips). Fraction I-I (A.), I-II (B.), IV-III (C.), III-III (D.), II-III (E.), V-II, (F.) and V-III (G.) are shown. Particles are shown at 153 000x.

Chapter 6- Studies in ANIT-treated mice

In collaboration with Dr. Lou Agellon at the University of Alberta, the effects of ANIT treatment (100 mg/kg) on both bile and plasma lipoprotein metabolism were initiated. Animal handling, plasma and liver lipid and lipoprotein analysis as presented in this thesis were performed by the author. Measurement of 7α-hydroxylase, cyp7 mRNA abundance, HMG CoA reductase activity and gallbladder lipid analysis were performed in the lab of Dr. Lou Agellon and are presented with permission to complement the data

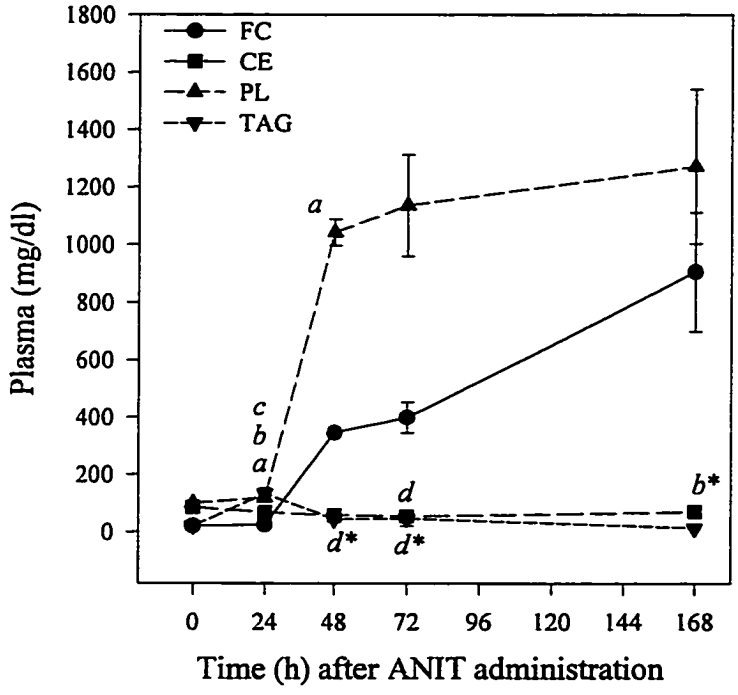

Figure 6.1- Mouse plasma lipids after ANIT administration
Points shown are for fasted mice and are the mean ± S.E.M. (0 h, n=6; 24 h n=2; 48 h n=10; 72 h n=3; 168 h n=3). The ANIT dosage was 100 mg/kg. ^{a}Free cholesterol (FC), ^{b}Cholesteryl ester (CE), ^{c}Phospholipid (PL) and ^{d}Triacylglycerol (TAG) measurements were not significantly different ($p < 0.05$) versus controls (0 h). *Points were not tested as the sample size was too small to reach a statistical conclusion.

collected by the author. This work is being continued through an on-going collaboration between the two labs.

Measurement of ANIT-treated C57BL/6 mouse plasma lipids (**Figure 6.1**), clearly demonstrated that 24 hours after ANIT administration, plasma phospholipid and free cholesterol began to rise with phospholipid reaching an apparent plateau between 48 and 168. Free cholesterol was elevated 17, 20 and 45 fold at 48, 72 and 168 hours respectively. Phospholipid was similarly increased by 10, 11 and 13 fold at 48, 72 and 168 hours. Cholesteryl ester was 60-80% of normal at all time points. These results are dramatically different than those observed in the ANIT-treated rat time course study (chapter 4), as the elevations in free cholesterol and phospholipid were significantly higher. Cholesteryl ester decreased in the ANIT-treated mouse and the CE/FC ratio dropped to 2% of normal by 168 hours with a concomitant reduction in cholesteryl ester mass. In the rat, cholesteryl ester mass increased and the CE/FC ratio was reduced to 25% of normal.

Table 6.1- Plasma parameters of liver damage and LCAT activity after ANIT treatment (48 h) in the mouse

LCAT activity was measured by a recombinant HDL method (described in methods). Bile acids, bilirubin, aspartate aminotransferase (AST) and alanine aminotransferase (ALT) were measured using kits.

		Control *n=4*	**ANIT 48 h** *n=5*	**Fold Change**
LCAT*	(nmol CE formed/ml/h)	10. 3±0.5	2.0±0.4	-5.2
Bile Acids*	(μmol/L)	11.9±3.5	3152±400	263
Bilirubin*	(μmol/L)	5.2±1.7	58.7±18.4	11
AST*	(I.U.)	26.6±6.1	197.3±64.0	7.4
ALT*	(I.U.)	1.5±0.5	6.4±1.7	1.5
AST/ALT		21.1±5.9	31.7±5.9	1.5

Mean ± S.E.M.

*Significant versus Control at $p<0.05$

This gross depletion of plasma cholesteryl ester observed in the ANIT-treated mouse was very suggestive of LCAT deficiency, an effect that was not observed in the ANIT-treated rat. Indeed, in the ANIT-treated mouse, LCAT activity was reduced to 20% of normal at 48 hours (**Table 6.1**). Forty eight hours after ANIT treatment, plasma bile acids were elevated 264 fold, and bilirubin levels, aspartate aminotransferase and alanine aminotransferase activities were increased. Although the elevation in plasma bile

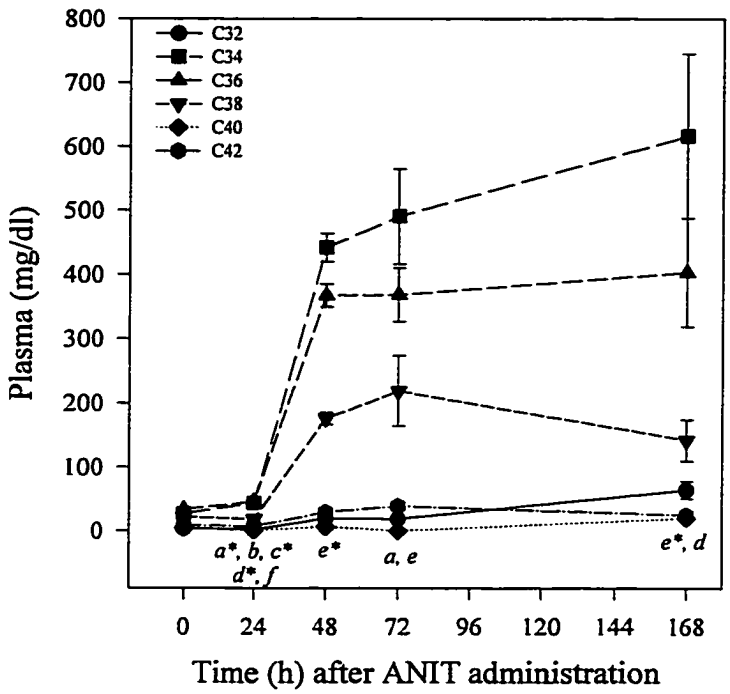

Figure 6.2- Mouse plasma phospholipid molecular species with time after ANIT administration (100 mg/kg)

Points shown are for fasted mice and are the mean ± S.E.M. (0 h, n=6; 24 h, n=2; 48 h, n=10; 72 h, n=3; 168 h, n=3). Carbon numbers in the legend refer to the total carbons from the two fatty acyl moieties and do not include the 3 carbons in the glycerol backbone. C-16/18, C-18/18 and C-18/20 are likely the major fatty acid combinations represented by C-34, C-36 and C-38 molecular species as identified by gas chromatographic total lipid profiling (174). ^{a}C-32, ^{b}C-34, ^{c}C-36, ^{d}C-38, ^{e}C-40 and ^{f}C-42 phospholipid measurements were not significantly different ($p < 0.05$) versus controls (0 h). *Points were not tested as the sample size was too small to reach a statistical conclusion.

acids was higher at 24 hours than at any time point in the ANIT treated rat, bilirubin levels were lower and the reduced activities of alanine and aspartate aminotransferases suggest that liver damage may be less severe in ANIT-treated mice (48 h). Plasma triacylglycerol (**Figure 6.1**) was elevated maximally (6.5 fold) 24 hours after ANIT administration with the major triacylglycerol molecular species being C54. C54 most likely corresponds to a triacylglycerol containing fatty acyl side chains of C18/18/18 and may indicate that by 24 hours there was a reduction in chylomicron remnant clearance that was exacerbated by the corn oil bolus used to administer ANIT.

Analysis of plasma phospholipid molecular species by gas chromatographic total lipid profiling (174) (**Figure 6.2**) indicated, as in the ANIT-treated rat, that the elevation of plasma phospholipids was due to those species containing medium chain length fatty acyl moieties. In particular, those containing 34, 36 and 38 carbons which likely correspond to phospholipids containing C16/18, C18/18 and C18/20 fatty acyl groups respectively. Phospholipid molecular species analysis of hepatic tissue (**Figure 6.3**) indicated that these same phospholipid molecular species were predominant in the liver; however, the relative proportions of C34:C36:C38 was inversely related to those in plasma. Thus either the majority of plasma phospholipid entering the plasma following ANIT treatment was not of hepatic tissue origin or there was a selective release of phospholipid molecular species. As the increased plasma phospholipid is thought be of biliary origin, refluxing into the plasma as a result of cholestasis, it may be pertinent to measure gallbladder bile phospholipid molecular species.

Analysis of plasma cholesteryl esters (**Figure 6.4**) demonstrated that the reduction in cholesteryl ester mass at 48 and 72 hours was due to C18 and C20 molecular species. Although there appears to be a slight increase in C16 cholesteryl ester mass at 48, 72 and 168 hours, this increase was either not statistically significant or the sample size was too small to reach a statistical conclusion using Dunns or Dunnetts multiple comparison procedure.

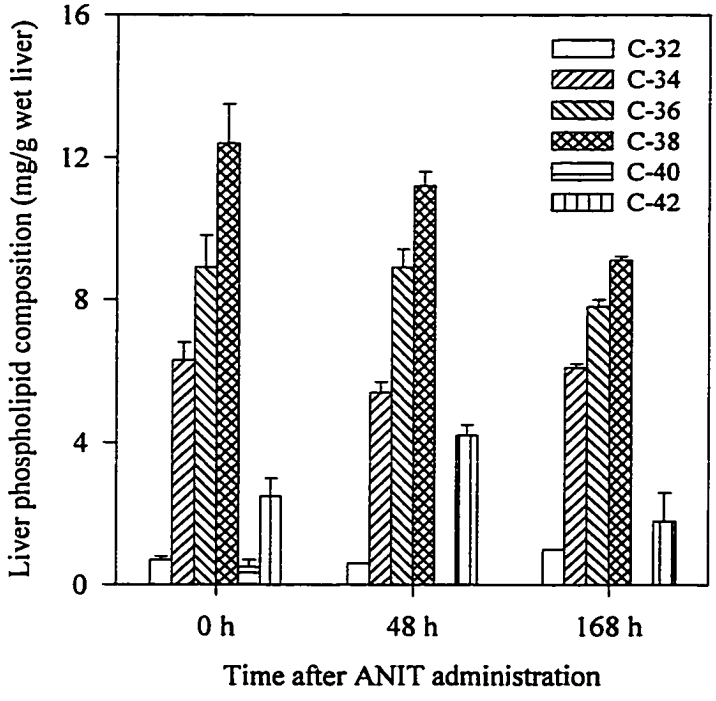

Figure 6.3- Mouse liver phospholipid molecular species with time after ANIT administration (100 mg/kg)

Points shown are for fasted mice and are the mean ± S.E.M. (0 h, n=6; 48 h, n=10; 168 h, n=3). Carbon numbers in the legend refer to the total carbons from the two fatty acyl moieties and do not include the 3 carbons in the glycerol backbone. C-16/18, C-18/18 and C-18/20 are likely the major fatty acid combinations represented by C-34, C-36 and C-38 molecular species as identified by gas chromatographic total lipid profiling (174).

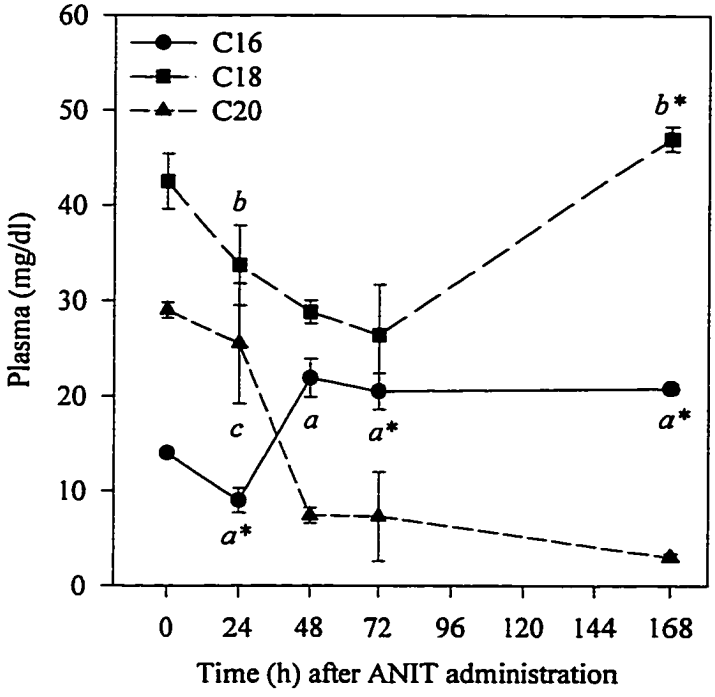

Figure 6.4- Mouse plasma cholesteryl ester molecular species with time after ANIT administration (100 mg/kg)

Points shown are for fasted rats and are the mean ± S.E.M. (0 h, n=6; 24 h, n=2; 48 h n=10; 72 h; n=3, 168 h; n=3). Carbon numbers in the legend refer to total fatty acyl chain carbons as determined by gas chromatographic total lipid profiling (174) and do not include carbons derived from cholesterol. ^{A}C-16, ^{b}C-18 and ^{c}C-20 cholesteryl ester measurements were not significantly different ($p < 0.05$) versus control (0 h). *Points were not tested as the sample size was too small to reach a statistical conclusion.

Measurement of hepatic tissue lipids (**Figure 6.5**) showed that with the exception of triacylglycerol (48 h), lipid content was virtually unchanged following ANIT treatment. The large elevation of liver triacylglycerol at 48 hours was abolished by 168 hours without a noticeable effect on plasma triacylglycerol (168 h). This suggests that VLDL synthesis and/or secretion may have been inhibited at 48 hours and then restarted at some point between 48 and 168 hours. If lipoprotein lipase was functional (not measured), as in the ANIT rat, VLDL triacylglycerol entering the plasma during this time span may have been normally hydrolyzed without an observable increase of plasma

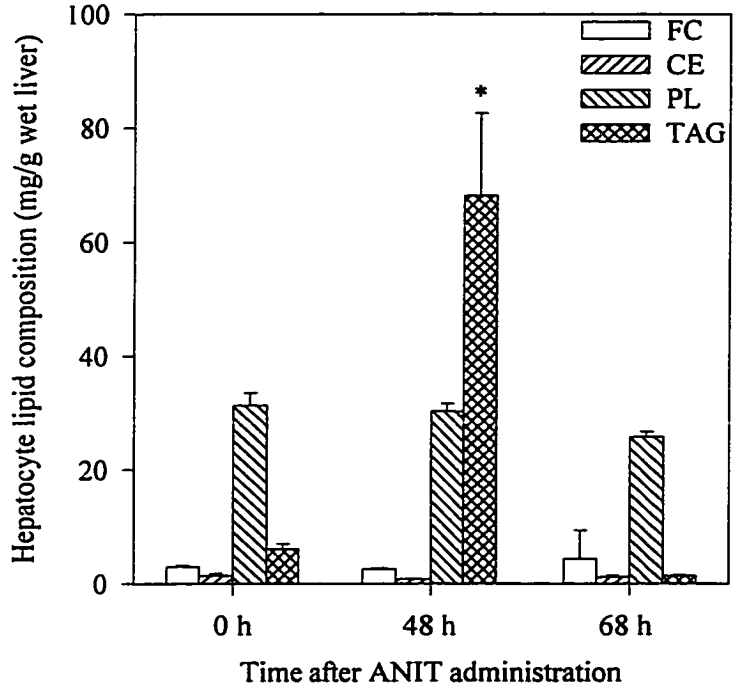

Figure 6.5- Mouse liver lipids following ANIT administration (100 mg/kg).
Points are the mean ± S.E.M. (0 h, n=6; 48 h, n=10; 168 h, n=3). FC, free cholesterol; CE, cholesteryl ester; PL, phospholipid; TAG, triacylglycerol. Lipids were measured by by gas chromatographic total lipid profiling (174) following extraction with 2:1 chloroform:methanol (175). *Significant versus control at $p < 0.05$, all other data was either not signifcant or the sample size was too small to reach a statistical conclusion.

triacylglycerol.

The fact that liver cholesterol and phospholipid content was virtually unchanged (**Figure 6.5**) following ANIT treatment, even though large increases of plasma phospholipid and free cholesterol of probable hepatic origin were observed, strongly suggests that liver phospholipid and cholesterol synthesis were functioning. Conformation of cholesterol synthesis by assay of HMG CoA reductase activity (**Figure 6.6**) clearly demonstrated a significant increase in liver microsomal HMG CoA reductase

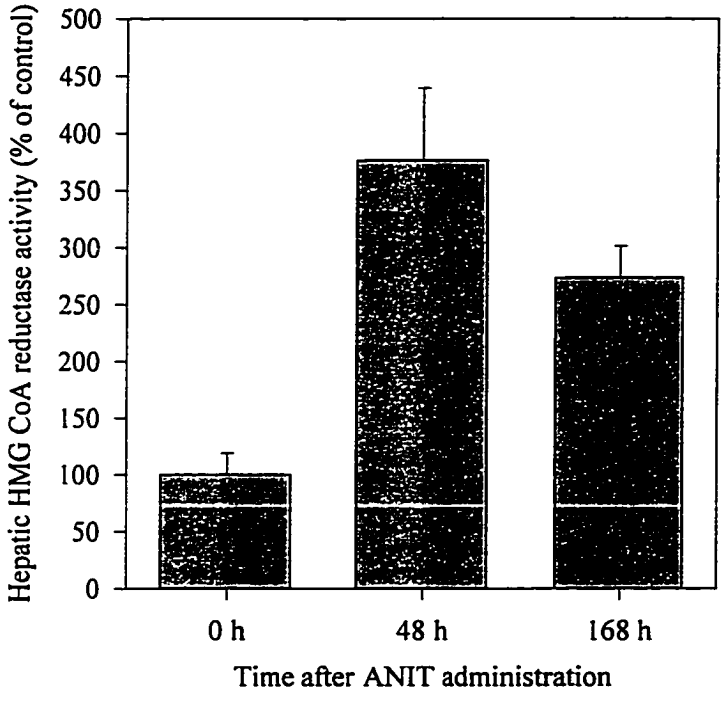

Figure 6.6- Mouse hepatic HMG CoA reductase activity with time after ANIT administration (100 mg/kg)

Points are shown as percent of control and are the mean ± S.E.M. (n=3). The data used in this figure was courtesy of Dr. Lou Agellon and was used with permission. The assay of HMG CoA reductase was based on the conversion of labelled HMG CoA to mevalonolactone by mouse liver microsomes (standardized by protein mass) and separation of the product by TLC as previously described (189). Measurements at both 48 and 168 h were significant versus controls at $p < 0.05$.

activity of 3.8 and 2.7 fold at 48 and 72 hours, respectively. While phospholipid synthesis was not measured, the stability of liver phospholipid levels following ANIT treatment indicated that it was normal or possibly elevated.

To characterize and compare the changes in mouse lipoprotein composition following ANIT-induced intrahepatic cholestasis, density gradient ultracentrifugation was performed on normal C57BL/6 (**Figure 6.7A**) and ANIT-treated (48 h) (**Figure 6.7B**) pooled mouse plasma. The alterations in lipoprotein density distribution were dramatic and consistent with plasma lipid levels at 48 hours. All fractions in the ANIT-treated mouse profile were highly enriched in phospholipid and free cholesterol and nearly devoid of neutral lipid. In the control profile, as would be expected for a mouse, almost all of the plasma lipid was located within the HDL density range (fractions 12-18) with the exception of fractions 5-11 which contained a small amount of LDL. Compared to the ANIT-treated rat at 48 hours, the alterations in the ANIT-treated mouse lipoprotein distribution were similar, but more extreme, as the fractions contained much less neutral lipid and an even larger percentage of plasma lipoproteins was found in the LDL density range (fractions 5-15).

Further analysis of the density gradient fractions by sodium dodecyl sulfate polyacrylamide gradient gel electrophoresis (5-19%) (**Figure 6.8A and B**) revealed minor alterations in the density distribution of plasma apolipoproteins. In the ANIT-treated mouse pool (**Figure 6.8B),** fractions 8-10 which were associated with the majority of plasma lipoprotein mass were composed of primarily apolipoprotein E, A-IV, some A-I and a small amount of B_{100} and B_{48}. In the corresponding control mouse fractions, as would be expected for LDL, apolipoprotein B_{100} and E were the primary constituents.

Interestingly, there was no apolipoprotein A-IV detected in these fractions and very little to none in any control mouse density fraction. In the ANIT-treated mouse (48 h) significant amounts of apolipoprotein A-IV was detected in fractions 8-16. The density distrubution of apolipoprotein B in the ANIT-treated mouse was similar to that observed in the ANIT-treated rat with detectable levels of both apolipoprotein B_{100} and B_{48} being observed well into the HDL density fractions. Thus in ANIT-induced intrahepatic cholestasis in the mouse, like the rat, there may be impaired remnant lipoprotein catabolism. The distribution of apolipoprotein A-I in ANIT-treated mouse HDL fractions (**Figure 6.8B**, fractions 12-22) was similar to that of the control mouse; however, there was an obvious increase in both apolipoprotein E and A-IV in the lower density HDL fractions (fractions 12-15), suggesting decreased uptake of HDL containing apolipoprotein E by the liver. While the function of apolipoprotein A-IV is not well understood, the presence of apolipoprotein A-IV in ANIT-treated HDL fractions may be indicative of its affinity for phospholipid.

Overall, the density gradient lipid and apolipoprotein composition data are consistent with the presence of Lp-X like vesicles in the LDL density range of the ANIT-treated mouse (48 h). However, three pieces of evidence suggest a cautious conclusion: firstly, no albumin (consistent with Lp-X) was present in these density gradient fractions; secondly, agar electrophoresis (not shown) was negative for Lp-X in ANIT-treated mouse plasma (48 h); and, thirdly the ANIT-treated rat particle purification failed to conclusively demonstrate Lp-X.

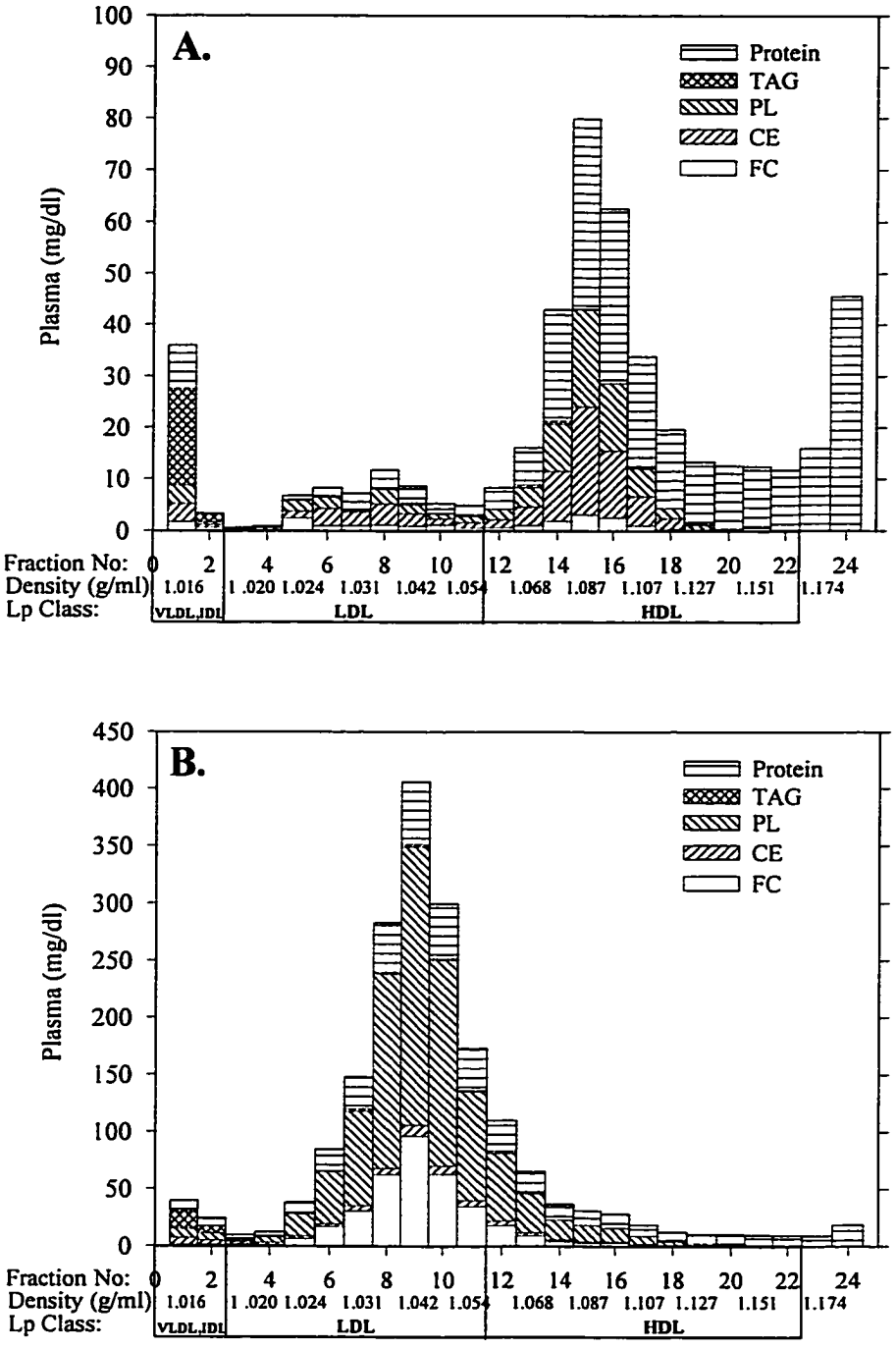

Figure 6.7A and B- Control and ANIT-treated (48 h) mouse lipoprotein mass distributions following density gradient ultracentrifugation

To obtain enough material for lipoprotein analysis the plasma from 6-10 mice was pooled. Control (A.); ANIT-treated (48 h) (B.). Only fractions 1-24 are shown, as fractions 25-30 were devoid of lipid. FC, free cholesterol; CE, cholesteryl ester; PL, phospholipid; TAG, triacylglycerol; Lp, lipoprotein.

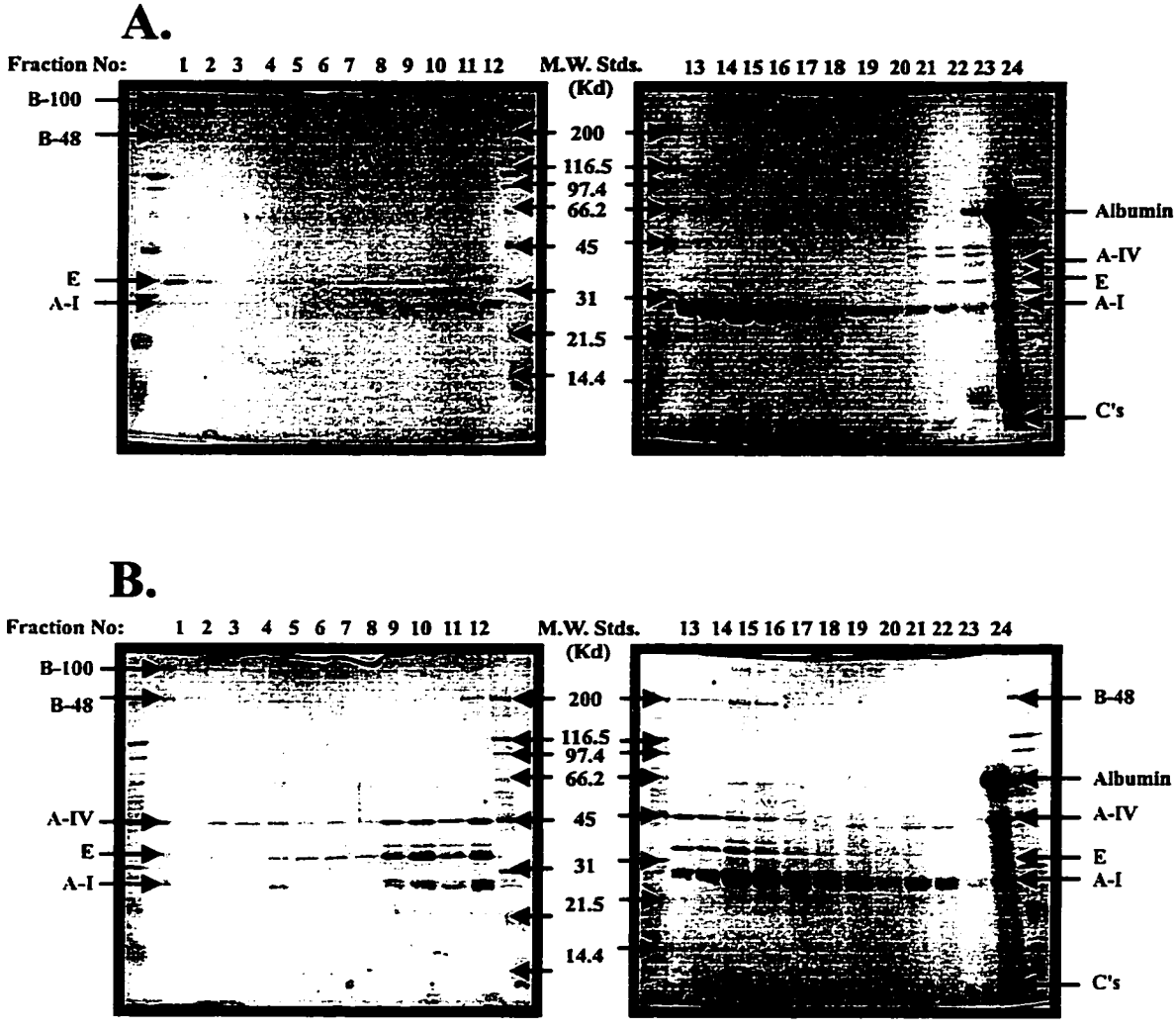

Figure 6.8A and B- Sodium dodecyl sulfate polyacrylamide gradient gels of mouse density gradient fractions 1-24 after density gradient ultracentrifugation

A control mouse pool (A.) is shown compared to an ANIT-treated (48 h) mouse pool (B.). Twenty μg of protein was loaded into each lane (Fig. 6.8A., fractions 1-12 <20 μg; Fig. 6.8B., fractions 1-8 <20 μg). Molecular weight standards were broad range (Bio-Rad) of the indicated molecular weights.

To better understand the effect of ANIT treatment on bile acid metabolism, cyp7 mRNA and 7α-hydroxylase (cyp7 gene product) activity were examined in mouse liver microsomes from control and ANIT-treated mice. 7α-hydroxylase activity (**Figure 6.9**) was reduced to 43% of control levels 48 hours after ANIT treatment; however, Statistically this was not a significant change. Measurements of 7α-hydroxylase activity were also performed at 24, 48 and 72 hours by an endogenous methodology. The results at all three time points were 24% , 22% and 15% of control levels, respectively, and the

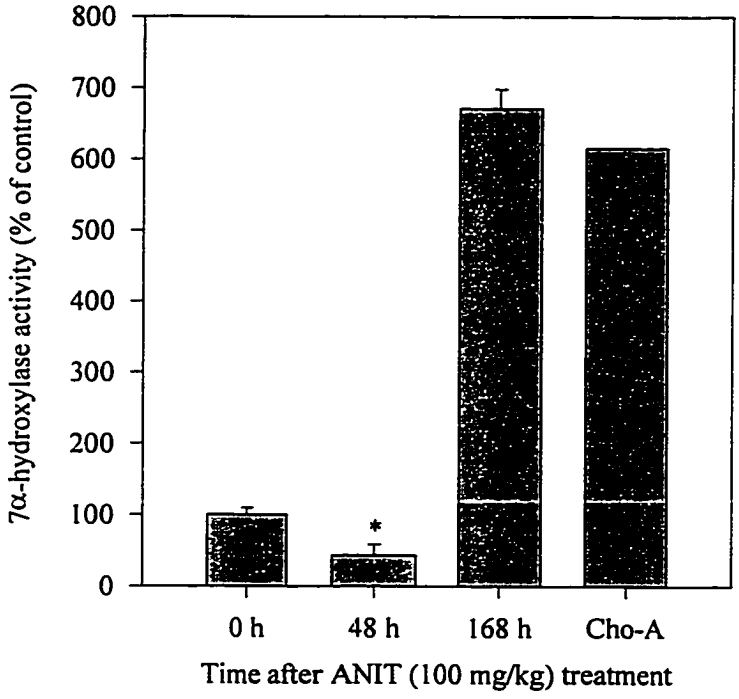

Figure 6.9- Mouse liver 7α-hydroxylase activity with time after ANIT treatment
Mouse liver microsomes (n=3, per time group, equal protein mass) were assayed by Dr. Lou Agellon's lab according to the reverse-phase HPLC method of Chiang (190) as outlined by Rudel *et al.* (191). Data is presented as the percent of control of 7α-hydroxy cholesterol peak areas. Liver microsomes from mice fed the bile acid sequesterant cholestyramine (Cho-A) were concurrently assayed as a high level control. *measurements were not significantly different ($p < 0.05$) versus controls (0 h).

48 hour value of 22% was consistent with 2 out of three 3 measurements used to calculate the mean 7α-hydroxylase activity at 48 hours (**Figure 6.9**). Unfortunately, due to the change in methodology, these values may be different than those shown as the assay did not differentiate between the relative contributions of the neutral and acidic bile acid synthesis pathways and assumes a constant cholesterol:protein ratio within the mouse liver microsomes. The results shown (**Figure 6.9**) were based on the conversion of exogenous radiolabelled cholesterol by 7α-hydroxylase to 7α-hydroxy cholesterol, which was quantitated by reverse-phase HPLC (190) as described by Rudel *et al.* (191). While it appears that 7α-hydroxylase was somewhat inhibited in the mouse following ANIT-induced intrahepatic cholestasis, between 24 and 72 hours, the effect was abolished by 168 hours with a 6.5 fold increase in enzymatic activity. This level of induction was comparable to that observed in cholestyramine treated mouse liver microsomes (**Figure 6.9**) used as a high level control.

Reverse transcriptase polymerase chain reaction (rt-PCR) analysis of cyp7 mRNA (**Figure 6.10**) showed that cyp7 gene transcription was completely inhibited at 24, 48 and 72 hours. This effect was reversed at 168 hours, as cyp7 mRNA abundance was approximately equal to or greater than the 0 hour time point. An induction in transcription at 168 hours would not be unreasonable given the large increase in 7α-hydroxylase activity observed. The lack of cyp7 mRNA at 24, 48 and 72 hours, suggests transcriptional regulation may be occurring due to either feedback inhibition by bile acids, liver cholesterol levels and/or ANIT-induced liver damage.

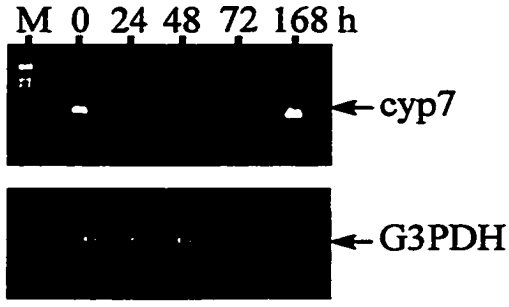

Figure 6.10- Mouse liver cyp7 mRNA abundance with time after ANIT administration cyp7 mRNA abundance was measured in the lab of Dr. Lou Agellon by a reverse transcriptase PCR method developed in-house. Glyceraldehyde-3-phosphate dehydrogenase (G3PDH) mRNA was measured concurrently as an internal control. 7α-hydroxylase is the enzyme product of the cyp7 gene. M, 1 Kb molecular weight standards (Gibco-BRL).

Preliminary enzymatic analysis of gallbladder biliary lipid and bile acid concentrations, cautiously (very small sample size) indicated in the mouse that ANIT-induced intrahepatic cholestasis results in a reduction of the ratio of both phospholipid and bile acids to cholesterol at 48 and 168 hours. These results potentially implicate the gallbladder bile as a potential source of the elevated plasma phospholipid and bile acids if biliary constituents are secreted into the intestine and reabsorbed normally. Unfortunately, gallbladder bile volume was not measured, such that absolute mass values for bile components could not be calculated.

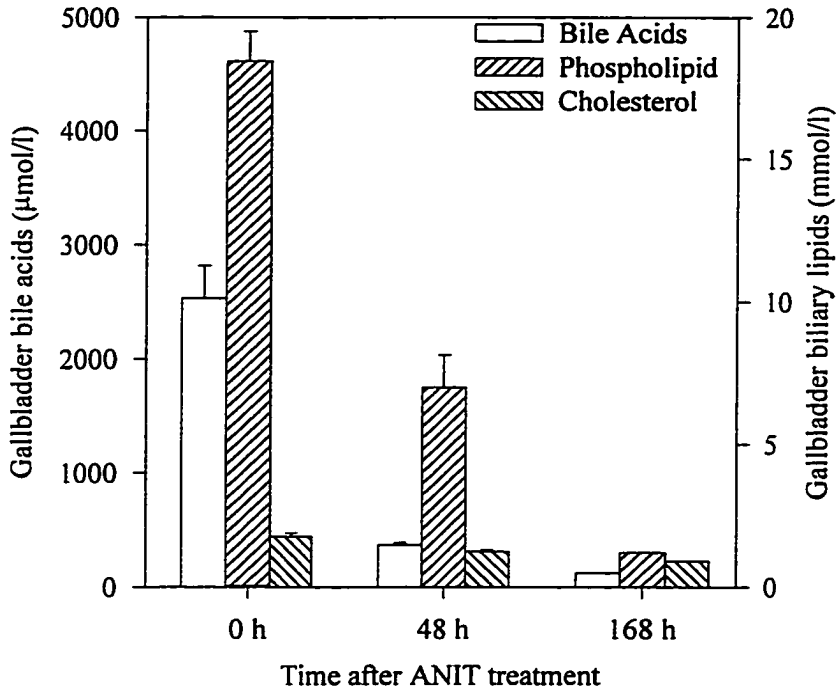

Figure 6.11- Mouse gallbladder biliary lipid and bile acid concentrations following ANIT administration

Mouse gallbladder bile, collected by the author, was analyzed by Dr. Lou Agellon at the University of Alberta. Total cholesterol (Sigma), phospholipids (WAKO) and bile acids (Sigma) were measured enzymatically with kits from the indicated manufacturers. (n=2, 0 h; n=2, 48 h; n=1, 168 h).

Chapter 7- ANIT-induced intrahepatic cholestasis in TgR[HuAI] rats

A transgenic rat strain (TgR[HuAI]) with a high level of liver specific human apolipoprotein A-I expression was developed by Swanson *et al.* (147) and obtained from Sandoz by Dr. Dolphin and the author. Analysis of plasma human and rat apolipoprotein A-I by immunological methods demonstrated that plasma from these rats contains a wide ranging concentration of both human and rat apolipoprotein A-I. Human apolipoprotein A-I levels measured in rats of the TgR[HuAI] rat strain were found to vary between 0 and greater than 1000 mg/dl. Circulating rat apolipoprotein A-I was rarely observed above 120 mg/dl (normal Spraque-Dawley rat approx. 80 mg/dl) and showed an inverse relationship to human apolipoprotein A-I. In most cases, TgR[HuAI] rats having a plasma human apolipoprotein A-I concentration greater than approximately 200 mg/dl did not have detectable rat apolipoprotein A-I. Plasma apolipoprotein E and B levels were measured in some TgR[HuAI] rats, however there was no apparent correlation between the levels of these apolipoproteins and human apolipoprotein A-I.

Correlation of human apolipoprotein A-I levels with plasma lipids by linear regression analysis (**Figure 7.1**) revealed a near linear relationship between human apolipoprotein A-I levels and plasma phospholipid, free cholesterol and cholesteryl ester. There was no apparent relationship between plasma triacylglycerol and human apolipoprotein A-I. This data combined with personal observations indicates that circulating human apolipoprotein A-I levels in TgR[HuAI] rats are proportional to HDL levels.

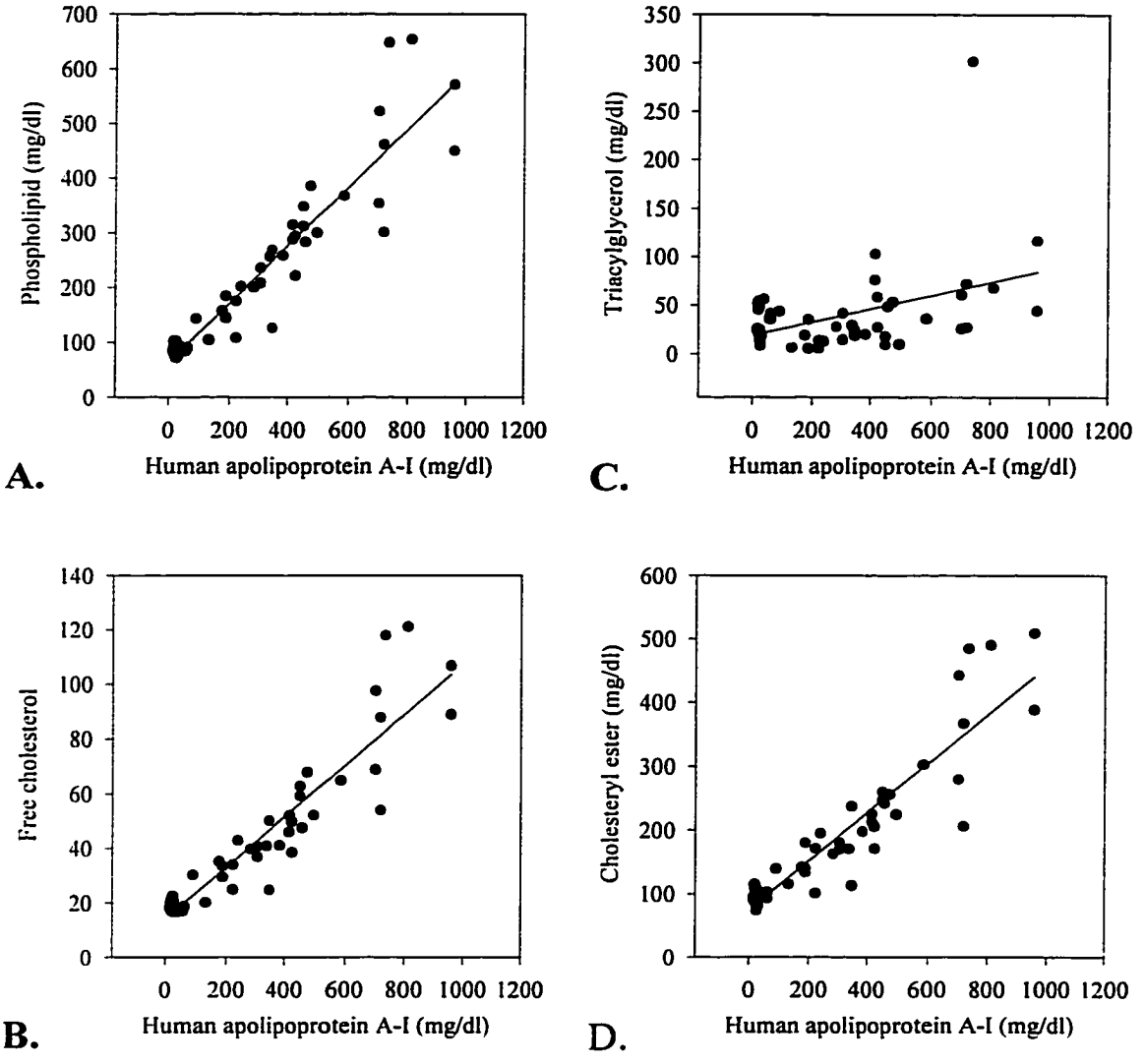

Figure 7.1- Correlation of human apolipoprotein A-I levels with plasma lipids in TgR[HuAI] rats

A random sampling (n=54) of TgR[HuAI] rat plasma was assayed for human apolipoprotein A-I by nephelometry (Behring). These values were correlated by linear regression analysis with plasma lipids measured by gas chromatographic total lipid profiling (174). Whole plasma human apolipoprotein A-I levels were found to most closely correlate with phospholipid (R=0.936) followed by free cholesterol and cholesteryl ester (R=0.929 and R=0.921 respectively). There was only a very weak correlation with plasma triacylglycerol (R=0.424).

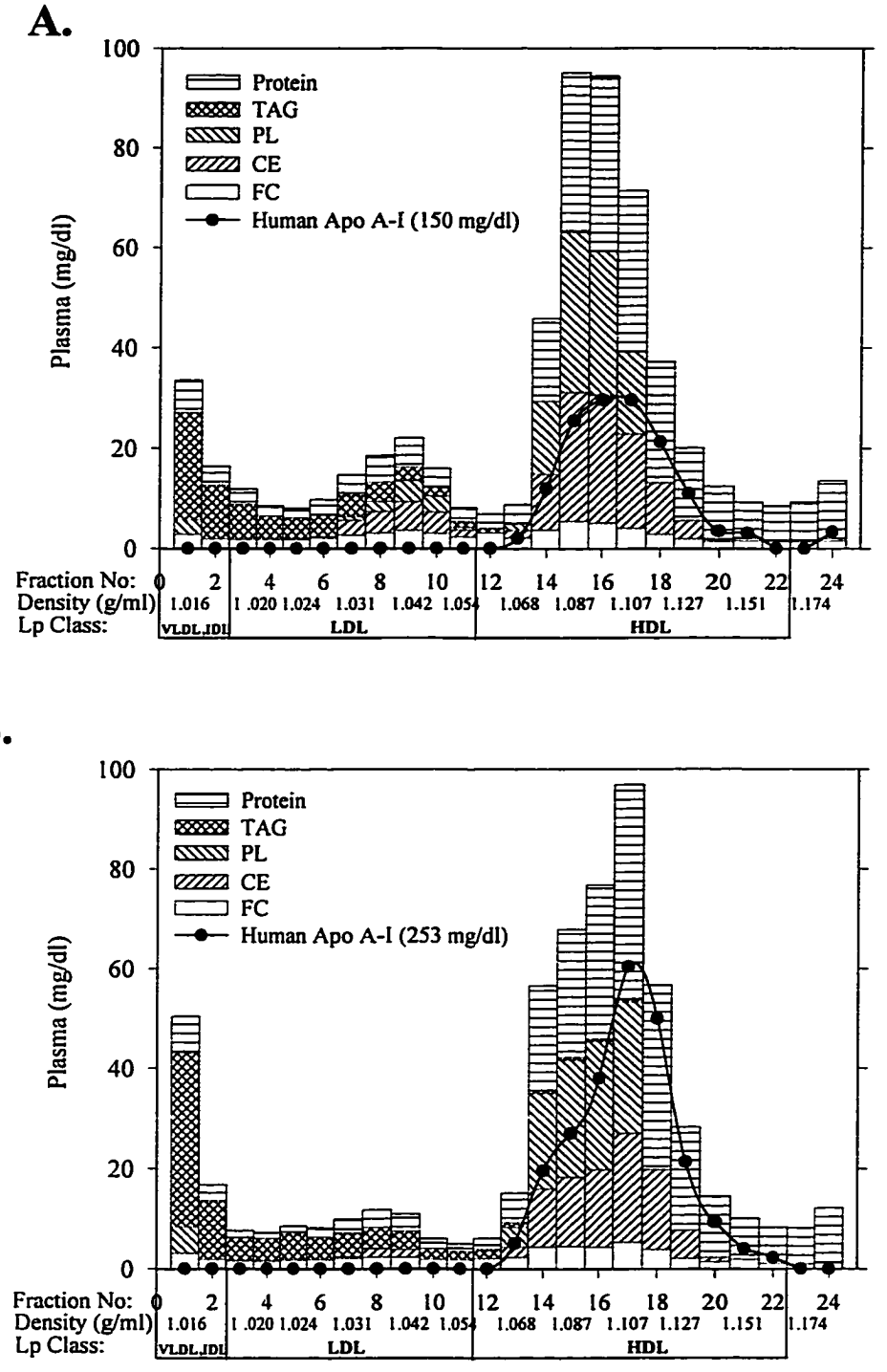

Figure 7.2A and B- Distribution of TgR[HuAI] rat plasma lipoproteins and human apolipoprotein A-I following density gradient ultracentrifugation

Lipids were measured enzymatically and human apolipoprotein A-I was determined by nephelometry (Behring). Plasma human apolipoprotein A-I levels were (A.) 150 mg/dl and (B.) 253 mg/dl. FC, free cholesterol; CE, cholesteryl ester; PL, phospholipid; TAG, triacylglycerol; apo, apolipoprotein.

Density gradient ultracentrifugation of two TgR[HuAI] rats (**Figure 7.2**) having human apolipoprotein A-I concentrations of 150 mg/dl (**Figure 7.2A**) and 253 mg/dl, (**Figure 7.2B**) demonstrated that these rats had an HDL distribution similar (fractions 12-22) to that of a non-transgenic rat of the same strain (**Figure 7.5A**). However, by comparison, the TgR[HuAI] rats had elevated HDL and a more defined separation between LDL and HDL suggesting that the increased HDL was HDL_2 and HDL_3, not HDL_1 which tends to float into the LDL density range by the density gradient ultracentrifugational method employed. This result was consistent with HDL_1 being primarily associated with apolipoprotein E while HDL_2 and HDL_3, were elevated and associated with apolipoprotein A-I. Analysis of human apolipoprotein A-I in density gradient fractions by nephelometry (**Figure 7.2**) confirmed that the observed increases in HDL_2 and HDL_3 were associated with human apolipoprotein A-I.

Further analysis of the distribution of plasma apolipoproteins amongst lipoprotein species in TgR[HuAI] rats was performed by Superose 6B gel filtration of plasma (**Figure 7.3**). **Figure 7.3A**, shows a gel filtration profile of a TgR[HuAI] rat expressing very low levels of human apolipoprotein A-I, **Figures 7.3 B** and **C** are profiles TgR[HuAI] rats that had significant concentrations of both human and rat apolipoprotein A-I and **Figure 7.3 D** is of a TgR[HuAI] rat that had significant human, but very little rat apolipoprotein A-I. In all three gel filtration profiles, both the major apolipoprotein B and E peaks eluted at similar volumes. In **Figures 7.3 B** and **C,** rat apolipoprotein A-I was primarily associated with larger HDL than human apolipoprotein A-I. Furthermore, the majority of rat apolipoprotein A-I co-eluted with apolipoprotein E containing HDL, whereas human apolipoprotein A-I was disproportionately associated with smaller HDL

(HDL_2 and HDL_3). Interestingly, rat apolipoprotein A-I in the non-transgenic rat (**Figure 7.3 A**) peaked at an elution volume intermediary to the rat and human apolipoprotein A-I peaks observed in **Figures 7.3 B** and **C**. Moreover, rat apolipoprotein A-I in this non-transgenic rat appeared to be more associated with small apolipoprotein E poor HDL than observed in **Figures 7.3 B** and **C**. In the TgR[HuAI] rat that had virtually no rat apolipoprotein A-I or E (**Figure 7.3 D**) there were two major human apolipoprotein A-I peaks. The first peak eluted at a volume that was associated with large apolipoprotein E containing lipoproteins in the other profiles, while the second peak co-migrated with smaller HDL.

These results indicate that the human apolipoprotein at low plasma concentrations (**Figure 7.3B and C**) preferentially binds smaller HDL (HDL_2 and HDL_3) in TgR[HuAI] rats displacing endogenous rat apolipoprotein A-I to larger HDL, possibly apolipoprotein E containing HDL. In TgR[HuAI] rats expressing moderately high levels of plasma human apolipoprotein A-I and very low levels of rat apolipoprotein A-I (**Figure 7.3D**), the absence of rat apolipoprotein A-I may be due to displacement by human apolipoprotein A-I in both large and small HDL (HDL_1, HDL_2 and HDL_3). Presumably, lipid-poor rat apolipoprotein A-I would then be catabolized. The lack of plasma apolipoprotein E in this TgR[HuAI] rat suggests that it may be similarly displaced by human apolipoprotein A-I; however, apolipoprotein E has only been measured in a small number of rats and it is not known whether apolipoprotein E levels are inversely proportional to human apolipoprotein A-I levels.

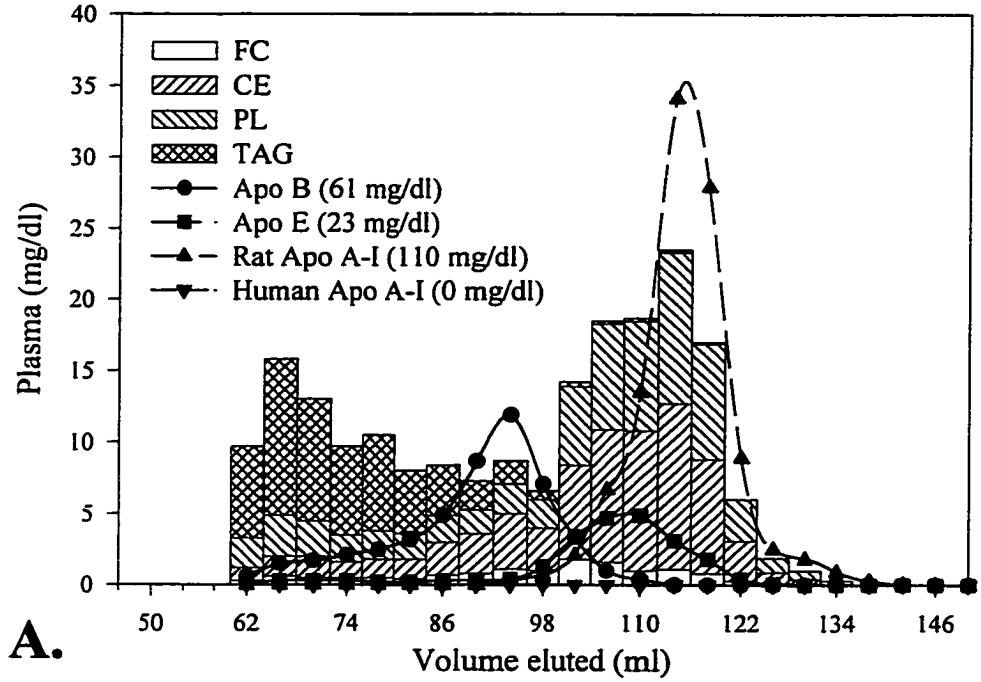

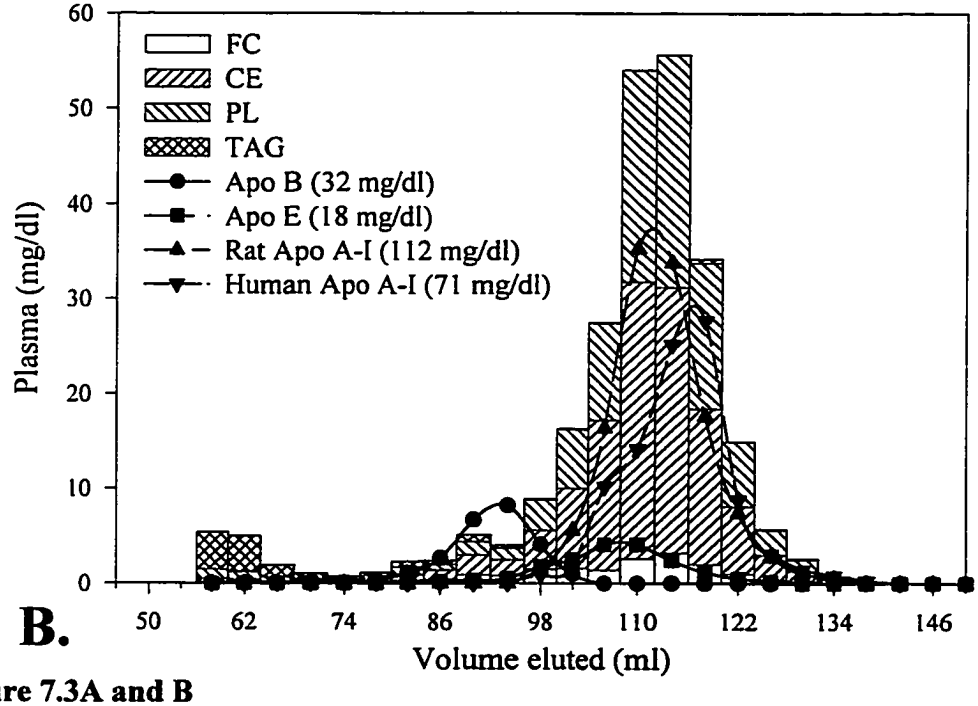

Figure 7.3A and B

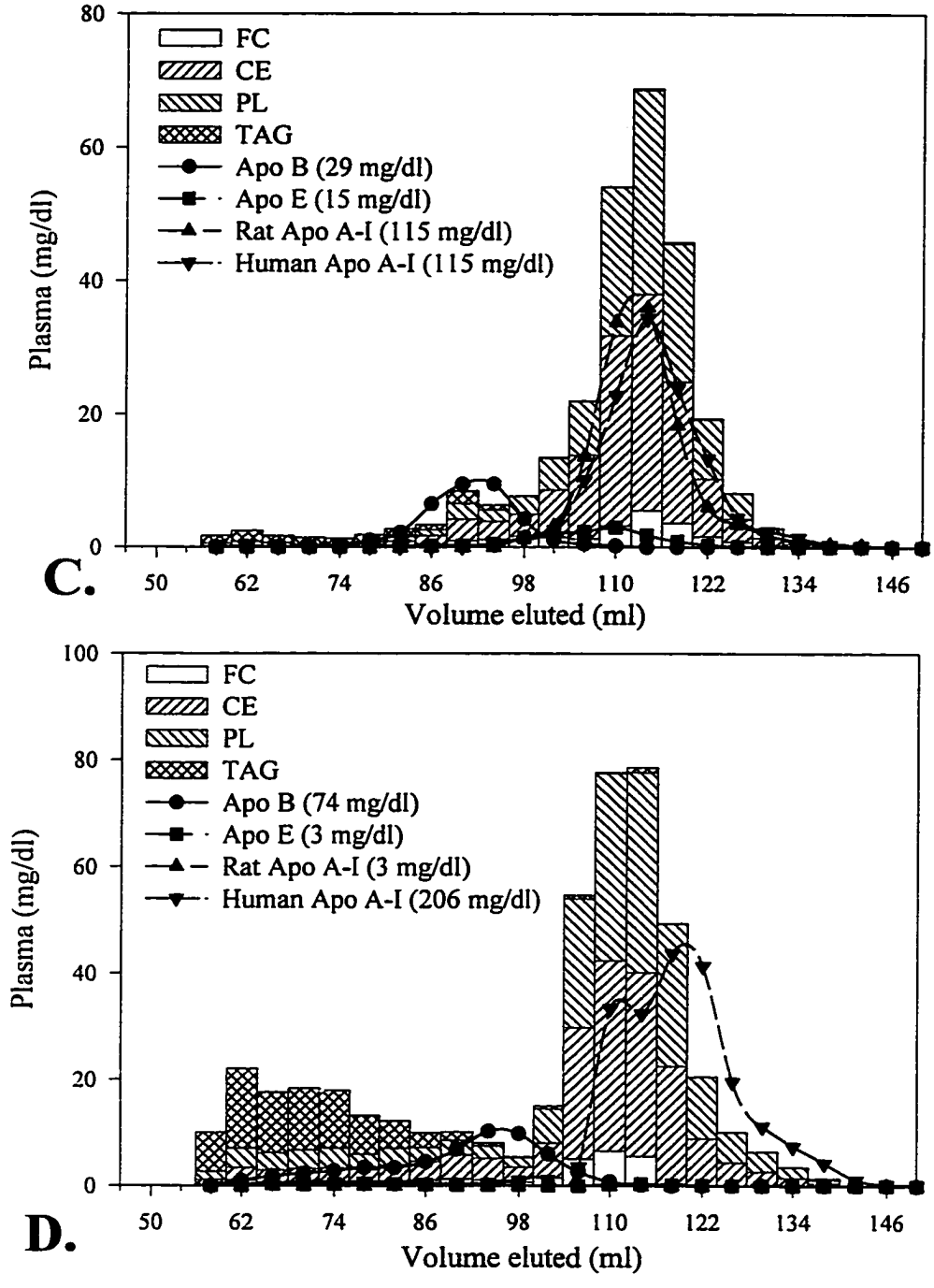

Figure 7.3A-D- Distribution of TgR[HuAI] rat plasma lipids and apolipoproteins following Superose 6B gel filtration of plasma

Individual fractions (4 ml) were analyzed for lipid content enzymatically and apolipoproteins were measured by an electroimmunoassay (180,181). FC, free cholesterol; CE, cholesterol ester; PL, phospholipid; TAG, triacylglycerol; Apo, apolipoprotein.

As demonstrated in the ANIT-treated rat time course study (chapter 4), administration of ANIT (100mg/kg) induced profound changes in the distribution of rat plasma lipoproteins at the 48 hour time point. In particular, plasma free cholesterol and phospholipid concentrations were dramatically elevated and the CE/FC ratio was reduced, even though LCAT was functional. Analysis of the lipoprotein distribution indicated that the majority of the increased phospholipid and free cholesterol was localized to the LDL density range and that these changes were fully reversible by 120 hours. It was hypothesised that the clearance of excess LDL phospholipid and free cholesterol was mediated by lipid-poor apolipoprotein A-I and/or apolipoprotein A-I rich HDL (Lp A-I HDL). Newly formed HDL, and/or phospholipid and free cholesterol enriched HDL, would then undergo cholesterol esterification by LCAT and be cleared by the liver. A process that was completed by 120 hours. To test the hypothesis that apolipoprotein A-I may mediate the clearance of excess phospholipid and free cholesterol within the LDL density range, ANIT (100 mg/kg) was administered to TgR[HuAI] rats to investigate the effect of plasma apolipoprotein A-I levels on the accumulation of material within the LDL density range.

As was expected, treatment of TgR[HuAI] rats with ANIT, resulted in substantial alterations to plasma lipid levels. While all ANIT-treated TgR[HuAI] rats (48 h) showed a varying reduction in their plasma CE/FC ratio and apparent elevations in phospholipid and free cholesterol, the wide range of plasma human apolipoprotein A-I concentrations made it difficult to determine an obvious effect.

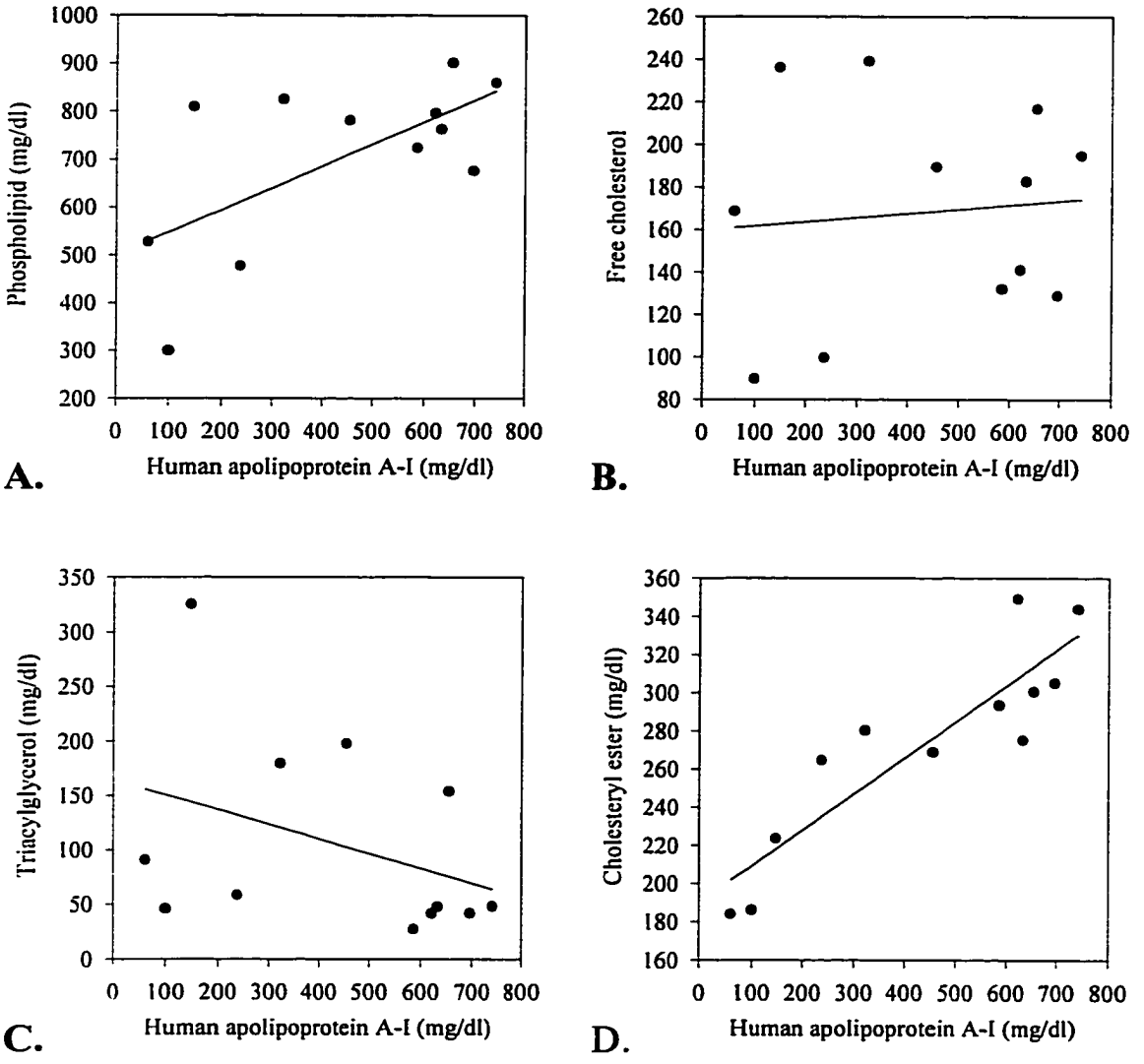

Figure 7.4- Correlation of human apolipoprotein A-I levels with plasma lipids in ANIT-treated TgR[HuAI] rats (48 h)

ANIT-treated TgR[HuAI] rat (n=12) plasma was assayed for human apolipoprotein A-I by nephelometry (Behring). These values were correlated by linear regression analysis with plasma lipids measured by gas chromatographic total lipid profiling (174). Whole plasma human apolipoprotein levels were found to be most closely correlated to cholesteryl ester (R=0.893) followed by phospholipid (R=0.644). There was no apparent correlation between plasma triacylglycerol (R=0.372) or free cholesterol (R=0.0967). R=0.785 for CE/FC (plot not shown).

However, linear regression analysis of plasma human apolipoprotein A-I and plasma lipids in ANIT-treated TgR[HuAI] rats (**Figure 7.4A-D**) was revealing. As previously shown (**Figure 7.1**) in TgR[HuAI] rats, plasma human apolipoprotein A-I levels were strongly correlated to plasma phospholipid, free cholesterol and cholesteryl ester, with the strongest relationship being observed with phospholipid. By contrast, in ANIT-treated TgR[HuAI] rats, human apolipoprotein A-I levels were most strongly correlated to cholesteryl ester (R=0.893) (**Figure 7.4 D**) and the CE/FC ratio (R=0.765) with a much weaker correlation to phospholipid (R=0.644) (**Figure 7.4 A**). There was no significant relationship between human apolipoprotein A-I and free cholesterol (R=0.097) or triacylglycerol (R=0.372) (**Figures 7.4B and C**). The correlation between plasma human apolipoprotein A-I levels and cholesteryl ester suggests that human apolipoprotein A-I facilitates the movement of LCAT substrates (phospholipid and free cholesterol) into lipoproteins (presumably HDL) that are good LCAT substrates. As demonstrated by an exogenous assay using a recombinant HDL substrate, plasma LCAT activity in TgR[HuAI] rats was not altered by ANIT treatment (TgR[HuAI] rats, 28±4 nmol CE formed/ml/h, n=8 and for ANIT-TgR[HuAI] rats, 27±5 nmol CE formed/ml/h, n=6). Thus, the inability of LCAT to cope with the influx of phospholipid and free cholesterol into the plasma of ANIT-treated rats does not necessarily reflect insufficient LCAT activity, but rather that apolipoprotein A-I facilitated generation of LCAT substrate lipoproteins was limiting.

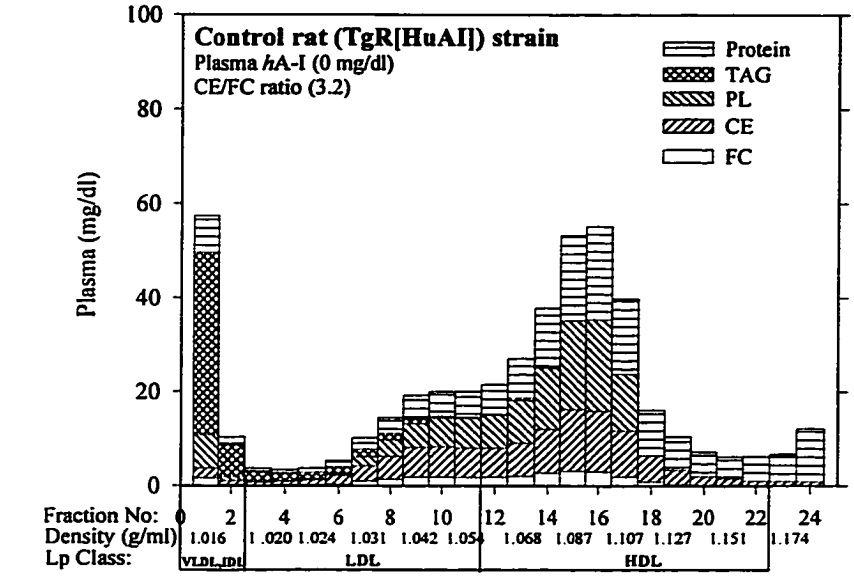

A.

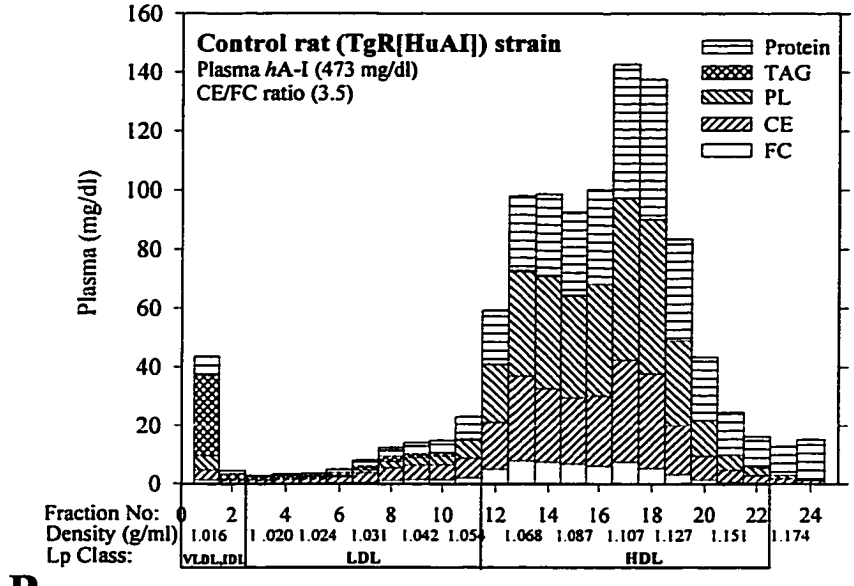

B.

Figure 7.5A and B- Distribution of TgR[HuAI] rat plasma lipoproteins following density gradient ultracentrifugation

Lipids were measured enzymatically and plasma human apolipoprotein A-I determined by nephelometry (Behring). Plasma human apolipoprotein A-I levels were (A.) 0 mg/dl and (B.) 473 mg/dl.

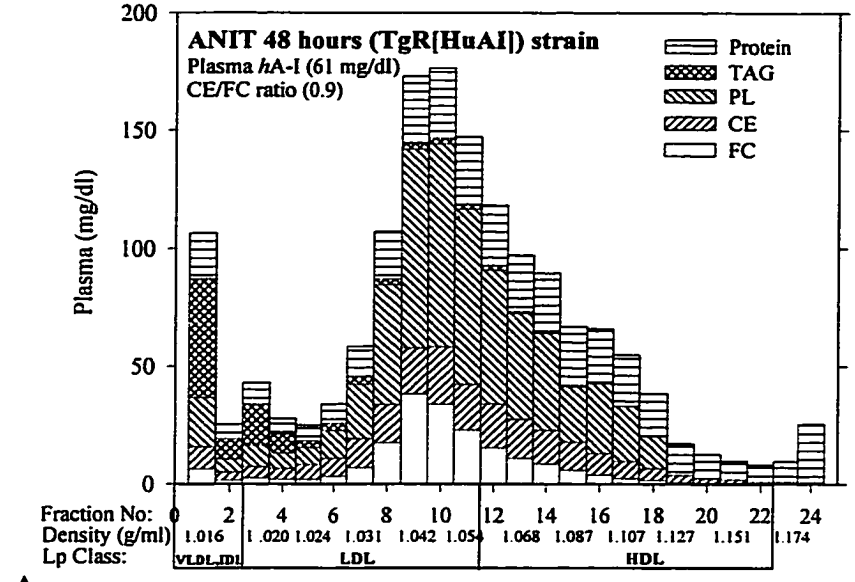

A.

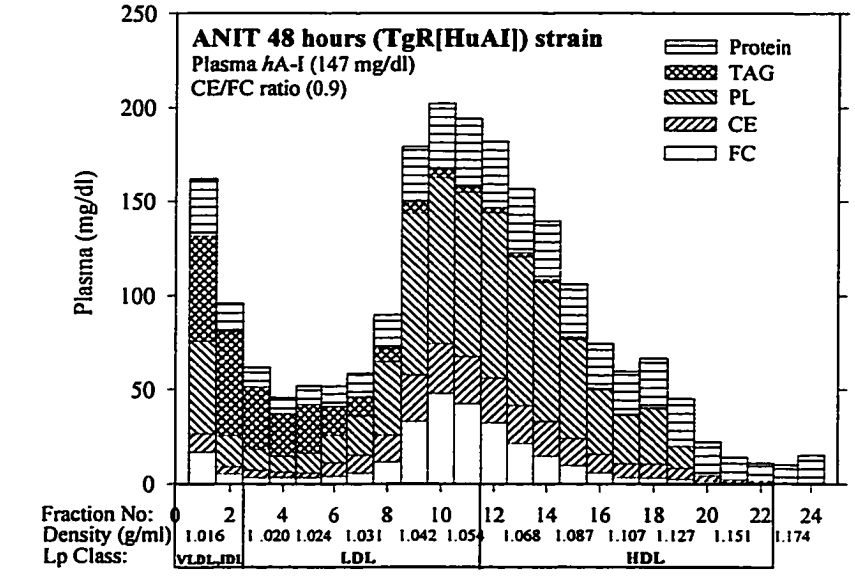

B.

Figure 7.6A and B

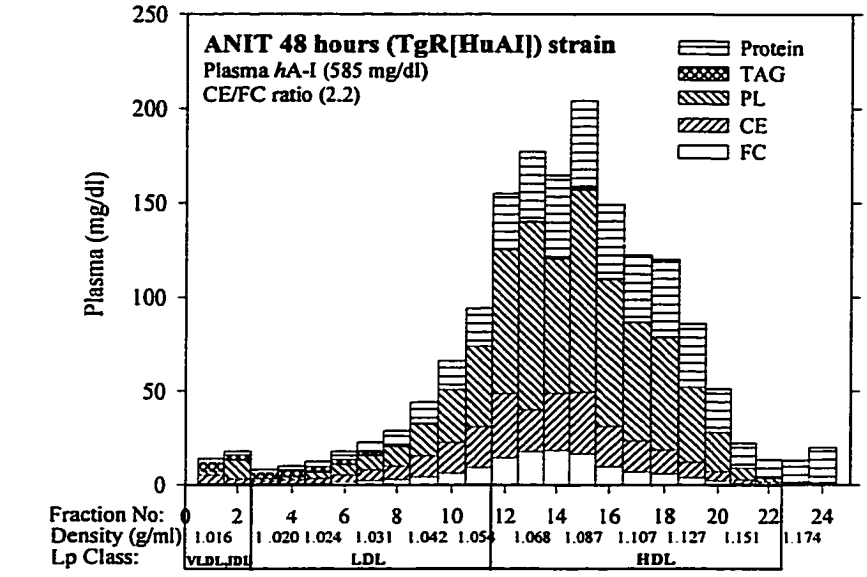

C.

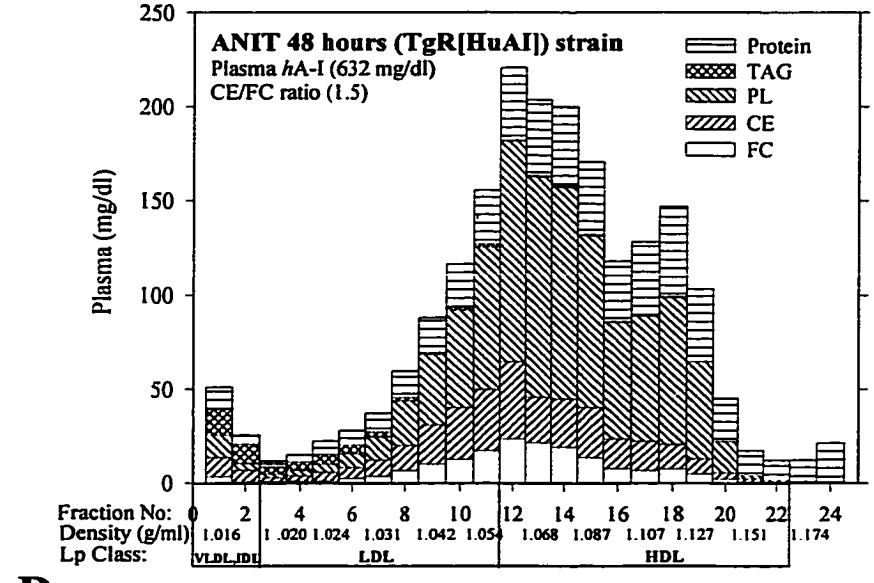

D.

Figure 7.6B and D

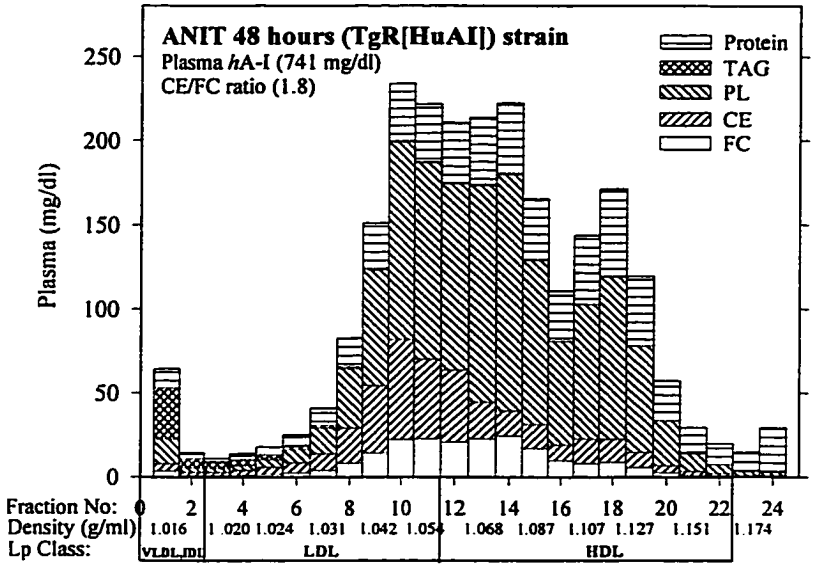

E.

Figure 7.6A-E- Distribution of TgR[HuAI] rat plasma lipoproteins by density gradient ultracentrifugation following ANIT treatment (48 h, 100 mg/kg)

Lipids were measured enzymatically and plasma human apolipoprotein A-I determined by nephelometry (Behring). Plasma human apolipoprotein A-I levels (mg/dl) were (A.) 61, (B.) 147, (C.) 585, (D.) 632 and (E.) 741.

To further examine this effect in ANIT-treated TgR[HuAI] rats, density gradient ultracentrifugation was performed on rat plasma of varying plasma human apolipoprotein A-I concentrations (**Figures 7.6A-E**). For comparitive purposes, density gradient profiles of two untreated TgR[HuAI] rats are shown (**Figure 7.5A-B**).

The series of density gradient ultracentrifugal profiles generated from ANIT-treated TgR[HuAI] rat plasma (**Figure 7.6**) clearly demonstrates that increased plasma apolipoprotein A-I concentration ameliorated the buildup of cholesteryl ester poor lipoproteins in the LDL density range. ANIT-treated rats with relatively low human plasma apolipoprotein A-I (**Figures 7.6 A and B**) levels tended to have lower CE/FC ratios and density gradient lipoprotein profiles similar to those observed at 48 hours in the ANIT-treated rat time course study (chapter 4). Similarly treated rats (**Figures 7.6 C-E**), with very high plasma levels of human apolipoprotein A-I had a marked reduction in lipoproteins within the LDL density range and a more normal CE/FC ratio. The wide density distribution of lipoproteins within the HDL density range of these rats (**Figures 7.6 C-E**), does not appear to be particularly abnormal for TgR[HuAI] rats with high plasma apolipoprotein A-I concentrations (**Figure 7.5B**). However, in comparison to untreated TgR[HuAI] rat HDL lipid composition (**Figure 7.5B**), HDL fractions were cholesteryl ester depleted (**Figures 7.6C-E**).

Sodium dodecyl sulfate density gradient polyacrylamide gel electrophoresis of density gradient fractions from both an ANIT-treated and untreated TgR[HuAI] rat (**Figure 7.7A and B**) were analyzed. The gels of an untreated TgR[HuAI] rat (**Figure 7.7A**) having a plasma human apolipoprotein A-I concentration of almost 500 mg/dl showed that apolipoprotein A-I was detectable and predominant in all fractions and other

plasma apolipoproteins were barely detectable. Analysis of density gradient fractions from an ANIT-treated TgR[HuAI] rat (**Figure 7.7B**) having a plasma human apolipoprotein A-I concentration of greater than 600 mg/dl showed a similar distribution of apolipoprotein A-I, but unlike the untreated TgR[HuAI] rat, considerable amounts of other apolipoproteins were present. In particular there were increased amounts of apolipoprotein E and B_{48}, as well as the C apolipoproteins within the LDL density fractions (fractions 6-12).

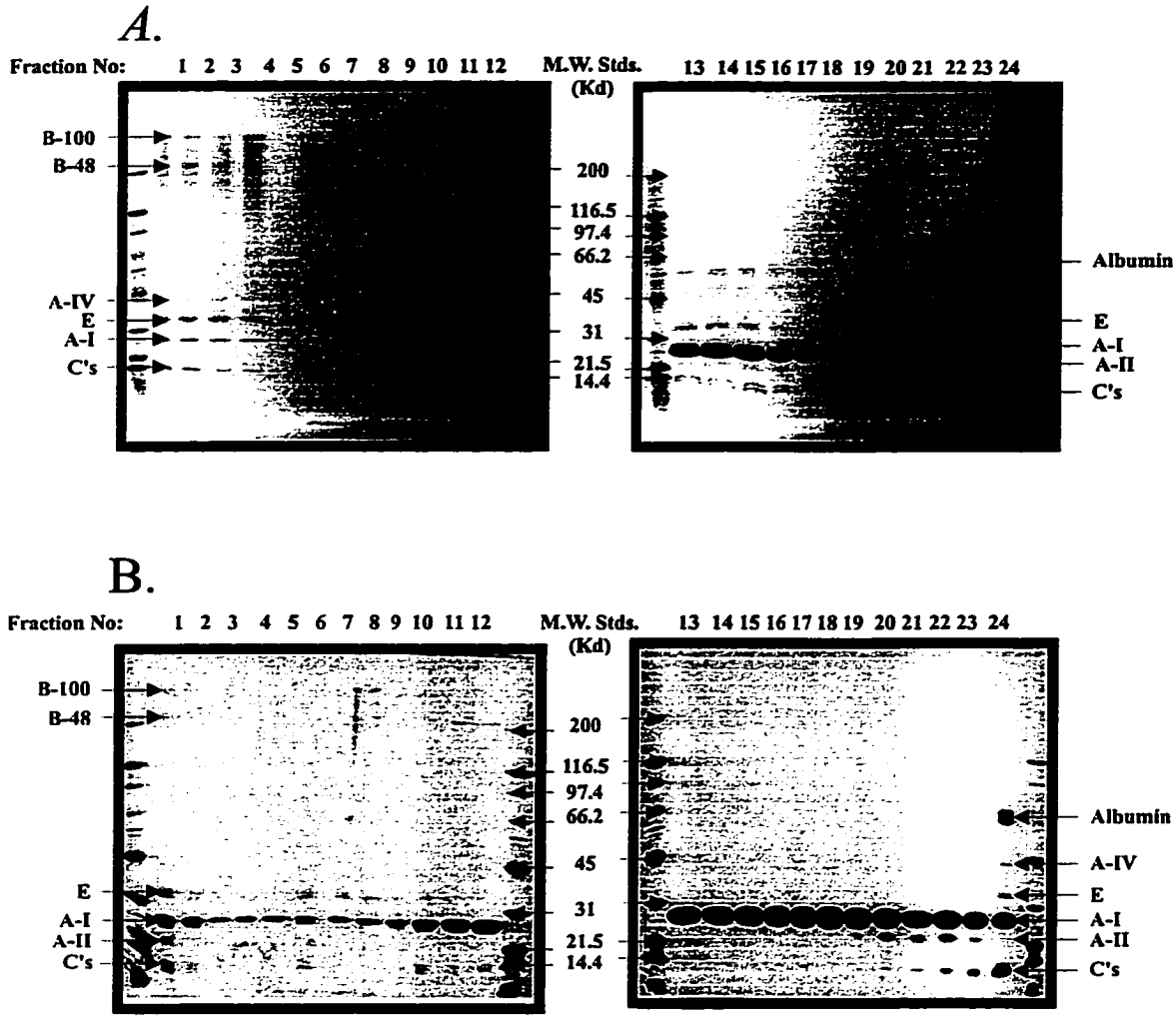

Figure 7.7- Sodium dodecyl sulfate polyacrylamide gradient gels of TgR[HuAI] rat density gradient fractions 1-24 after ultracentrifugation

An ANIT-treated TgR[HuAI] rat (48 h) (A.) is shown compared to an untreated TgR[HuAI] rat (B.). Twenty μg of protein was loaded into each lane and molecular weight standards were broad range (Bio-Rad) of the indicated molecular weights. Plasma human apolipoprotein A-I concentrations were 632 mg/dl (A.) and 473 mg/dl (B.).

Chapter 8- Discussion

8.1 The D-(+) galactosamine rat

D-(+) galactosamine-HCl induced experimental hepatitis in the rat results in the manifestation of many changes in plasma lipoproteins that are similar to those found in familial LCAT deficiency, including cholesteryl ester depleted, phospholipid and free cholesterol enriched lipoproteins. Subspecies analysis of HDL indicates the presence of polydisperse HDL, including an apolipoprotein E rich discoidal HDL (192). Work presented in this thesis and the compositional analysis of lipoproteins in the LDL density range as reported by others (127,193,194) is suggestive of the presence of a small amount of Lp-X. However, conclusive proof of the presence of Lp-X in D-(+) galactosamine induced experimental hepatitis has never been demonstrated.

The development of abnormal lipoproteins in this model is not only attributable to a deficiency in plasma LCAT activity, but also to severe reductions in both lipoprotein lipase and hepatic lipase activities. Deficiencies in these lipolytic enzymes (chapter 3) and also apolipoproteins A-I, A-II A-IV and the C's have been previously described (193,195). These findings are not surprising when the mechanism of D-(+) galactosamine induced hepatitis is considered. D-(+) galactosamine has been shown to sequester cellular UTP pools and effectively inhibit glycosylation, glycolipid and nucleic acid synthesis. Thus, a wide range of cellular processes are affected including transcription, protein synthesis and post-translational glycosylation of proteins (195-198). It is uncertain whether D-(+) galactosamine affects tissues and organs other than the liver,

athough Keppler *et al.* have reported that only the liver in treated animals appeared abnormal on visual examination (196).

Studies by the author have confirmed the reversibility and time course of the drug (750 mg/kg) affects. Moreover, the dramatic deficiencies in plasma lipolytic activity were reconfirmed. While the deficiency of both lipoprotein and hepatic lipases caused the author to have reservations about the use of this model, the possible unknown effects of D-(+) galactosamine on the liver and possibly other tissues was the most disconcerting. However, it was the lack of plasma lipids particularly evident after density gradient ultracentrifugation that precipitated the final decision to discontinue work in the D-(+) galactosamine rat. Low plasma lipid concentrations would make analysis and conclusive identification of Lp-X very difficult, as well as limit the types of metabolic experiments possible.

However, the deficiency of lipolytic activity might make this an interesting model for studying the fate of exogenously administered lipoproteins. In particular, insight into the metabolism of Lp-X might be gained by an intravenous injection of a large dose of Lp-X containing radiolabelled albumin. Would the particle remain in plasma or be metabolized? If metabolism occurred would it be through tissue uptake and deposition of lipid or by movement into other lipoproteins?

8.2 Studies in the ANIT-treated rat

ANIT, when administered in a single dosage (100 mg/kg by gavage in corn oil) to rats, promotes a transient, reversible intrahepatic cholestasis resulting in marked perturbations to plasma lipids and lipoproteins. The onset of cholestasis is followed by

elevated levels of bile acids, bilirubin, medium chain length phospholipids, free cholesterol and plasma enzyme markers of liver damage. All of these increased levels return to near normal by 120 hours.

Although increased cholesteryl ester mass was observed, the CE/FC ratio was reduced even though LCAT activity was near normal. In severe human cholestasis, hepatitis, chronic liver failure, late stage primary biliary cirrhosis (199,200) and galactosamine-induced hepatitis in rats (127) (chapter 3), LCAT activity is decreased. As LCAT activity is increased when hepatic damage appears to be light such as in ANIT-treatedrats, mild cases of human cholestasis and early stage primary biliary cirrhosis (199,200), the synthesis and secretion of the enzyme does not appear to be impaired. A low CE/FC ratio in the presence of near normal LCAT activity suggests LCAT activity was either initially overloaded by the large amount of phospholipid and free cholesterol entering the plasma compartment or alternatively, the free cholesterol and phospholipid were sequestered in particles that did not function as good LCAT substrates.

The Lp-X-like particle (**Figure 4.11B**) observed 48 hours after ANIT treatment in the time course study would be a likely candidate. Whether or not Lp-X is an LCAT substrate *in vivo* remains controversial and is probably dependent upon whether the vesicles contain significant quantities of the surface bound LCAT activating apolipoprotein, A-I. Lp-X vesicles are thought to normally contain very little if any apolipoprotein A-I (95,96). However, the majority of these characterizations have been performed using Lp-X separated by ultracentrifugation, such that disassociation of weakly bound apolipoprotein A-I or HDL complexes may occur.

Thus, the failure of LCAT to maintain the plasma CE/FC ratio may be due to a combination of factors which include:

1) In the early-mid stages of ANIT treatment, much of the phospholipid and free cholesterol is localized to Lp-X-like particles and as such is not presented to LCAT in an ideal substrate form.
2) In order for the excess phospholipid and cholesterol to be metabolized, it must either be removed by direct uptake of the Lp-X particle or be moved to appropriate HDL substrates containing the obligatory LCAT-activating apolipoproteins.

8.3 Possible mechanisms for the formation of Lp-X

Lp-X vesicles may be formed under the following physiological conditions.

1) In the case of some types of human obstructive liver disease, bile-duct ligation or possibly ANIT treatment, there is a reflux of biliary lipids including phospholipid and free cholesterol into the plasma compartment. Manzato *et al.* (96) have shown that biliary lipid complexes form Lp-X-like vesicles when albumin or plasma is added (presumably by binding bile salts) and conversely Lp-X can be transformed into bile-like micelles upon addition of bile salts. Moreover, studies in the perfused rat liver have shown that bile lipids are secreted in an almost constant 12:1 phospholipid:free cholesterol ratio (201). Thus for Lp-X (1:1 molar phospholipid:free cholesterol) (96) to form, extrabiliary free cholesterol must be taken up from both endothelial and erythrocyte membranes as well as plasma lipoproteins. Hydrolysis of

phospholipid and/or movement of phospholipid to other lipoproteins may contribute to this process. Indeed, Quarfordt *et al.* (202) have calculated that biliary lipid efflux as a result of cholestasis does not completely account for the large increases in plasma cholesterol and phospholipid usually observed.

2) In cases of familial LCAT deficiency (78,79), Lp-X is possibly formed from the excess surface phospholipid and free cholesterol produced by lipolysis of triacylglycerol-rich chylomicrons and VLDL (106). The surface material may simply vesicularize trapping plasma albumin and proceed to remove phospholipid and cholesterol from membranes and other lipoproteins to form the most stable particles.

3) Infusion of 10% Intralipid™ into rats (203) and man (204) results in lipolysis of the triacylglycerol-rich, phospholipid emulsion, such that a large excess of phospholipid is produced resulting in the formation of Lp-X by a mechanism similar to that described for familial LCAT deficiency.

In advanced cholestasis, cirrhosis and other types of liver disease, secondary LCAT deficiency would further contribute to Lp-X formation. In the ANIT-treated rat and possibly in some types of human liver disease, hepatic lipase activity (rarely ever measured) is also reduced. A deficiency in hepatic lipase might further promote the formation of phospholipid and free cholesterol-rich vesicles through reduced phospholipid hydrolysis of phospholipid rich lipoproteins. Since hepatic lipase has also been implicated in the regeneration of lipid-poor apolipoprotein A-I and/or pre-β1 HDL

through the remodeling of HDL subspecies (65,67,68), the capacity of HDL to accept free cholesterol and phospholipid may be reduced.

8.4 Catabolism of Lp-X like vesicles

In normal rats, Walli *et al.* have demonstrated that intravenously injected Lp-X containing radiolabelled albumin in the core is cleared from the plasma with the spleen accumulating the most radioactivity on a mass basis (113). The difficulty in interpreting these results is not knowing whether this is evidence for the uptake of intact Lp-X particles or simply clearance of core albumin after catabolism of the vesicle. Williams *et al.* have demonstrated in fibroblasts that Lp-X-like vesicles containing apolipoprotein E from the plasma of humans treated with Intralipid™ or having cholestasis compete with LDL for binding to the LDL receptor and are internalized with a concomitant regulatory effect on LDL uptake (115). Since cholestatic liver disease is often accompanied by hepatic cholesterolgenesis, a function expected to be down-regulated by Lp-X uptake via the LDL receptor, this mechanism may not occur under the physiological conditions of cholestasis. However, although the data of Walli *et al.* (113) showed that the spleen accumulated the most radioactivity on a tissue mass basis, the liver actually accumulated the most radioactivity. Thus, these results could be interpreted to mean that both uptake of intact Lp-X by the liver and plasma catabolism of Lp-X occur simultaneously in normal rats.

Catabolism of Lp-X through the movement of phospholipid and cholesterol into HDL may proceed by one or both of the following mechanisms:

1) transfer to and formation of HDL-like substrates facilitated by the binding of lipid-poor apolipoprotein A-I, pre-β1 HDL and/or the formation of complexes with other existing HDL species;

2) phospholipid and free cholesterol movement out of Lp-X and into HDL by a gradient established as a result of LCAT mediated depletion of HDL phospholipid and free cholesterol.

Situations where this may occur have been observed in some cases of human cholestatic liver disease (199,200), bile-duct ligation (205) and Intralipid™ infusion (203) were LCAT activity was not significantly reduced. However, the relative importance of catabolism by tissue uptake of Lp-X, as opposed to LCAT-mediated metabolism of phospholipid and free cholesterol moved into HDL, remains unclear.

8.5 ANIT treatment of TgR[HuAI] rats

Consistent with the concept that apolipoprotein A-I may mediate the catabolism of the abnormal lipoproteins present in the LDL density range of ANIT-treated rats (48 h), it was postulated that overexpression of human apolipoprotein A-I resulting in high levels of plasma human apolipoprotein A-I might facilitate the movement of phospholipid and free cholesterol into the HDL density range. Treatment of TgR[HuAI] rats with low to very high plasma human apolipoprotein A-I levels with ANIT (100 mg/kg) demonstrated an apparent decrease in lipid accumulation within the LDL density range and increased HDL. This effect appeared most significant in rats expressing high levels of human apolipoprotein A-I and was followed by increases in the CE/FC ratio.

Correlation of ANIT-treated TgR[HuAI] rat, human apolipoprotein A-I levels with plasma lipids by linear regression analysis demonstrated a clear positive relationship between human apolipoprotein A-I, cholesteryl ester and the CE/FC ratio. Phospholipid was correlated to a lesser extent and there was no apparent relationship with plasma triacylglycerol or free cholesterol. These results provide evidence that the apolipoprotein A-I facilitated movement of phospholipid and free cholesterol into HDL prior to LCAT mediated esterification may be a key determining factor in whether or not phospholipid and free cholesterol entering the plasma accumulates in the LDL density range or is esterified by LCAT into spherical HDL. Thus while LCAT activity may be normal or slightly elevated in ANIT-induced cholestasis in the rat (48 h), LCAT is not overwhelmed by influx of phospholid and free cholesterol, but rather apolipoprotein A-I mediated movement of the material into LCAT substrate lipoproteins is rate-limiting.

8.6 Similarities between the ANIT-treated rat and bile-duct ligation

Ritland and Bergan (105) have shown in bile-duct ligated and cholecystectomized dogs that Lp-X is generated and that its levels vary inversely with LCAT activity. Felker *et al.* (206) have comprehensively evaluated the changes in lipoprotein metabolism in the plasma and perfused liver of bile-duct ligated rats. The major alterations observed were increased plasma phospholipid and free cholesterol, a decreased plasma CE/FC ratio, the presence of an Lp-X-like particle, moderately increased plasma apolipoprotein B, enhanced secretion of apolipoprotein A-I and phospholipid-enriched and cholesteryl ester depleted HDL. As a result of the reduced CE/FC ratio and Lp-X, Felker *et al.* speculated that LCAT activity was reduced. In contrast, others have reported increased activity

(207). The similarities between the changes in lipoprotein metabolism as a result of bile-duct ligation and those observed in the ANIT-treated rat are striking.

8.7 Plasma apolipoproteins in liver disease

The role of plasma apolipoproteins in liver disease must also be considered. Plasma apolipoprotein A-I levels are increased in the ANIT-treated rat (**Figure 4.4**), and possibly bile-duct ligated rats (206); however, they are often reduced in cases of human liver disease (116) and LCAT deficiency (79). In humans LCAT deficiency and alcoholic hepatitis, increased catabolism of apolipoprotein A-I due to decreased apolipoprotein A-I binding to HDL has been implicated (88) possibly due to low levels of core cholesteryl ester. How this relates to LCAT activity and the increased apolipoprotein A-I levels observed in cholestatic rats remains unclear. Emerging evidence in transgenic mice and rats does indicate that human apolipoprotein A-I may have a higher binding affinity for smaller spherical HDL than rat apolipoprotein A-I (62,71,72,149), such that rat apolipoprotein A-I may bind larger cholestatic and discoidal HDL better than human apolipoprotein A-I resulting in a reduction of rat apolipoprotein A-I turnover.

Increased apolipoprotein E levels were observed in the ANIT-treated rat and have been similarly reported in liver disease (116) and LCAT deficiency (79). Apolipoprotein E discoidal particles have been observed in LCAT deficiency and secondary LCAT deficiency resulting from liver disease (116). In the ANIT-treated rat, increased apolipoprotein E may also prove to be associated with triacylglycerol-rich lipoproteins, their remnants and/or large HDL particles.

8.8 Impaired remnant metabolism in liver disease

The appearance of apolipoprotein B-48 in the HDL density range of plasma from ANIT-treated rats (fractions 13-16, **Figure 4.10B**) 48 hours post-treatment strongly suggests the presence of either VLDL or chylomicron remnants. Defective remnant clearance in the presence of Lp-X has been noted in bile-duct ligation (113,114) and some types of human liver disease (90). Walli *et al.* (113) have demonstrated that Lp-X competitively inhibits remnant uptake by the hepatic apolipoprotein-E remnant receptor. However, hepatic damage may also be a factor, resulting in decreased receptor numbers and/or dysfunction.

8.9 Characterization of the abnormal lipoproteins in the ANIT-treated rat

Purification of the abnormal lipoproteins in the ANIT-treated rat (48 h, 150 mg/kg) yielded results that were consistent with ANIT-treated rat data (48 h, 100 mg/kg) obtained in the time course study. As the severity of cholestasis was assessed by the CE/FC ratio and plasma lipid concentrations, the changes in lipoprotein metabolism in the rats used for particle purification appear to be comparable to those in the time course study (48 h, 100 mg/kg).

All isolated lipoprotein fractions, separated by a combination of single-spin ultracentrifugation (d_{15}=1.21 g/ml), Heparin-Sepharose affinity chromatography and Superose 6B gel filtration chromatography, were enriched in free cholesterol and phospholipid and depleted of cholesteryl ester. HDL was found to contain a polydisperse population of particles that were approximately the same median diameter or slightly larger than that found in a normal rat. The estimated median size for HDL_1/ HDL_2/ HDL_3

for ANIT and control rats respectively were 18.5/13.5/13 and 16/13/12.5 nm. However, the size range of individual HDL species in the ANIT-treated rat was much broader than in the normal rat as indicated in **Table 5.1**. In both ANIT (**Figure 5.5**, fraction II-III) and control(**Figure 4.11C**) HDL_3, there appear to be small HDL_3 corresponding to 7 and 8 nm. These may correspond to small apolipoprotein A-I containing HDL_3; however, these were identified only on the basis of protein staining such that apolipoprotein A-I or lipid association was not conclusively shown. HDL from the ANIT-treated rat pool tended to have a lower surface:core lipid ratio, due to relative cholesteryl ester enrichment, than LDL or unbound Heparin-Sepharose chromatography fractions (I-I and I-II). This finding is compatible with normal LCAT mediated esterification of ANIT HDL.

The fraction identified as being analogous to LDL (fraction V-II) was found to be extremely abnormal with a virtual absence of neutral core lipid and a median diameter slightly larger than control LDL. The apolipoprotein content, ($E>>B_{100}\approx B_{48}$) of the putative ANIT LDL suggests that this fraction may be heterogeneous and contain both apolipoprotein B_{100} and B_{48} remnant lipoproteins that were not cleared from the plasma due impaired remnant and/or LDL uptake. Alternatively, this may prove to be an artifact of the single-spin ultracentrifugation step.

Two free cholesterol and phospholipid rich lipoprotein fractions were separated by gel filtration of the unbound Heparin-Sepharose chromatography fraction of the ANIT pool. Lp-X was expected to comprise this fraction; however, compositional analysis indicated significantly more core triacylglycerol and cholesteryl ester was associated than is characteristic of Lp-X. Apolipoprotein analysis showed that these fractions were also

associated with apolipoprotein B_{100} and B_{48}. While one could speculate on the reasons for the lack of binding to Heparin-Sepharose by these particles and the possible origin of the excess phospholipid and free cholesterol, it seems much more likely that these particles were artifacts of the single-spin ultracentrifuge method. Thus, fractions I-I and I-II are likely composed of aggregates of VLDL, LDL and/or remnants and possibly Lp-X.

The problems associated with the purification methodology presented in this thesis may most easily be overcome by replacing, prior to chromatography, the d_{15}<1.21 g/ml lipoprotein fraction obtained by single spin ultracentrifugation with pooled fractions 1-24 (d<1.21 g/ml) from a single spin density gradient ultracentrifugation. However, the results presented here also indicate that purification of these large unbound Heparin-Sepharose particles may be possible by either a Heparin-Manganese precipitation modified to Heparin-Sepharose chromatography initial binding conditions or alternatively Heparin-Sepharose chromatography of fresh dialyzed ANIT-treated rat plasma. Although preferable, direct chromatography of plasma was not performed in these experiments due to the difficulty in completely separating plasma proteins from lipoproteins by the chromatography methods employed. However, in this case, the particles in the unbound fractions (I-I and I-II) should be large enough such that Superose 6B gel filtration will fully separate them from any plasma proteins present in the Heparin-Sepharose unbound fraction. Provided the vast majority of plasma proteins do not bind to Heparin-Sepharose, it may be possible to obtain purified lipoproteins free of plasma proteins by gel filtration of the Heparin-Sepharose chromatography fractions. The major advantage to purifying lipoproteins from plasma in this way is that ultracentrifugal artifacts may be avoided, and the separation could be performed in a shorter period of time.

8.10 Studies in ANIT-treated mice

The effect of ANIT treatment on the lipoprotein and bile acid metabolism in mice was investigated in collaboration with Dr. Lou Agellon of the University of Alberta. The authors primary goal was to compare alterations in the plasma lipoprotein metabolism of mice with those previously characterized in the rat. The second collaborative goal was to extend these studies into the area of bile acid metabolism in order to better understand the origin of the biliary lipid and bile acids within the plasma compartment and the overall effect of intrahepatic cholestasis on bile acid metabolism. While this collaborative investigation is on-going, a number of interesting observations have been made to date.

In comparison to the rat, changes in plasma lipid levels were extreme with phospholipid and free cholesterol being elevated at 48, 72, 168 hours by 10/11/13 and 17/20/45 fold, respectively. These massive elevations were accompanied by a reduction in plasma cholesteryl ester to levels 60-80% of normal. The failure of cholesteryl ester concentrations to rise with the influx of phospholipid and free cholesterol resulted in CE/FC ratios at 0, 24, 48 72, 168 hours of 4.3/2.7/0.17/0.14/0.08 respectively. Consistent with these changes, plasma LCAT activity was reduced to 20% of control levels by an exogenous assay (48 h) and may have been further inhibited endogenously by highly elevated levels of bile acids (3152±400 μmol/l). This elevation was very high compared to the rat (715±57, 24 h; 538±58, 48 h). Calandra *et al.* (208) have shown that human LCAT activity is decreased *in vitro* by high concentrations of bile acids, an effect that was independent of the bile acid species used. LCAT activity was reduced to approximately 50% with 1000 μmol/l and 25% with 2000 μmol/l of added bile acids.

These concentrations are lower than those measured at 48 hours in the ANIT-treated mouse, such that mouse LCAT activity *in vivo*, due to the 8-16 fold dilution of plasma used in the exogenous assay, may be much less than 20% (48 h). This would be consistent with the severe decrease in cholesteryl ester mass observed.

Increases in plasma phospholipid, like in the rat, were due to those molecular species containing fatty acyl carbons numbering C34 (18/16), C36 (18/18) and C38 (18/20) with the relative proportions being C34 >C36 >C38. Interestingly, the relative proportions were inversely related to those observed in the livers of ANIT-treated mice. While at least part of the increase in phospholipid is thought to be of biliary origin (202), the precise source remains unknown. Measurement of phospholipid molecular species in the gallbladder might provide insight into whether the majority of phospholipid is from biliary, plasma, tissue or dietary sources.

The changes to plasma lipids and lipoprotein distribution observed in ANIT-treated mice suggest that liver damage may be more severe than observed in the rat. This assumption was not supported by plasma measurements of liver aminotransferases or bilirubin. However, in the mouse, the cholestatic time course appears to be prolonged as plasma lipids remained elevated even after 168 hours, such that the lower plasma aminotransferase activities (48 h) may simply be due to 48 hours not being the period of peak liver damage. In humans, multiple linear regression analysis of various parameters of liver damage correlated LCAT activity, total plasma cholesterol, alkaline phosphatase and bile acids as being the best indicators of the severity of liver damage (209). Provided this correlation holds true for mice, all of the parameters measured in both rats and mice support the conclusion that liver damage may be more severe in ANIT-treated mice (100

mg/kg, 48 h).

In the mouse, like in the rat, there appears to be an inhibition of remnant clearance as indicated by the presence of both apolipoprotein B_{48} and B_{100} in the HDL density fractions (**Figure 6.8B**). This inhibition of remnant uptake by the LDL receptor or LRP may in part be responsible for the large increase in hepatic cholesterol synthesis observed after ANIT treatment (**Figure 6.6**). However, since hepatic cholesteryl ester concentrations were relatively unchanged, increased cholesterol synthesis may be more reflective of a physiological response to liver membrane cholesterol depletion by cholestatic lipoproteins. This effect would further enhance the accumulation of cholesterol in the plasma of ANIT-treated mice.

To better understand the alterations in bile acid metabolism occurring in ANIT-induced cholestasis in the mouse, the activity of 7α-hydroxylase, the enzyme regulating bile acid synthesis was measured. 7α-hydroxylase activity was reduced 48 hours after treatment and elevated by 168 hours to approximately the same level as observed in cholestyramine treated mice. Cholestyramine functions by sequestering intestinal bile acids thereby preventing their reabsorption by the intestinal endothelium prior to transport via the circulatory system back to the liver. These bile acids are thought to regulate bile acid synthesis transcriptionally through a putative BARE (bile acid responsive element) (44,173,210). Thus, an induction of bile acid synthesis at 168 hours may indicate derepression of cyp7 (7α-hydroxylase gene) gene transcription due to re-establishment of bile acid secretion and flow, resulting in a decrease in repressive bile acids within the liver. Repression of cyp7 was verified by a virtual absence of cyp7

mRNA at 24, 48 and 72 hours and an apparent induction at 168 hours. The caveat to this apparent feedback regulation by bile acids is that 7α-hydroxylase being a cytochrome-P450 isozyme may be partially inhibited by ANIT or liver damage. It is not clear whether 7α-hydroxylase is involved in the oxidation of substrates other than cholesterol; however, if so, some of the reported reduction (138,139) in cytochrome-P450 mixed function oxidase activity might be due to down regulation of 7α-hydroxylase by bile acids. Li *et al.* (211) have reported that in the rat, transcriptional regulation of cyp7 is paralleled by reductions in 7α-hydroxylase activity due to a rapid turnover of the enzyme. The present data suggests that 7α-hydroxylase may have a relatively long half-life as the reduction in enzymatic activity was not nearly as large as the change in cyp7 mRNA abundance. These contradictory results may be due to physiological differences between the rat and mouse and/or be suggestive of alternative post-translational regulation.

To further elucidate the alterations in bile acid metabolism in the mouse, both gallbladder and plasma bile acids need to be measured at a number of time points. To facilitate a more complete understanding of the alterations in bile acid metabolism occurring in the ANIT-treated mouse, the functional status of both the intestinal and hepatic bile acid transporters needs to be confirmed. Furthermore, the time course should be extended to confirm the reversibility of the cholestasis and to examine the activities of lipoprotein and hepatic lipase at various time points.

From the accumulated data, a hypothetical series of events can be assembled to describe the alterations in lipoprotein and bile acid metabolism. For descriptive purposes the time course in the ANIT-treated mouse will be used.

1) Administration of ANIT to the mouse results in down-regulation of cytochrome P-450 mediated mixed function oxidases and bioactivation of ANIT to a secondary metabolite that results in the blockage of bile canniculi, through possible fibroblast proliferation.
2) The blockage of bile secretion causes increased osmotic pressure within the cell causing eventual expulsion of biliary material through gaps in hepatic tight junctions. As a protective mechanism, the liver preferentially synthesizes trihydroxy bile acids (may not be true in the mouse) which are less damaging to membranes than hydrophobic species.
3) Increased concentrations of bile acids within the hepatocytes repress cyp7 gene transcription causing an eventual reduction but not complete inhibition of 7α-hydroxylase mediated bile acid synthesis.
4) Plasma phospholipid, free cholesterol and bile acids continue to rise as the result of continued reflux from permeable cellular tight junctions and this material is supplemented with free cholesterol and phospholipid from lypolysis of intestinally derived lipoproteins and bile acids reabsorbed from the intestine.
5) The influx of phospholipid and free cholesterol into the plasma combined with a deficiency in both hepatic lipase and LCAT activities results in development of abnormal vesicles. These vesicles may then promote efflux of free cholesterol from cellullar membranes until approximately a 1:1 molar ratio of phospholipid to free cholesterol is attained, as is consistent with Lp-X.

6) The efflux of free cholesterol into the plasma combined with an absence of LDL receptor mediated down regulation of HMG CoA reductase due to reduced uptake of remnant lipoproteins and possibly LDL, results in hepatic cholesterolgenesis.

7) At some point prior to 168 hours, the liver, through regeneration, reestablishes bile secretion and flow through the bile canniculi resulting in derepression of cyp7 transcription and increased bile acid synthesis. As liver functions begin to normalize, plasma bile acid concentrations begin to drop and LCAT and hepatic lipase activities return towards normal. Apolipoprotein A-I mediated movement of phospholipid and free cholesterol into HDL and subsequent esterification begins the process of clearing excess plasma phospholipid and free cholesterol and thereby returning the plasma CE/FC ratio to normal.

8.11 General Conclusions

In conclusion, the ANIT-treated rat is a transient, fully reversible and non-surgical model of intrahepatic cholestasis where LCAT is functional. The ANIT-treated mouse although not fully characterized appears to be a model of intrahepatic cholestasis with secondary LCAT deficiency and may be a useful model for the study of plasma lipoproteins in familial LCAT deficiency and intrahepatic cholestasis. ANIT treatment of rodents, like bile-duct ligated rats and dogs, many types of liver disease, Intralipid™ infusion and familial LCAT deficiency, results in the genesis of abnormal lipoprotein species like Lp-X, remnants and phospholipid-enriched, cholesteryl ester depleted HDL. As in bile-duct ligation in rats, Intralipid infusion and unlike many types of Lp-X positive

liver disease and familial LCAT deficiency, these particles in the ANIT-treated rat are generated in the presence of increased LCAT activity. As with any experimental rodent model of lipoprotein metabolism, the differences in rodent versus human lipoprotein metabolism must be considered. Certainly, this model like the bile-duct ligated rat is not an exact duplication of the human cholestatic situation. However, given the similarities to many aspects of human liver disease and the fact that bile-duct ligation is currently one of the only experimental models available for the in-depth study of abnormal cholestatic lipoproteins, the ANIT-treated rat and mouse models may be valuable alternative tools for elucidating the underlying mechanisms involved in the generation and catabolism of abnormal lipoproteins.

Results in the ANIT-treated TgR[HuAI] rats clearly provide evidence that this tool (ANIT-induced cholestasis) in combination with other available resources can be used to better understand plasma lipoprotein metabolism. In the case of the ANIT-treated TgR[HuAI] rats, a unique system has been provided to better understand the role of apolipoprotein A-I in the clearance of abnormal phospholipid and free cholesterol rich lipoproteins.

Furthermore, initial collaborative evaluation of the ANIT-mouse has indicated that this system may be a valuable resource for better understanding not only bile acid metabolism and regulation, but also its intimate relationship to whole animal cholesterol homeostasis.

Appendix A

A.1 Biobead preparation

To facilitate the removal of cholate, the binding properties of Biorad SM-2 Biobeads were exploited. The polystyrene biobeads were prepared and activated by incubating 20 g of dry beads in 100 ml of cold MeOH at 4 °C for 15 minutes. The beads were then washed with 2 L of Milli-Q H_2O followed by 500 ml TBS pH 8.0 by vacuum aspiration on a 500 ml scintered glass funnel. The beads were then suspended in 200 ml TBS pH 8.0 and stored at 4 °C until used.

A.2 Preactivation of ITLC SG TLC plates

Gelman ITLC SG thin layer chromatography plates (ITLC SG Plates, Gelman, Cat# 61886) were divided into 8-10 lanes with a pencil and preactivated by preheating in a 120 °C laboratory oven for 2-4 hours.

References

1. Wilson, M.D., Rudel, L.L. 1994. Review of cholesterol absorption with emphasis on dietary and biliary cholesterol. *J. Lipid Res.* **35:** 943-55.

2. Brindley, D.N. 1991. Metabolism of triacylglycerols. Vance, D.E. and Vance, J. editors. In Biochemistry of Lipids, Lipoproteins and Membranes. Elsevier, New York. 171-203.

3. Lindgren, F.T. 1980. The plasma lipoproteins: Historical developments and nomenclature. Scanu, A.M. and Landsberger, F.R. editors. In Lipoprotein structure. The New York Academy of Sciences, New York, New York. 1-15.

4. Herz, J., Willnow, T.E. 1995. Lipoprotein and receptor interactions in vivo. *Curr. Opin. Lipidol.* **6:** 97-103.

5. Glomset, J.A. 1968. The plasma lecithin:cholesterol acyltransferase reaction. *J. Lipid Res.* **9:** 155-67.

6. Fielding, C.J., Fielding, P.E. 1995. Molecular physiology of reverse cholesterol transport. *J. Lipid Res.* **36:** 211-28.

7. Barter, P.J., Rye, K.A. 1996. Molecular mechanisms of reverse cholesterol transport. *Curr. Opin. Lipidol.* **7:** 82-7.

8. Rothblat, G.H., Mahlberg, F.H., Johnson, W.J., Phillips, M.C. 1992. Apolipoproteins, membrane cholesterol domains, and the regulation of cholesterol efflux. *J. Lipid Res.* **33:** 1091-7.

9. Barrans, A., Jaspard, B., Barbaras, R., Chap, H., Ferret, B., Collet, X. 1996. Pre-beta HDL: Structure and metabolism. *Biochim. Biophys. Acta* **1300:** 73-85.

10. Fielding, P.E., Fielding, C.J. 1996. Dynamics of lipoprotein transport in the human circulatory system. Vance, D.E. and Vance, J. editors. In Biochemistry of Lipids, Lipoproteins and Membranes. Elsevier, New York. 495-516.

11. Castro, G.R., Fielding, C.J. 1988. Early incorporation of cell-derived cholesterol into pre-beta-migrating high-density lipoprotein. *Biochemistry* **27:** 25-9.

12. Francone, O.L., Gurakar, A., Fielding, C. 1989. Distribution and functions of lecithin:cholesterol acyltransferase and cholesteryl ester transfer protein in plasma lipoproteins. Evidence for a functional unit containing these activities together with apolipoproteins A-I and D that catalyzes the esterification and transfer of cell-derived cholesterol. *J. Biol. Chem.* **264:** 7066-72.

13. Davis, R.A., Vance, J.E. 1996. Structure, assembly and secretion of lipoproteins. Vance, D.E. and Vance, J. editors. In Biochemistry of Lipids, Lipoproteins and Membranes. Elsevier, New York. 473-93.

14. Karathanasis, S.K. 1985. Apolipoprotein multigene family: tandem organization of human apolipoprotein AI, CIII, and AIV genes. *Proc. Natl. Acad. Sci. U. S. A.* **82:** 6374-8.

15. Walsh, A., Azrolan, N., Wang, K., Marcigliano, A., O'Connell, A., Breslow, J.L. 1993. Intestinal expression of the human apoA-I gene in transgenic mice is controlled by a DNA region 3' to the gene in the promoter of the adjacent convergently transcribed apoC-III gene. *J. Lipid Res.* **34:** 617-23.

16. Dolphin, P.J., Forsyth, S.J., Krul, E.S. 1986. Post-secretory acquisition of apolipoprotein E by nascent rat hepatic very-low-density lipoproteins in the absence of cholesteryl ester transfer. *Biochim. Biophys. Acta* **875:** 21-30.

17. Havel, R.J., Kane, J.P., Kashyap, M.L. 1973. Interchange of apolipoproteins between chylomicrons and high density lipoproteins during alimentary lipemia in man. *J. Clin. Invest.* **52:** 32-8.

18. Chen, S.H., Habib, G., Yang, C.Y., Gu, Z.W., Lee, B.R., Weng, S.A., Silberman, S.R., Cai, S.J., Deslypere, J.P., Rosseneu, M., et al. 1987. Apolipoprotein B-48 is the product of a messenger RNA with an organ-specific in-frame stop codon. *Science* **238:** 363-6.

19. Innerarity, T.L., Boren, J., Yamanaka, S., Olofsson, S.O. 1996. Biosynthesis of apolipoprotein B48-containing lipoproteins. Regulation by novel post-transcriptional mechanisms. *J. Biol. Chem.* **271:** 2353-6.

20. Johnson, D.F., Poksay, K.S., Innerarity, T.L. 1993. The mechanism for apo-B mRNA editing is deamination. *Biochem. Biophys. Res. Commun.* **195:** 1204-10.

21. Davidson, N.O., Innerarity, T.L., Scott, J., Smith, H., Driscoll, D.M., Teng, B., Chan, L. 1995. Proposed nomenclature for the catalytic subunit of the mammalian apolipoprotein B mRNA editing enzyme: APOBEC-1 [letter]. *RNA* **1:** 3.

22. Greeve, J., Altkemper, I., Dieterich, J.H., Greten, H., Windler, E. 1993. Apolipoprotein B mRNA editing in 12 different mammalian species: hepatic expression is reflected in low concentrations of apoB-containing plasma lipoproteins. *J. Lipid Res.* **34:** 1367-83.

23. LaRosa, J.C., Levy, R.I., Herbert, P., Lux, S.E., Fredrickson, D.S. 1970. A specific apoprotein activator for lipoprotein lipase. *Biochem. Biophys. Res. Commun.* **41:** 57-62.

24. Eisenberg, S. 1984. High density lipoprotein metabolism. *J. Lipid Res.* **25:** 1017-58.

25. Havel, R.J. 1995. Chylomicron remnants: hepatic receptors and metabolism. *Curr. Opin. Lipidol.* **6:** 312-6.

26. Hamilton, R.L., Wong, J.S., Guo, L.S., Krisans, S., Havel, R.J. 1990. Apolipoprotein E localization in rat hepatocytes by immunogold labeling of cryothin sections. *J. Lipid Res.* **31:** 1589-603.

27. Brown, M.S., Herz, J., Kowal, R.C., Goldstein, J.L. 1991. The low-density lipoprotein receptor-related protein. *Curr. Opin. Lipidol.* **2:** 65-72.

28. Von Eckardstein, A., Jauhiainen, M., Huang, Y.D., Metso, J., Langer, C., Pussinen, P., Wu, S.L., Ehnholm, C., Assmann, G. 1996. Phospholipid transfer protein mediated conversion of high density lipo proteins generates beta(1)-HDL. *Biochim. Biophys. Acta* **1301:** 255-62.

29. van Ree, J.H., Hofker, M.H., van den Broek, W.J., van Deursen, J.M., van der Boom, H., Frants, R.R., Wieringa, B., Havekes, L.M. 1995. Increased response to cholesterol feeding in apolipoprotein C1-deficient mice. *Biochem. J.* **305:** 905-11.

30. Ginsberg, H.N. 1995. Synthesis and secretion of apolipoprotein B from cultured liver cells. *Curr. Opin. Lipidol.* **6:** 275-80.

31. Thompson, G.R., Naoumova, R.P., Watts, G.F. 1996. Role of cholesterol in regulating apolipoprotein B secretion by the liver. *J. Lipid Res.* **37:** 439-47.

32. Wu, X., Sakata, N., Dixon, J., Ginsberg, H.N. 1994. Exogenous VLDL stimulates apolipoprotein B secretion from HepG2 cells by both pre- and post-translational mechanisms. *J. Lipid Res.* **35:** 1200-10.

33. Nakahara, D.H., Lingappa, V.R., Chuck, S.L. 1994. Translocational pausing is a common step in the biogenesis of unconventional integral membrane and secretory proteins. *J. Biol. Chem.* **269:** 7617-22.

34. Wu, X., Zhou, M., Huang, Y.D., Wetterau, J., Ginsberg, H.N. 1996. Demonstration of a physical interaction between microsomal triglyceride transfer protein and apolipoprotein B during the assembly of apo-B-containing lipoproteins. *J. Biol. Chem.* **271:** 10277-81.

35. Ricci, B., Sharp, D., O'Rourke, E., Kienzle, B., Blinderman, L., Gordon, D., Smith Monroy, C., Robinson, G., Gregg, R.E., Rader, D.J., et al. 1995. A 30-amino acid truncation of the microsomal triglyceride transfer protein large subunit disrupts its interaction with protein disulfide-isomerase and causes abetalipoproteinemia. *J. Biol. Chem.* **270:** 14281-5.

36. Sharp, D., Blinderman, L., Combs, K.A., Kienzle, B., Ricci, B., Wager Smith, K., Gil, C.M., Turck, C.W., Bouma, M.E., Rader, D.J., et al. 1993. Cloning and gene defects in microsomal triglyceride transfer protein associated with abetalipoproteinaemia. *Nature* **365:** 65-9.

37. Boren, J., Rustaeus, S., Olofsson, S.O. 1994. Studies on the assembly of apolipoprotein B-100- and B-48-containing very low density lipoproteins in McA-RH7777 cells. *J. Biol. Chem.* **269:** 25879-88.

38. Ritland, S., Stokke, K.T., Gjone, E., Torsvik, H., Berg, K., Magnani, H.N., McConathy, J., Alaupovic, P. 1976. Changes in the concentration of lipoprotein-X during incubation of postheparin plasma from patients with familial lecithin: cholesterol acyltransferase (LCAT) deficiency. *Clin. Chim. Acta* **67:** 63-9.

39. Tall, A.R. 1995. Plasma cholesteryl ester transfer protein and high-density lipoproteins: new insights from molecular genetic studies. *J. Intern. Med.* **237:** 5-12.

40. Tall, A.R. 1993. Plasma cholesteryl ester transfer protein. *J. Lipid Res.* **34:** 1255-74.

41. Brown, M.S., Goldstein, J.L. 1986. A receptor-mediated pathway for cholesterol homeostasis. *Science* **232:** 34-47.

42. Dietschy, J.M., Turley, S.D., Spady, D.K. 1993. Role of liver in the maintenance of cholesterol and low density lipoprotein homeostasis in different animal species, including humans. *J. Lipid Res.* **34:** 1637-59.

43. Goldstein, J.L., Brown, M.S. 1990. Regulation of the mevalonate pathway. *Nature* **343:** 425-30.

44. Russell, D.W., Setchell, K.D. 1992. Bile acid biosynthesis. *Biochemistry* **31:** 4737-49.

45. Wilson, P.W., Abbott, R.D., Castelli, W.P. 1988. High density lipoprotein cholesterol and mortality. The Framingham Heart Study. *Arteriosclerosis* **8:** 737-41.

46. Castelli, W.P., Garrison, R.J., Wilson, P.W., Abbott, R.D., Kalousdian, S., Kannel, W.B. 1986. Incidence of coronary heart disease and lipoprotein cholesterol levels. The Framingham Study. *JAMA* **256:** 2835-8.

47. Fielding, C.J., Fielding, P.E. 1981. Evidence for a lipoprotein carrier in human plasma catalyzing sterol efflux from cultured fibroblasts and its relationship to lecithin:cholesterol acyltransferase. *Proc. Natl. Acad. Sci. U. S. A.* **78:** 3911-4.

48. Reichl, D., Hathaway, C.B., Sterchi, J.M., Miller, N.E. 1991. Lipoproteins of human peripheral lymph. Apolipoprotein AI-containing lipoprotein with alpha-2 electrophoretic mobility. *Eur. J. Clin. Invest.* **21:** 638-43.

49. Asztalos, B.F., Sloop, C.H., Wong, L., Roheim, P.S. 1993. Comparison of apo A-I-containing subpopulations of dog plasma and prenodal peripheral lymph: evidence for alteration in subpopulations in the interstitial space. *Biochim. Biophys. Acta* **1169:** 301-4.

50. Rothblat, G.H., Phillips, M.C. 1982. Mechanism of cholesterol efflux from cells. Effects of acceptor structure and concentration. *J. Biol. Chem.* **257:** 4775-82.

51. Oram, J.F., Brinton, E.A., Bierman, E.L. 1983. Regulation of high density lipoprotein receptor activity in cultured human skin fibroblasts and human arterial smooth muscle cells. *J. Clin. Invest.* **72:** 1611-21.

52. Oram, J.F. 1990. Cholesterol trafficking in cells. *Curr. Opin. Lipidol.* **1:** 416-21.

53. Hokland, B., Mendez, A.J., Oram, J.F. 1992. Cellular localization and characterization of proteins that bind high density lipoprotein. *J. Lipid Res.* **33:** 1335-42.

54. Hokland, B.M., Slotte, J.P., Bierman, E.L., Oram, J.F. 1993. Cyclic AMP stimulates efflux of intracellular sterol from cholesterol-loaded cells. *J. Biol. Chem.* **268:** 25343-9.

55. Mendez, A.J., Oram, J.F., Bierman, E.L. 1991. Protein kinase C as a mediator of high density lipoprotein receptor-dependent efflux of intracellular cholesterol. *J. Biol. Chem.* **266:** 10104-11.

56. Schmitz, G., Assmann, G., Robenek, H., Brennhausen, B. 1985. Tangier disease: a disorder of intracellular membrane traffic. *Proc. Natl. Acad. Sci. U. S. A.* **82:** 6305-9.

57. Hui, S.W. 1996. The spatial distribution of cholesterol in membranes. Yeagle, P.L. editor. In Biology of Cholesterol. CRC Press, Boca Raton, FL. 213-31.

58. Schroeder, F., Jefferson, J.R., Kier, A.B., Knittel, J., Scallen, T.J., Wood, W.G., Hapala, I. 1991. Membrane cholesterol dynamics: cholesterol domains and kinetic pools. *Proc. Soc. Exp. Biol. Med.* **196:** 235-52.

59. Tabas, I., Tall, A.R. 1984. Mechanism of the association of HDL_3 with endothelial cells, smooth muscle cells, and fibroblasts. Evidence against the role of specific ligand and receptor proteins. *J. Biol. Chem.* **259:** 13897-905.

60. Leblond, L., Marcel, Y.L. 1991. The amphipathic alpha-helical repeats of apolipoprotein A-I are responsible for binding of high density lipoproteins to HepG2 cells. *J. Biol. Chem.* **266:** 6058-67.

61. Segrest, J.P., Jones, M.K., De Loof, H., Brouillette, C.G., Venkatachalapathi, Y.V., Anantharamaiah, G.M. 1992. The amphipathic helix in the exchangeable apolipoproteins: a review of secondary structure and function. *J. Lipid Res.* **33:** 141-66.

62. Fournier, N., Moya, M.D., Burkey, B.F., Swaney, J.B., Paterniti, J., Moatti, N., Atger, V., Rothblat, G.H. 1996. Role of HDL phospholipid in efflux of cell cholesterol to whole serum: Studies with human apoA-I transgenic rats. *J. Lipid Res.* **37:** 1704-11.

63. Glass, C., Pittman, R.C., Weinstein, D.B., Steinberg, D. 1983. Dissociation of tissue uptake of cholesterol ester from that of apoprotein A-I of rat plasma high density lipoprotein: selective delivery of cholesterol ester to liver, adrenal, and gonad. *Proc. Natl. Acad. Sci. U. S. A.* **80:** 5435-9.

64. Liang, H.Q., Rye, K.A., Barter, P.J. 1994. Dissociation of lipid-free apolipoprotein A-I from high density lipoproteins. *J. Lipid Res.* **35:** 1187-99.

65. Clay, M.A., Newnham, H.H., Forte, T.M., Barter, P.I. 1992. Cholesteryl ester transfer protein and hepatic lipase activity promote shedding of apo A-I from HDL and subsequent formation of discoidal HDL. *Biochim. Biophys. Acta* **1124:** 52-8.

66. Clay, M.A., Newnham, H.H., Barter, P.J. 1991. Hepatic lipase promotes a loss of apolipoprotein A-I from triglyceride-enriched human high density lipoproteins during incubation in vitro. *Arterioscler. Thromb.* **11:** 415-22.

67. Barrans, A., Collet, X., Barbaras, R., Jaspard, B., Manent, J., Vieu, C., Chap, H., Perret, B. 1994. Hepatic lipase induces the formation of pre-beta 1 high density lipoprotein (HDL) from triacylglycerol-rich HDL2. A study comparing liver perfusion to in vitro incubation with lipases. *J. Biol. Chem.* **269:** 11572-7.

68. Horowitz, B.S., Goldberg, I.J., Marab, J., Vanni, T., Ramatrishnan, R., Ginsberg, H.N. 1992. Role of the kidney in increased clearance of apolipoprotein A-I in subjects with reduced high density lipoprotein cholesterol concentrations. Miller, N.E. and Tall, A.R. editors. In High density lipoproteins and atherosclerosis III. Excerpta Medica, New York. 215-22.

69. Forte, T.M., Bielicki, J.K., Goth Goldstein, R., Selmek, J., McCall, M.R. 1995. Recruitment of cell phospholipids and cholesterol by apolipoproteins A-II and A-I: formation of nascent apolipoprotein-specific HDL that differ in size, phospholipid composition, and reactivity with LCAT. *J. Lipid Res.* **36:** 148-57.

70. Czarnecka, H., Yokoyama, S. 1995. Lecithin:cholesterol acyltransferase reaction on cellular lipid released by free apolipoprotein-mediated efflux. *Biochemistry* **34:** 4385-92.

71. Rubin, E.M., Ishida, B.Y., Clift, S.M., Krauss, R.M. 1991. Expression of human apolipoprotein A-I in transgenic mice results in reduced plasma levels of murine apolipoprotein A-I and the appearance of two new high density lipoprotein size subclasses. *Proc. Natl. Acad. Sci. U. S. A.* **88:** 434-8.

72. Chajek Shaul, T., Hayek, T., Walsh, A., Breslow, J.L. 1991. Expression of the human apolipoprotein A-I gene in transgenic mice alters high density lipoprotein (HDL) particle size distribution and diminishes selective uptake of HDL cholesteryl esters. *Proc. Natl. Acad. Sci. U. S. A.* **88:** 6731-5.

73. Bamberger, M., Lund Katz, S., Phillips, M.C., Rothblat, G.H. 1985. Mechanism of the hepatic lipase induced accumulation of high-density lipoprotein cholesterol by cells in culture. *Biochemistry* **24:** 3693-701.

74. Bamberger, M., Glick, J.M., Rothblat, G.H. 1983. Hepatic lipase stimulates the uptake of high density lipoprotein cholesterol by hepatoma cells. *J. Lipid Res.* **24:** 869-76.

75. Busch, S.J., Barnhart, R.L., Martin, G.A., Fitzgerald, M.C., Yates, M.T., Mao, S.J., Thomas, C.E., Jackson, R.L. 1994. Human hepatic triglyceride lipase expression reduces high density lipoprotein and aortic cholesterol in cholesterol-fed transgenic mice. *J. Biol. Chem.* **269:** 16376-82.

76. Fan, J., Wang, J., Bensadoun, A., Lauer, S.J., Dang, Q., Mahley, R.W., Taylor, J.M. 1994. Overexpression of hepatic lipase in transgenic rabbits leads to a marked reduction of plasma high density lipoproteins and intermediate density lipoproteins. *Proc. Natl. Acad. Sci. U. S. A.* **91:** 8724-8.

77. Marques Vidal, P., Azema, C., Collet, X., Vieu, C., Chap, H., Perret, B. 1994. Hepatic lipase promotes the uptake of HDL esterified cholesterol by the perfused rat liver: a study using reconstituted HDL particles of defined phospholipid composition. *J. Lipid Res.* **35:** 373-84.

78. Torsvik, H., Berg, K., Magnani, H.N., McConathy, J., Alaupovic, P., Gjone, E. 1972. Identification of the abnormal cholestatic lipoprotein (Lp-X) in familial lecithin:cholesterol acyltransferase deficiency. *FEBS Lett.* **24:** 165-8.

79. Guerin, M., Dolphin, P.J., Chapman, M.J. 1993. Familial lecithin:cholesterol acyltransferase deficiency: further resolution of lipoprotein particle heterogeneity in the low density interval. *Atherosclerosis* **104:** 195-212.

80. Ritland, S., Gjone, E. 1975. Quantitative studies of lipoprotein-X in familial lecithin: cholesterol acyltransferase deficiency and during cholesterol esterification. *Clin. Chim. Acta* **59:** 109-19.

81. Seidel, D., Gjone, E., Blomhoff, J.P., Geisen, H.P. 1974. Plasma lipoproteins in patients with familial plasma lecithin: cholesterol acyltransferase (LCAT) deficiency--studies on the apolipoprotein composition of isolated fractions with identification of LP-X. *Horm. Metab. Res.* **Suppl 4:** 6-11.

82. Flint, A. 1862. Experimental researches into a new excretory function of the liver; consisting of the removal of cholesterine from the blood, and its discharge from the body in the form of stercorine. *Amer. J. Med. Sci.* **44:** 305-65.

83. Widal, F., Weill, A., Laudat, M. 1912. La lipémie des brightiques: rapports de la rétinite des brightiques aves l'azotémie et al cholestérémie. *Semaine Medicale* **32:** 529-31.

84. Man, E.B., Kartin, B.L. 1945. The lipids of serum and liver in patients with hepatic diseases. *J. Clin. Invest.* **24:** 623-43.

85. Phillips, G.B. 1960. The lipid composition of serum in patients with liver disease. *J. Clin. Invest.* **39:** 1639-50.

86. Miller, J.P. 1990. Dyslipoproteinaemia of liver disease. *Baillieres. Clin. Endocrinol. Metab.* **4:** 807-32.

87. Jauhiainen, M., Dolphin, P.J. 1986. Human plasma lecithin-cholesterol acyltransferase. An elucidation of the catalytic mechanism. *J. Biol. Chem.* **261:** 7032-43.

88. Seidel, D., Greten, H., Geisen, H.P., Wengeler, H., Wieland, H. 1972. Further aspects on the characterization of high and very low density lipoproteins in patients with liver disease. *Eur. J. Clin. Invest.* **2:** 359-64.

89. Agorastos, J., Fox, C., Harry, D.S., McIntyre, N. 1978. Lecithin--cholesterol acyltransferase and the lipoprotein abnormalities of obstructive jaundice. *Clin. Sci. Mol. Med.* **54:** 369-79.

90. Muller, P., Fellin, R., Lamprecht, J., Agostini, B., Wieland, H., Rost, W., Seidel, D. 1974. Hypertriglyceridemia secondary to liver disease. *Eur. J. Clin. Invest.* **4:** 419-28.

91. Komai, K., Sabesin, S.M., Weidman, S.W. 1987. Inhibition of hepatic triglyceride secretion and exogenous triglyceride clearance in the cholestatic rat. *Atherosclerosis* **64:** 147-53.

92. Kostner, G.M., Laggner, P., Prexl, H.J., Holasek, A. 1976. Investigation of the abnormal low-density lipoproteins occurring in patients with obstructive jaundice. *Biochem. J.* **157:** 401-7.

93. Felker, T.E., Hamilton, R.L., Havel, R.J. 1978. Secretion of lipoprotein-X by perfused livers of rats with cholestasis. *Proc. Natl. Acad. Sci. U. S. A.* **75:** 3459-63.

94. Seidel, D., Alaupovic, P., Furman, R.H., McConathy, W.J. 1970. A lipoprotein characterizing obstructive jaundice. II. Isolation and partial characterization of the protein moieties of low density lipoproteins. *J. Clin. Invest.* **49:** 2396-407.

95. Patsch, J.R., Aune, K.C., Gotto, A.M., Jr., Morrisett, J.D. 1977. Isolation, chemical characterization, and biophysical properties of three different abnormal lipoproteins: LP-X_1, LP-X_2, and LP-X_3. *J. Biol. Chem.* **252:** 2113-20.

96. Manzato, E., Fellin, R., Baggio, G., Walch, S., Neubeck, W., Seidel, D. 1976. Formation of lipoprotein-X. Its relationship to bile compounds. *J. Clin. Invest.* **57:** 1248-60.

97. Chisholm, J.W., Dolphin, P.J. 1996. Abnormal lipoproteins in the ANIT-treated rat: A transient and reversi ble animal model of intrahepatic cholestasis. *J. Lipid Res.* **37:** 1086-98.

98. Blomhoff, J.P., Holme, R., Ostrem, T. 1978. Plasma cholesterol esterification and plasma lipoproteins in bile-duct-ligated dogs. *Scand. J. Gastroenterol.* **13:** 693-702.

99. Jung, K., Schimmelpfennig, W., Wack, R., Neumann, R. 1978. Lecithin: cholesterol acyltransferase activity in patients with chronic liver diseases and positive LP-X tests. *Digestion* **17:** 445-8.

100. Weinberg, R.B., Singh, K.K. 1989. Short-term parenteral nutrition with glucose and Intralipid: effects on serum lipids and lipoproteins. *Am. J. Clin. Nutr.* **49:** 794-8.

101. Griffin, E., Breckenridge, W.C., Kuksis, A., Bryan, M.H., Angel, A. 1979. Appearance and characterization of lipoprotein X during continuous intralipid infusions in the neonate. *J. Clin. Invest.* **64:** 1703-12.

102. Tomsits, E., Rischak, K., Molnar, M., Filiczky, I., Szollar, L. 1995. Effects of administration of different intravenous lipid emulsions on plasma LP-X concentrations in the rat. *JPEN* **19:** 369-72.

103. Miyahara, T., Fujiwara, H., Yae, Y., Okano, H., Okochi, K., Torisu, M. 1979. Abnormal lipoprotein appearing in plasma of patients who received a ten percent soybean oil emulsion infusion. *Surgery* **85:** 566-74.

104. Hinton, R.H., Mullock, B.M. 1978. Changes in rat serum lipoproteins following ligation of the bile duct. *Clin. Chim. Acta* **82:** 31-44.

105. Ritland, S., Bergan, A. 1975. Plasma concentration of lipoprotein-X (LP-X) in experimental bile duct obstruction. *Scand. J. Gastroenterol.* **10:** 17-24.

106. Glomset, J.A., Norum, K.R., Nichols, A.V., King, W.C., Mitchell, C.D., Applegate, K.R., Gong, E.L., Gjone, E. 1975. Plasma lipoproteins in familial lecithin: cholesterol acyltransferase deficiency: effects of dietary manipulation. *Scand. J. Clin. Lab. Invest. Suppl.* **142:** 3-30.

107. Wengeler, H., Seidel, D. 1973. Does lipoprotein-X (LP-X) act as a substrate for the lecithin: cholesterol acyltransferase (LCAT)? *Clin. Chim. Acta* **45:** 429-32.

108. Utermann, G., Menzel, H.J., Adler, G., Dieker, P., Weber, W. 1980. Substitution in vitro of lecithin-cholesterol acyltransferase. Analysis of changes in plasma lipoproteins. *Eur. J. Biochem.* **107:** 225-41.

109. Patsch, J.R., Soutar, A.K., Morrisett, J.D., Gotto, A.M., Jr., Smith, L.C. 1977. Lipoprotein-X: a substrate for lecithin: cholesterol acyltransferase. *Eur. J. Clin. Invest.* **7:** 213-7.

110. O, K., Frolich, J. 1995. Role of lecithin:cholesterol acyltransferase and apolipoprotein A-I in cholesterol esterification in lipoprotein-X in vitro. *J. Lipid Res.* **36:** 2344-54.

111. Sauar, J., Ritland, S., Holme, R., Horn, R. 1978. The effect of lipoprotein lipase and hepatic lipase on the electrophoretic mobility of lipoprotein-X. *Clin. Chim. Acta* **88:** 461-7.

112. Ritland, S., Sauar, J., Holme, R., Blomhoff, J.P. 1977. The electrophoretic mobility of lipoprotein X in postheparin plasma. *Clin. Chim. Acta* **75:** 129-35.

113. Walli, A.K., Seidel, D. 1984. Role of lipoprotein-X in the pathogenesis of cholestatic hypercholesterolemia. Uptake of lipoprotein-X and its effect on 3-hydroxy-3-methylglutaryl coenzyme A reductase and chylomicron remnant removal in human fibroblasts, lymphocytes, and in the rat. *J. Clin. Invest.* **74:** 867-79.

114. Larsson, B., Nilsson, A. 1980. Inhibition of hepatic chylomicron remnant uptake in the cholestatic rat. *Scand. J. Gastroenterol.* **15:** 959-67.

115. Williams, K.J., Tall, A.R., Tabas, I., Blum, C. 1986. Recognition of vesicular lipoproteins by the apolipoprotein B,E receptor of cultured fibroblasts. *J. Lipid Res.* **27:** 892-900.

116. Clifton, P.M., Barter, P.J., Mackinnon, A.M. 1988. High density lipoprotein particle size distribution in subjects with obstructive jaundice. *J. Lipid Res.* **29:** 121-35.

117. Mitchell, C.D., King, W.C., Applegate, K.R., Forte, T., Glomset, J.A., Norum, K.R., Gjone, E. 1980. Characterization of apolipoprotein E-rich high density lipoproteins in familial lecithin:cholesterol acyltransferase deficiency. *J. Lipid Res.* **21:** 625-34.

118. Danielsson, B., Ekman, R., Petersson, B.G. 1975. An abnormal high density lipoprotein in cholestatic plasma isolated by zonal ultracentrifugation. *FEBS Lett.* **50:** 180-4.

119. Coulhon, M.P., Tallet, F., Yonger, J., Agneray, J., Raichvarg, D. 1985. Changes in human high density lipoproteins in patients with extra-hepatic biliary obstruction. *Clin. Chim. Acta* **145:** 163-72.

120. Norum, K.R., Glomset, J.A., Nichols, A.V., Forte, T., Albers, J.J., King, W.C., Mitchell, C.D., Applegate, K.R., Gong, E.L., Cabana, V., et al. 1975. Plasma lipoproteins in familial lecithin: cholesterol acyltransferase deficiency: effects of incubation with lecithin: cholesterol acyltransferase in vitro. *Scand. J. Clin. Lab. Invest.* **35 Suppl 142:** 31-55.

121. Glomset, J.A., Norum, K.R., Gjone, E. 1983. Familial lecithin:cholesterol acyltransferase deficiency. Stanbury, J.B., Wyngaarden, J.B., Fredrickson, D.S., Goldstein, J.L., and Brown, M.S. editors. In The Metabolic Basis of Inherited Disease. McGraw-Hill, New York. 643-54.

122. Hovig, T., Blomhoff, J.P., Holme, R., Flatmark, A., Gjone, E. 1978. Plasma lipoprotein alterations and morphologic changes with lipid deposition in the kidney of patients with hepatorenal syndrome. *Lab. Invest.* **38:** 540-9.

123. Gjone, E., Blomhoff, J.P., Skarbovik, A.J. 1974. Possible association between an abnormal low density lipoprotein and nephropathy in lecithin: cholesterol acyltransferase deficiency. *Clin. Chim. Acta* **54:** 11-8.

124. Blomhoff, J.P., Hovig, T., Stokke, K.T., Holme, R., Bergan, A., Ostrem, T., Gjone, E. 1979. Lipid deposition in kidneys in experimental liver disease: a study in dogs with choledochocaval anastomosis. *Eur. J. Clin. Invest.* **9:** 267-80.

125. Breslow, J.L. 1994. Lipoprotein metabolism and atherosclerosis susceptibility in transgenic mice. *Curr. Opin. Lipidol.* **5:** 175-84.

126. Paigen, B., Plump, A.S., Rubin, E.M. 1994. The mouse as a model for human cardiovascular disease and hyperlipidemia. *Curr. Opin. Lipidol.* **5:** 258-64.

127. Sabesin, S.M., Kuiken, L.B., Ragland, J.B. 1975. Lipoprotein and lecithin: cholesterol acyltransferase changes in galactosamine-induced rat liver injury. *Science* **190:** 1302-4.

128. Goldfarb, S., Singer, E.J., Popper, H. 1962. Experimental cholangitis due to alpha-naphthylisothiocyanate (ANIT). *Am. J. Pathol.* **40:** 685-95.

129. Capizzo, F., Roberts, R.J. 1971. α-naphthylisothiocyanate (ANIT)-induced hepatotoxicity and disposition in various species. *Toxicol. Appl. Pharmacol.* **19:** 176-87.

130. Plaa, G.L., Priestly, B.G., Ungar, H., Moran, E., Eisner, M., Eliakim, M. 1976. Intrahepatic cholestasis induced by drugs and chemicals. *Pharmacol. Rev.* **28:** 207-73.

131. Ungar, H., Moran, E., Eisner, M., Eliakim, M. 1962. Rat intrahepatic biliary tract lesions from alpha-naphthylisothiocyanate. *Arch. Pathol.* **73:** 427-35.

132. Desmet, V.J., Krstulovic, B., Van Damme, B. 1968. Histochemical study of rat liver in alpha-naphthyl isothiocyanate (ANIT) induced cholestasis. *Am. J. Pathol.* **52:** 401-21.

133. Kossor, D.C., Meunier, P.C., Handler, J.A., Sozio, R.S., Goldstein, R.S. 1993. Temporal relationship of changes in hepatobiliary function and morphology in rats following alpha-naphthylisothiocyanate (ANIT) administration. *Toxicol. Appl. Pharmacol.* **119:** 108-14.

134. Roberts, R.J., Plaa, G.L. 1965. Potentiation and inhibition of α-naphthylisothiocyanate-induced hyperbilirubinemia and cholestasis. *J. Pharmacol. Exp. Ther.* **150:** 499-506.

135. Traiger, G.J., Vyas, K.P., Hanzlik, R.P. 1985. Effect of inhibitors of alpha-naphthylisothiocyanate-induced hepatotoxicity on the in vitro metabolism of alpha-naphthylisothiocyanate. *Chem. Biol. Interact.* **52:** 335-45.

136. Traiger, G.J., Vyas, K.P., Hanzlik, R.P. 1984. Effect of thiocarbonyl compounds on alpha-naphthylisothiocyanate-induced hepatotoxicity and the urinary excretion of [35S]alpha-naphthylisothiocyanate in the rat. *Toxicol. Appl. Pharmacol.* **72:** 504-12.

137. Dahm, L.J., Roth, R.A. 1991. Protection against alpha-naphthylisothiocyanate-induced liver injury by decreased hepatic non-protein sulfhydryl content. *Biochem. Pharmacol.* **42:** 1181-8.

138. El Hawari, A.M., Plaa, G.L. 1979. Impairment of hepatic mixed-function oxidase activity by alpha-and beta-naphthylisothiocyanate: relationship to hepatotoxicity. *Toxicol. Appl. Pharmacol.* **48:** 445-58.

139. Schaffner, F., Scharnbeck, H.H., Hutterer, F., Denk, H., Greim, H.A., Popper, H. 1973. Mechanism of cholestasis. VII. -Naphthylisothiocyanate-induced jaundice. *Lab. Invest.* **28:** 321-31.

140. Plaa, G.L., Rogers, L.A., Fouts, J.R. 1965. Effect of acute alpha-naphthylisothiocyanate administration on hepatic microsomal drug metabolism in the mouse. *Proc. Soc. Exp. Biol. Med.* **119:** 1045-8.

141. Krell, H., Hoke, H., Pfaff, E. 1982. Development of intrahepatic cholestasis by alpha-naphthylisothiocyanate in rats. *Gastroenterology* **82:** 507-14.

142. Becker, B.A., Plaa, G.L. 1965. Quantitative and temporal delineation of various parameters of liver dysfunction due to alpha-naphthylisothiocyanate. *Toxicol. Appl. Pharmacol.* **7:** 708-18.

143. Becker, B.A., Plaa, G.L., AU, K.V., AU, W.D. 1965. The nature of alpha-naphthylisothiocyanate-induced cholestasis. *Toxicol. Appl. Pharmacol.* **7:** 680-5.

144. Katterman, V.R., Wolfrum, D.I. 1970. cholesterinstoffwechsel und lecithin-cholesterin-acyl-transferase im plasma bei experimenteller hepatitis und cholestase and der ratte. *Z. klin. Chem. u. klin. Biochem.* **8:** 413-9.

145. Cooper, A.D., Ockner, R.K. 1974. Studies of hepatic cholesterol synthesis in experimental acute biliary obstruction. *Gastroenterology* **66:** 586-95.

146. Mitamura, T. 1984. Alterations of high density lipoproteins in experimental intrahepatic cholestasis in the rat induced by administration of alpha-naphthylisothiocyanate. *J. Biochem. Tokyo.* **95:** 29-36.

147. Swanson, M.E., Hughes, T.E., Denny, I.S., France, D.S., Paterniti, J.R., Jr., Tapparelli, C., Gfeller, P., Burki, K. 1992. High level expression of human apolipoprotein A-I in transgenic rats raises total serum high density lipoprotein cholesterol and lowers rat apolipoprotein A-I. *Transgenic Res.* **1:** 142-7.

148. Bisaha, J.G., Simon, T.C., Gordon, J.I., Breslow, J.L. 1995. Characterization of an enhancer element in the human apolipoprotein C-III gene that regulates human apolipoprotein A-I gene expression in the intestinal epithelium. *J. Biol. Chem.* **270:** 19979-88.

149. Burkey, B.F., France, D., Wang, H., Ma, X., Brand, B., Abuhani, C., Diffenderfer, M.R., Marsh, J.B., Paterniti, J.R., Jr., Fisher, E.A. 1995. Overexpression of human apolipoprotein A-I in transgenic rats and the hyperlipoproteinemia associated with experimental nephrosis. *J. Lipid Res.* **36:** 1463-73.

150. Marsh, J.B., Diffenderfer, M.R., Fisher, E.A., Sowden, M., Dong, M., Paterniti, J.R., Burkey, B.F. 1996. Effect of experimental nephrosis on hepatic lipoprotein secretion and urinary lipoprotein excretion in rats expressing the human apolipoprotein A- I gene. *J Lipid Res* **37:** 1113-24.

151. Patsch, W., Patsch, J.R., Kunz, F., Sailer, S., Braunsteiner, H. 1977. Studies on the degradation of lipoprotein-X. *Eur. J. Clin. Invest.* **7:** 523-30.

152. Rubin, E.M., Krauss, R.M., Spangler, E.A., Verstuyft, J.G., Clift, S.M. 1991. Inhibition of early atherogenesis in transgenic mice by human apolipoprotein AI. *Nature* **353:** 265-7.

153. Liu, A.C., Lawn, R.M., Verstuyft, J.G., Rubin, E.M. 1994. Human apolipoprotein A-I prevents atherosclerosis associated with apolipoprotein[a] in transgenic mice. *J. Lipid Res.* **35:** 2263-7.

154. Plump, A.S., Scott, C.J., Breslow, J.L. 1994. Human apolipoprotein A-I gene expression increases high density lipoprotein and suppresses atherosclerosis in the apolipoprotein E-deficient mouse. *Proc. Natl. Acad. Sci. U. S. A.* **91:** 9607-11.

155. Paszty, C., Maeda, N., Verstuyft, J., Rubin, E.M. 1994. Apolipoprotein AI transgene corrects apolipoprotein E deficiency-induced atherosclerosis in mice. *J. Clin. Invest.* **94:** 899-903.

156. Vlahcevic, Z.R., Hylemon, P.B., Chiang, J.Y.L. 1994. Hepatic cholesterol metabolism. Arias, I.M., Boyer, J.L., Fausto, N., Jakoby, W.B., Schachter, D.A., and Stanbury, J.B. editors. In The Liver: Biology and Pathobiology. 3rd ed. Raven Press Ltd. New York. 379-89.

157. Pedersen, J.I., Gustafsson, J. 1980. Conversion of 3 alpha, 7 alpha, 12 alpha-trihydroxy-5 beta-cholestanoic acid into cholic acid by rat liver peroxisomes. *FEBS Lett.* **121:** 345-8.

158. Lazarow, P.B., Fujiki, Y. 1985. Biogenesis of peroxisomes. *Annu. Rev. Cell Biol.* **1:** 489-530.

159. Kase, B.F., Bjorkhem, I. 1989. Peroxisomal bile acid-CoA:amino-acid N-acyltransferase in rat liver. *J. Biol. Chem.* **264:** 9220-3.

160. Danielsson, H. 1973. The Bile Acids. Nair, P.P. and Kritchevsky, D. editors. Plenum Press, New York. 1-32.

161. Nathanson, M.H., Boyer, J.L. 1991. Mechanisms and regulation of bile secretion. *Hepatology* **14:** 551-66.

162. Carey, M.C. 1982. The Liver: Biology and Pathobiology. Arias, I.M., Popper, H., Schachter, D.A., and Shafritz, D.A. editors. Raven Press, New York. 429-465.

163. Vlahcevic, Z.R., Pandak, W.M., Heuman, D.M., Hylemon, P.B. 1992. Function and regulation of hydroxylases involved in the bile acid biosynthesis pathways. *Semin. Liver Dis.* **12:** 403-19.

164. Gurantz, D., Hofmann, A.F. 1984. Influence of bile acid structure on bile flow and biliary lipid secretion in the hamster. *Am. J. Physiol.* **247:** G736-48.

165. Elferink, R.P.J.O., Ottenhoff, R., vanWijland, M., Frijters, C.M.G., vanNieuwkerk, C., Groen, A.K. 1996. Uncoupling of biliary phospholipid and cholesterol secretion in mice w ith reduced expression of mdr2 P-glycoprotein. *J. Lipid Res.* **37:** 1065-75.

166. Wilson, F.A. 1981. Intestinal transport of bile acids [editorial]. *Am. J. Physiol.* **241:** G83-92.

167. Dawson, P.A., Oelkers, P. 1995. Bile acid transporters. *Curr. Opin. Lipidol.* **6:** 109-14.

168. Hofmann, A.F. 1993. The enterohepatic circulation of bile acids in health and disease. Sleisenger, M.H. and Fordtran, J.S. editors. In Gastrointestinal disease. Pathophysiology, diagnosis, management. 5th ed. W.B. Saunders Co. Philadelphia. 127-50.

169. Turley, S.D., Dietschy, J.M. 1982. The Liver: Biology and Pathobiology. Arias, I.M., Popper, H., Schachter, D.A., and Shafritz, D.A. editors. Raven Press, New York. 467-492.

170. Pandak, W.M., Stravitz, R.T., Lucas, V., Heuman, D.M., Chiang, J.Y.L. 1996. Hep G2 cells: A model for studies on regulation of human cholesterol 7 alpha-hydroxylase at the molecular level. *Amer. J. Physiol. Gastrointest. L.* **33:** G401-10.

171. Stravitz, R.T., Hylemon, P.B., Heuman, D.M., Hagey, L.R., Schteingart, C.D., Ton Nu, H.T., Hofmann, A.F., Vlahcevic, Z.R. 1993. Transcriptional regulation of cholesterol 7 alpha-hydroxylase mRNA by conjugated bile acids in primary cultures of rat hepatocytes. *J. Biol. Chem.* **268:** 13987-93.

172. Heuman, D.M., Vlahcevic, Z.R., Bailey, M.L., Hylemon, P.B. 1988. Regulation of bile acid synthesis. II. Effect of bile acid feeding on enzymes regulating hepatic cholesterol and bile acid synthesis in the rat. *Hepatology* **8:** 892-7.

173. Ramirez, M.I., Karaoglu, D., Haro, D., Barillas, C., Bashirzadeh, R., Gil, G. 1994. Cholesterol and bile acids regulate cholesterol 7 alpha-hydroxylase expression at the transcriptional level in culture and in transgenic mice. *Mol. Cell Biol.* **14:** 2809-21.

174. Kuksis, A., Myher, J.J., Geher, K., Hoffman, A.G., Breckenridge, W.C., Jones, G.J., Little, J.A. 1978. Comparative determination of plasma cholesterol and triacylglycerol levels by automated gas--liquid chromatographic and autoanalyzer methods. *J. Chromatogr.* **146:** 393-412.

175. Folch, J., Lees, M., Sloane-Stanley, G.H. 1957. A Simple Method for the Isolation and Purification of total Lipids from Animal Tissues. *J. Biol. Chem.* **226:** 497-509.

176. Chen, C.H., Albers, J.J. 1982. Characterization of proteoliposomes containing apoprotein A-I: a new substrate for the measurement of lecithin: cholesterol acyltransferase activity Characterization of proteoliposomes containing apoprotein A-I: a new substrate for the measurement of lecithin: cholesterol acyltransferase activity. *J. Lipid Res.* **23:** 680-91.

177. Sparks, D.L., Anantharamaiah, G.M., Segrest, J.P., Phillips, M.C. 1995. Effect of the cholesterol content of reconstituted LpA-I on lecithin:cholesterol acyltransferase activity. *J. Biol. Chem.* **270:** 5151-7.

178. Jackson, R.I., MacLean, L.R. 1991. Human postheparin plasma lipoprotein lipase and hepatic triglyceride lipase. *Methods Enzymol.* **197:** 339-45.

179. Nilsson Ehle, P., Schotz, M.C. 1976. A stable, radioactive substrate emulsion for assay of lipoprotein lipase. *J. Lipid Res.* **17:** 536-41.

180. Krul, E.S., Dolphin, P.J. 1982. Isolated hepatocytes from hypercholesterolemic rats secrete discoidal lipoproteins. *FEBS Lett.* **139:** 259-64.

181. Dolphin, P.J., Breckenridge, W.C., Dolphin, M.A., Tan, M.H. 1984. The lipoproteins of human umbilical cord blood apolipoprotein and lipid levels. *Atherosclerosis* **51:** 109-22.

182. Chapman, M.J., Goldstein, S., Lagrange, D., Laplaud, P.M. 1981. A density gradient ultracentrifugal procedure for the isolation of the major lipoprotein classes from human serum. *J. Lipid Res.* **22:** 339-58.

183. Markwell, M.A., Haas, S.M., Bieber, L.L., Tolbert, N.E., AU, J.R., AU, M.L. 1978. A modification of the Lowry procedure to simplify protein determination in membrane and lipoprotein samples. *Anal. Biochem.* **87:** 206-10.

184. Irwin, D., O'Looney, P.A., Quinet, E., Vahouny, G.V. 1984. Application of SDS gradient polyacrylamide slab gel electrophoresis to analysis of apolipoprotein mass and radioactivity of rat lipoproteins. *Atherosclerosis* **53:** 163-72.

185. Asztalos, B.F., Sloop, C.H., Wong, L., Roheim, P.S. 1993. Two-dimensional electrophoresis of plasma lipoproteins: recognition of new apo A-I-containing subpopulations. *Biochim. Biophys. Acta* **1169:** 291-300.

186. Nichols, A.V., Krauss, R.M., Musliner, T.A. 1986. Nondenaturing polyacrylamide gradient gel electrophoresis. *Methods Enzymol.* **128:** 417-31.

187. Weisgraber, K.H., Mahley, R.W. 1986. Characterization of apolipoprotein E-containing lipoproteins. *Methods Enzymol.* **128:** 145-65.

188. Forte, T.M., Nordhausen, R.W. 1986. Electron microscopy of negatively stained lipoproteins. *Methods Enzymol.* **128:** 442-57.

189. Ingebritsen, T.S., Gibson, D.M. 1981. Assay of enzymes that modulate S-3-hydroxy-3-methylglutaryl-CoA reductase by reversible phosphorylation. *Methods Enzymol.* **71:** 486-97.

190. Chiang, J.Y.L. 1991. Reverse-phase high-performance liquid chromatography assay of 7α-hydroxylase. *Methods Enzymol.* **206:** 483-91.

191. Rudel, L., Deckelman, C., Wilson, M., Scobey, M., Anderson, R. 1994. Dietary cholesterol and downregulation of cholesterol 7 alpha-hydroxylase and cholesterol absorption in African green monkeys. *J. Clin. Invest.* **93:** 2463-72.

192. Matsuura, J.E., Swaney, J.B. 1991. High density lipoprotein subpopulations from galactosamine-treated rats and their transformation by lecithin:cholesterol acyltransferase. *J. Lipid Res.* **32:** 581-94.

193. Cartwright, C.K., Ragland, J.B., Weidman, S.W., Sabesin, S.M. 1982. Alterations in lipoprotein composition associated with galactosamine-induced rat liver injury. *J. Lipid Res.* **23:** 667-79.

194. Sirowej, H., Assmann, G., Kattermann, R. 1980. Lipoproteins and apolipoprotein patterns in rat plasma after liver injury induced by D-galactosamine. *Hoppe Seylers. Z. Physiol. Chem.* **361:** 1417-25.

195. Black, D.D., Freeman, M.R., Sabesin, S.M. 1982. Lipoprotein lipase and hepatic lipase deficiencies associated with impaired chylomicron clearance in D-(+) galactosamine hepatitis. *Metabolism* **31:** 620-6.

196. Keppler, D., Lesch, R., Reutter, W., Decker, K. 1968. Experimental hepatitis induced by D-galactosamine. *Exp. Mol. Pathol.* **9:** 279-90.

197. Konishi, Y., Shinozuka, H., Farber, J.L. 1974. The inhibition of rat liver nuclear ribonucleic acid synthesis by galactosamine and its reversal by uridine. *Lab. Invest.* **30:** 751-6.

198. Shinozuka, H., Farber, J.L., Konishi, Y., Anukarahanonta, T. 1973. D-galactosamine and acute liver cell injury. *Fed. Proc.* **32:** 1516-26.

199. Ritland, S., Blomhoff, J.P., Gjone, E. 1973. Lecithin: cholesterol acyl-transferase and lipoprotein-X in liver disease. *Clin. Chim. Acta* **49:** 251-9.

200. Wengeler, H., Greten, H., Seidel, D. 1972. Serum cholesterol esterification in liver disease. Combined determinations of lecithin: cholesterol acyltransferase and lipoprotein-X. *Eur. J. Clin. Invest.* **2:** 372-8.

201. Baumgartner, U., Scholmerich, J., Leible, P., Farthmann, E.H. 1992. Cholestasis, metabolism and biliary lipid secretion during perfusion of rat liver with different bile salts. *Biochim. Biophys. Acta* **1125:** 142-9.

202. Quarfordt, S.H., Oelschlaeger, H., Krigbaum, W.R., Jakoi, L., Davis, R. 1973. Effect of biliary obstruction on canine plasma and biliary lipids. *Lipids* **8:** 522-30.

203. Breckenridge, W.C., Kakis, G., Kuksis, A. 1979. Identification of lipoprotein X-like particles in rat plasma following Intralipid infusion. *Can. J. Biochem.* **57:** 72-82.

204. Tashiro, T., Mashima, Y., Yamamori, H., Horibe, K., Nishizawa, M., Sanada, M., Okui, K. 1991. Increased lipoprotein X causes hyperlipidemia during intravenous administration of 10% fat emulsion in man. *JPEN. J. Parenter. Enteral. Nutr.* **15:** 546-50.

205. Calandra, S., Martin, M.J., O'Shea, M.J., McIntyre, N. 1972. The effect of experimental biliary obstruction on the structure and lipid content of rat erythrocytes. *Biochim. Biophys. Acta* **260:** 424-32.

206. Felker, T.E., Hamilton, R.L., Vigne, J.L., Havel, R.J. 1982. Properties of lipoproteins in blood plasma and liver perfusates of rats with cholestasis. *Gastroenterology* **83:** 652-63.

207. Williams, D.R., Barter, P.J., Mackinnon, A.M. 1981. Serum lecithin: cholesterol acyltransferase activity in the bile duct-ligated rat. *Digestion* **21:** 273-8.

208. Calandra, S., Martin, M.J., McIntyre, N. 1971. Plasma lecithin: cholesterol acyltransferase activity in liver disease. *Eur. J. Clin. Invest.* **1:** 352-60.

209. Simko, V., Kelley, R.E., Dincsoy, H.P. 1985. Predicting severity of liver disease: twelve laboratory tests evaluated by multiple regression. *J. Int. Med. Res.* **13:** 249-54.

210. Chiang, J.Y., Stroup, D. 1994. Identification and characterization of a putative bile acid-responsive element in cholesterol 7 alpha-hydroxylase gene promoter. *J. Biol. Chem.* **269:** 17502-7.

211. Li, Y.C., Wang, D.P., Chiang, J.Y. 1990. Regulation of cholesterol 7 alpha-hydroxylase in the liver. Cloning, sequencing, and regulation of cholesterol 7 alpha-hydroxylase mRNA. *J. Biol. Chem.* **265:** 12012-9.

IMAGE EVALUATION TEST TARGET (QA-3)

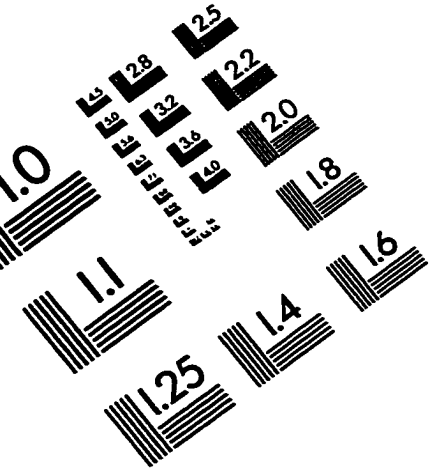

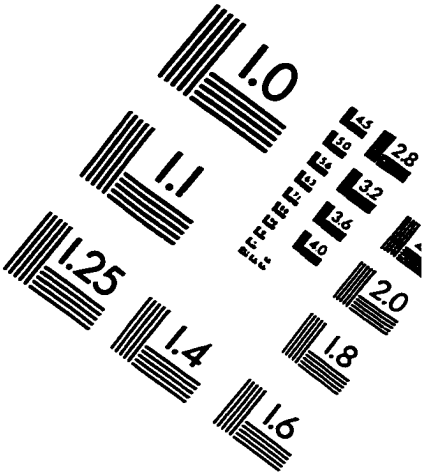

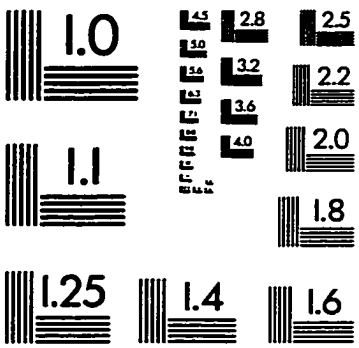

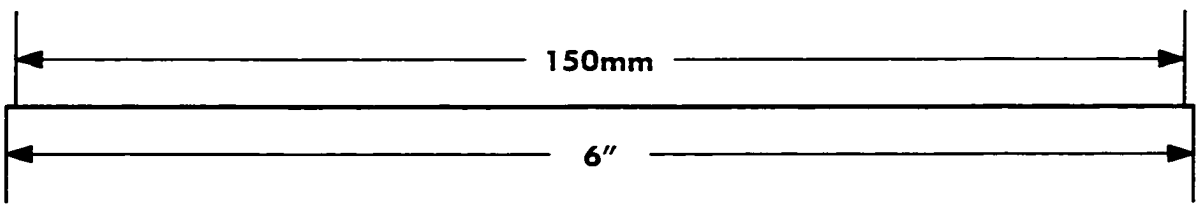

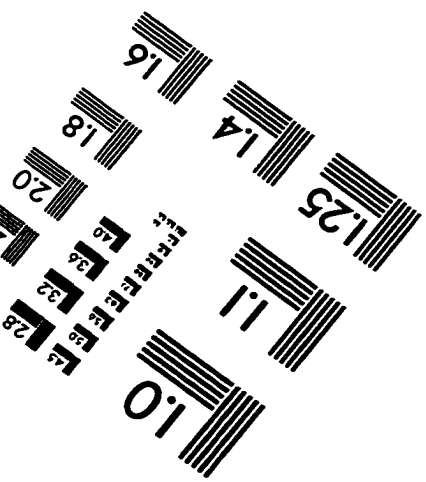

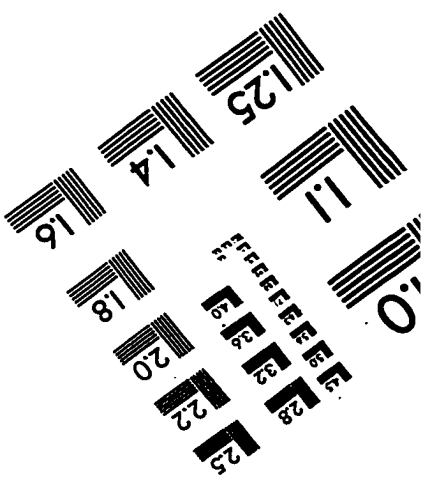

APPLIED IMAGE, Inc
1653 East Main Street
Rochester, NY 14609 USA
Phone: 716/482-0300
Fax: 716/288-5989